TABLE OF CONTENTS

Technical Papers on Flow Assurance, Energy and Management

International Conference on Petroleum Engineering 2016 (ICPE-2016)
Bangladesh University of Engineering & Technology (BUET)
Dhaka-1000, Bangladesh

ICPE (2016-002)

Material Planning and Control -A case study of TGTDCL

***Md. Shamsuzzoha**[1]*
Titas Gas Transmission and Distribution Company Ltd, Kawranbazar, Dhaka-1215, Bangladesh

ABSTRACT

Titas Gas Transmission and Distribution Company Limited (TGTDCL) is a public Limited (75% share of government) Company responsible for distributing natural gas to customers at the household, commercial and industrial level. In order to deliver it services more efficiently, the company needs to address a number of Material Planning and cost control issues such as supplier problems, accurate technical information, bureaucratic and administrative barriers, audit and tax burden, as well as financial and customer services. Titas Gas personnel use manual procedure to purchase material and to manage of inventory. TGTDCL need to purchase material in case of unavoidable conditions. For this, some of the items go to pile up and some of them go shortages when materials need. The purpose of this paper is to investigate the role of material management in a downstream Natural Gas Company. This paper discusses the current procedure material planning and controls of traditional model of Titas gas. It also outlines strategies for improving material management in the downstream Oil & Gas Company. Finally, this paper introduces a case study that shows how material management model of TGTDCL can be improved and thereby make the material planning and customer service of TGTDCL more efficient.

Key Words: Material Plan, cost control, Innovation, Public procurement rules (PPR), Inventory control, Supply Chain, customer service.

THEORY BACKGROUND

Material Requirements Planning is a time phased priority-planning technique that calculates material requirements and schedules supply to meet demand across all products and parts in a service company [1]. Material management is a scientific technique, concerned with Planning, Organizing & Controlling of flow of materials, from their initial purchase to destination. Usually, materials, information, capital, labor, technology, financial assets, and other resources flow through the material planning and inventory control processes. The main theme of Material Planning is "getting the right materials to the right place, right price at the right time" [5, 6]. Information Technology, Enterprise Resource Planning (ERP) plays a major role in designing and implementing Material requirements. Planning systems and processes as it provides information about service needs (linked with customer demand) as well as information about inventory levels. It clearly known that inventories have a direct impact upon the firms' profit and proper inventory management is a major contributing factor to fluctuations in business activity. Thus both from operational

* Corresponding Author address
Email: zoha.shamsu@gmail.com

and profitability point of view, maintaining an optimum level of inventory is very important for any business enterprise. Inventory control is not only the control of physical goods owned by an enterprise but also the control of the amount of funds invested in inventories of each type. The good understanding of sensitivity analysis, sound capital rationing and use of correct investment appraisal technique are all-imperative for a material manager [13]. As a Material Planner, the manager needs to maintain good personal relation with proper supplier and good information systems, be informed about government policy and community plan, environmental impact and nature conservation, compatibility with existing uses, economics benefit, interdepartmental harmony and consistency with quality service. Besides, terms of personal circumstances, private interests, moral or religious considerations, political or ideological interest, cost of development, ownership. There are three main steps [2] of material planning: a) identification of material requirements, b) creating suggestion (Critical, expedite, delay items), c) firming suggestion (Purchasing order, various reports). Planners need to think about the dimension of Inventory, priorities and capacity before doing material planning. Recognition of business and technical opportunity, solving the inventory problems consideration of motivational factors of MRP is also important [7].

The problem of lot sizing is one of satisfying the requirements while trying to minimize holding and setup costs. A variety of lot sizing rules has been proposed. The vital aspect of inventory planning is to find out and maintain the optimum level of inventory in an enterprise. The ideal inventory level is a material's Economic Order Quantity (EOQ) [6]. EOQ is a mathematical formula designed to minimize the combination of annual holding costs and ordering costs. EOQ is amount when an order has placed to consider. It can be determined by, EOQ = average monthly consumption X Lead Time (in months) + safety Stock - Stock in Hand. Here, Lead-time is the time between placing order and receipt of material. Ideally, lead-time should be between 2-6 weeks. Next, Planners need to determine Safety Stock (SS). This is the amount that one should have remaining when the EOQ arrives. Safety stock is the average bare minimum that will have at any given time and EOQ+SS are the average maximum amount that will have at any given point in time. This should be intuitive because safety is what we have when our shipment arrives and when the order arrives (EOQ) it gets added to the safety stock. A sound, mathematical approach to safety stock will not only justify the required inventory levels to business leaders, but also balance the conflicting goals of maximizing customer services and minimizing inventory cost.

Safety Stock = {Z*SQRT (Avg. Lead Time*Standard Deviation of Demand^2 + Avg. Demand^2*Standard Deviation of Lead Time^2}, Z= Z score [3]

The best way to deal with variable supply is to have high level of communication with the vendor and not to count on safety stock. At the end of each day, the MRP (Material requirement planning) system will run to identify items as critical, expedite, or delay. The MRP system will suggest if we need to order more of a certain material by classifying into the three categories. There are different methods to do plan material [1] such as ABC (Always Better Control) based on cost criteria, VET (Vital, Essential, Desirable) based on critical and shortage cost of an item, SDE (Scarce, Difficult, Essentially available) based on availability, FSN (Fast, Slow, Nonmoving) based on utilization, HML (Highest, Medium, Low) based on cost. Material Planner should think about latest technology, opportunity cost, repair facility within shortage downtime, post warranty and repair, proper installation and procedures, reputation of manufacturer and available spare parts and outside agency, environmental effects. Inventory management is important to keep material at optimum level and reduce the losses against deterioration, obsolescence and wastage, minimize inventory-ordering costs. Efficient inventory management process involves controlling the level of units in stock in order to prevent the inventory from becoming too high and a good inventory management controls the costs associated with the inventory, both from the perspective of the total value of the goods included and the tax burden generated by the cumulative value of the inventory [7, 8]. One need normally set a time framework of 12 months for implementing MRP. In case of Material

Planning, Cost is specified in terms of % of total effort and represents labor (i.e., in person – months). Nevertheless, Cost associated with capital acquisition (hardware or software) is not included.

As a material planner, one should consider shareholders expectation such as sustainable growth, sustainable dividend growth, accurate forecasts, good governance & reputations, clear strategic directions, regulatory and legal compliances. She / he needs to consider Confidence in Board and Management, Government and regulatory body's expectation such as public safety, innovation and economic growth, industry leadership, workplace safety, infrastructure investment, reduce emission, good regulatory outcomes. Material plan is vital for safety and reliability, reasonable price, timely response, to complaints and queries, innovative solution. Shareholder's expectation is normally sustainable growth, sustainable dividend growth, accurate forecasts, good governance & reputations, clear strategic directions, regulatory and legal compliances [10]. Confidence in Board and Management and Government and regulatory body's expectation is public safety, innovation and economic growth, industry leadership, workplace safety, infrastructure investment; reduce emission, good regulatory outcomes. Material Planner should consider that Material would not unduly stress under normal operating conditions such that full-required demand can met.

CASE STUDY – TITAS GAS TRANSMISSION AND DISTRIBUTION COMPANY LIMITED (TGTDCL)

MATERIAL PROCUREMNT PLANNING AND PROCEDURE AT TGTDCL:

TGTDCL is a Government Company, so strategic national plan needs to consider for developing a material plan. Government circular and PPR, orders, statutory instruments, guidance and advice needs to follow when one considers material plan. The flow diagram-1 shows the material planning of TGTDCL performed by Material Engineering and Control Department (MECD). This is a traditional, classic and well-defined system, but it is not a dynamic system, that can apply to the modern world. MECD does not enjoy the independency according to the current system. Titas Board and approval authority (Managing Director) can get troubles according to this system. MECD send MR (material requisition) and note sheet to the Finance Department for budget clearance after completing every procedure and taking expertise advice and approval from Managing Director. Sometimes, Finance Department raises voice about technical matters; such that type and number of materials etcetera instead of financial matters that can delay the material purchase. As a result, sometimes MECD needs to change preplan material that affects the customer services and user departments' requirements and company's goodwill. In addition, MECD needs to take information user department. Some of the concerned official does not know the material specification and installation date of equipments upon his/her tenure / jurisdiction due to installation of material and equipment did long time ago and previous persons didn't keep all reports proper way. Moreover, some officials do not know how to write requisition of material specification due to lack of training. In that case, MECD can get wrong idea or information. MECD personnel need to be intuitive with proper training, planning, maintenance, procurement, operational, cost administrative experience.

Two envelops single systems of international tendering method is used to purchase material and equipment according to CPTU and Public Procurement Rule (PPR)-2008. One envelop of tender documents examine technical matters of tender, if Technical evaluation subcommittee takes responsive action then open the tender for economic matters. Purchaser, pursuant to Rule 94 of the Public Procurement Rules, 2008 shall make Tender Documents available immediately to the potential Bidders, requesting and willing to purchase at the corresponding price if the advertisement has published in the newspaper pursuant to Rule 90 of the Public Procurement Rules, 2008. Nevertheless, MECD emerges some traditional and cultural factors instead of PPR.

Flow diagram-1

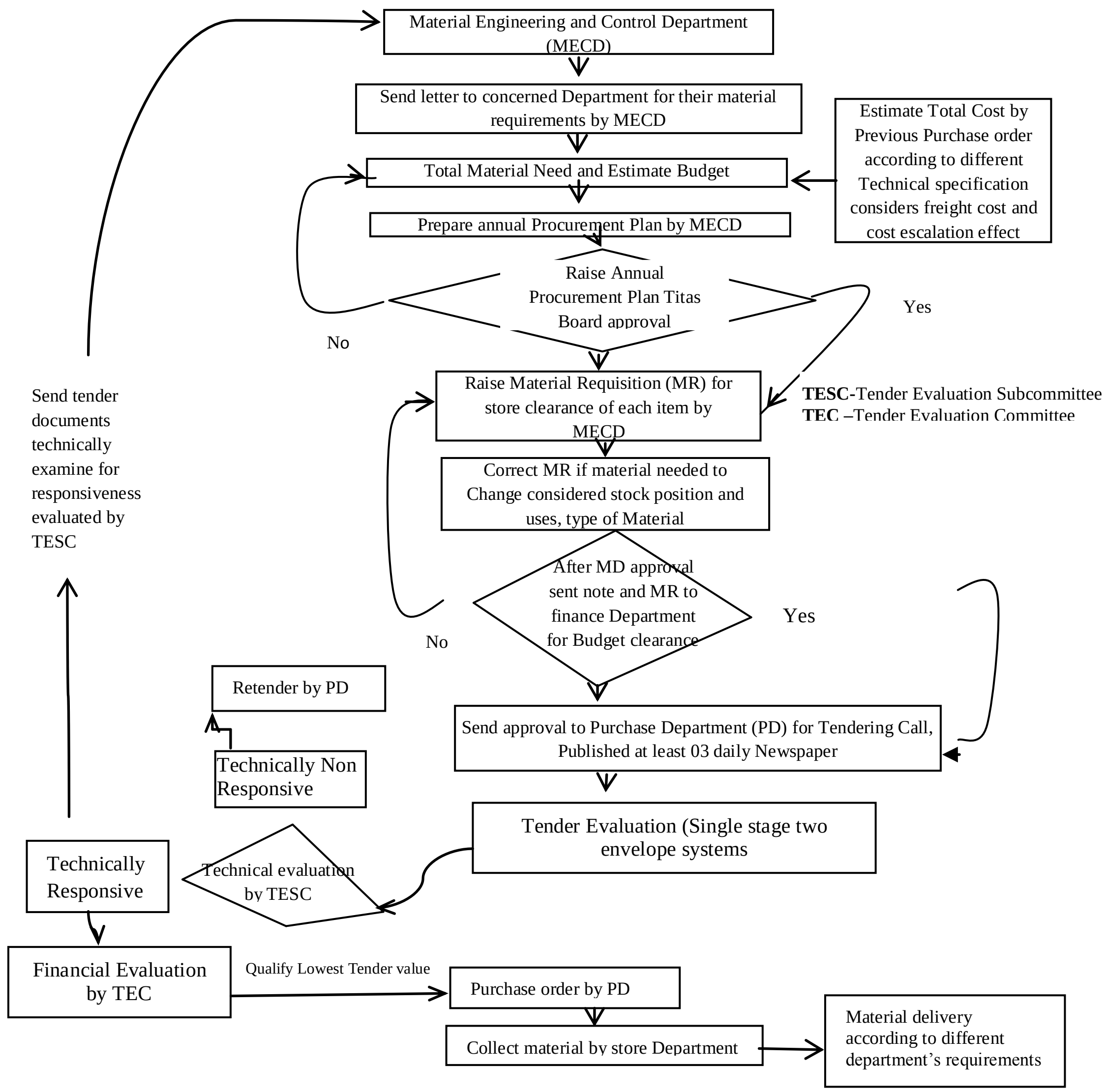

PROCEDURE AND COSTING OF MATERIAL AT TGTDCL

As a Service and Government public Limited company TGTDCL, customer service must focus on considering benefits verses costs of each decision. Like all other oil gas company in the world, TGTDCL almost all significant and important operations are planned. Thus, the whole procedure needs to fine-tune in to a high performance moneymaking machine. In that case, if the company acts best interest to optimize its profit can jeopardize customer service and satisfaction. There are two sections of MECD such as MEES (Material Engineering and Evaluation Section) and MPCS (Material Planning and Control Section). MEES of MECD prepares Technical specification of different material and equipment's. This is a vital task for material Planning and Costing. Technical specification (TS) determines material quality and availability, supplier availability and costing, transparent and fair neutral competition among suppliers. Concerned Committee approves TS. MEES arranges meeting for evaluation of international tender technical matters by TESC (Tender Evaluation Sub-Committee) for technically responsive. Those submitted tenders qualify technically responsive are evaluated financially by TEC (Tender Evaluation Committee) only. TEC should advise to give purchase order to the lowest bidder (+- 5% of estimated price according to PPR-2006) and this procedure is done by Purchase Department. Relations of different departments at TGTDCL regarding material requirements plan and purchase are following Fig-1:

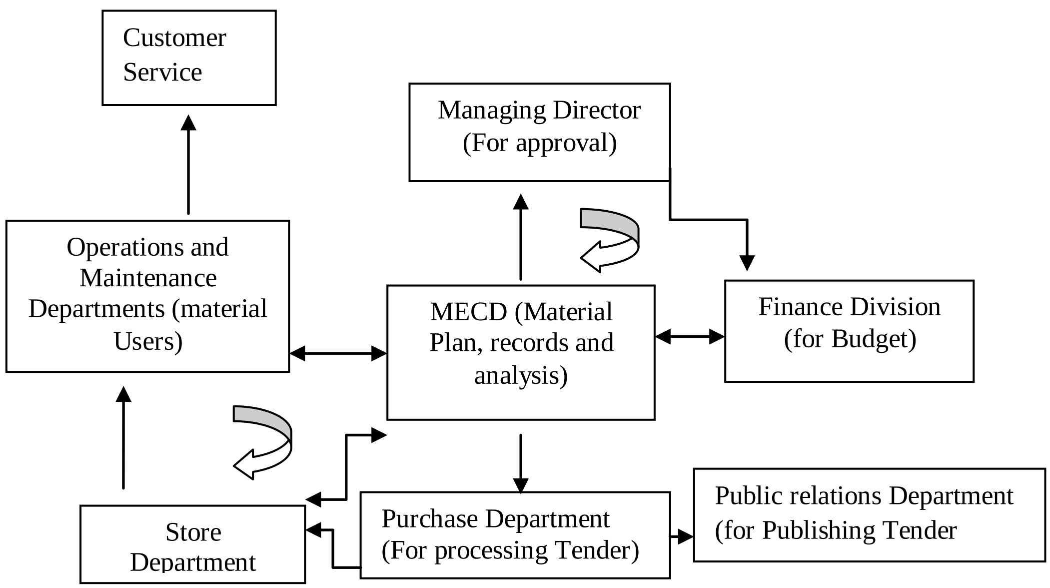

Fig-1: Departmental relations regarding material Plan and Purchase, TGTDCL

On the other hand, MPCS takes action material and cost estimation according to concerned Technical specification. They normally estimate unit cost considering the previous purchase order. Here, intuitive decision, information and practical experience of MPCS personnel play vital role. EOQ (economic order quantity), previous use, present stock and user department advice normally considers before to prepare material requirements plan. MEES makes technical specification by taking advice from concerned committee according to different required British, American and Canadian standard. MPCS needs to prepare annual procurement plan after collecting data from relevant department. They also prepare material requisition (MR), material transport Order/ voucher (MTO/MTV) and they take action budget clearance from finance department. They need to estimate unit price and budget considering previous purchase order. MPCS considers reconciliation cost, freight and delay of materials also. They normally use excel sheet to estimate instead of commercial software. They face challenges to estimate price of materials especially if they do not have previous purchase order of that materials. MPCS should follow strict rules and regulations (Public procurements rules, PPR-2008, act 2006) because of TGTDCL as a Government Company. Coordination with store department and store accounts section is vital to take decision how many items need to buy. Here, MPCS faces bureaucratic barrier. They have restriction to communicate any suppliers in tradition. Although, there are no problems to communicate perspective's supplier according to PPR keeping transparency and impartiality. As a third world country, TGTDCL face human, political and cultural restrictions. Sometimes, Material planners lose their motivational factors. In addition, they face questions difficulty under or over price estimation. The rest of the procedure regarding procurement such as Tendering and publish tender to daily newspaper, purchase contract, procurement method, monitor order status, reception of material, reconciliation are done by Purchase Department (PD).

PROBLEMS BACKGROUND OF MATERIAL PLANNING AT TGTDCL

Titas gas deals with complex gas distribution services, it has active valve and metering station involves meeting stringent safety regulations and follow other government requirements related to existing and new gas distribution networks. TGTDCL also needs integration with decision supports systems, business functions such as design, engineering, gas line construction and networks analysis etc. This paper discuss about the foreign purchase of TGTDCL material to support the whole systems operations. The drawback of TGTDCL material planning is repressive interdependency and time consuming of financing systems. In addition, there is restriction to communicate tenderers and manufacturer from MECD keeping secrecy. MECD sometimes does not get budget timely, as per demanding of regulator-meter, materials continue to increase. Most of the cases, finance arises question about number of proposed items to be purchased and audit matters. As a consequence, This affects general customer services. Finance division should consider that Innovation and competition resulted in greater efficiency of the performance of financial function. Sometimes, user department cannot be able to supply specific material/instruments. Therefore, Operation and Engineering services department do not be able to install accurate sizes of meter, regulator and other materials due to lack of available proper sizes of materials. In that case, they install alternative instruments in to the existing operating systems that affect the measuring systems and eventually TGTDCL loses money. Titas engineering services departments need to install higher capacity meter and regulator which increase installation and investment cost due to lack of proper material. It also affects planning of these items. Means, some of the material can lose out within short time and some may increase to block or pile up the store and inventory. Total setup material and spare parts also can hinge customer services and measurement systems. In addition, some of the material needs special technical specification and updated technology. In that case, Store personnel needs training to adapt themselves in the technical matters those who do not have relevant experience. According to Store accounts/Accounts department, about TK 19.33 crore, number of 10849 items did not use from the last five years from 2005 to 2013 (Dead Stock Committee interim report, TGTDCL) equivalent materials or these are slow/dead items. However, Committee decided that about Tk. 5.56 crore (about 685 number items) equivalent items has had definitely usable conditions and Tk. 3.32 crore (376 number items) have had usable conditions, but they need to justify whether it can be used present operating conditions. Rest of the TK 10.18 crore 9788 number items are obsolete, cannot be used under present operating conditions due to technological change, quality, future requirements. The most of the 9788 items (Automobile items) purchased long time ago (during 1970-1990 years). Here, as a downstream gas company, material manager often purchase products months ahead through forward contracts. Material manager considers price risk supplying material by a short notice. Dead material can be the cause of technological change, ignorance of management or ignorance of user department. However, that does not mean TGTDCL will not purchase regular items for proper operations of existing systems and serve customer services. After formation of MECD in 2009, they try to establish updated technique avoid unnecessary financial burden.

Table-1

Procurement Plan	Approved Plan (Lac Taka)		Actual Execution (Lac Taka)		% of Execution		Note
	Local	Foreign	Local	Foreign	Local	Foreign	
FY 2011-12	990.02	3732.09	410.09	2526.62	41.42	67.69	
FY 2012-13	2313.28	3770.88	1195.17	1215.48	51.66	32.23	
FY 2013-14	5229.43	4328.80	4317.73	1097.96	82.56	25.36	
FY 2014-15	6698.22	3849.40	5968.81	2359.87	89.11	61.30	
FY 2015-16	14165.29	13281.32					

Sources: MECD, TGTDCL

Table-2

Procurement Plan	Approved Plan (Lac Taka)		Actual Execution (Lac Taka)		% of Execution		Note
	Local	Foreign	Local	Foreign	Local	Foreign	
FY 2011-12	990.02	3732.09	410.09	3284.05			For carry over
FY 2012-13	2313.28	3770.88	1195.17	5496.60			For carry over
FY 2013-14	5229.43	4056.60	4317.73	975.67			
FY 2014-15	6698.22	3849.40	5968.81	919.67			
FY 2015-16	14165.29	13281.32		1409.35			

Source store accounts, Department of Accounts, TGTDCL

The table-1 and 2 show that the actual percentage of execution of plan does not consider as satisfactory level. Sources of the two section's data also show the coordination level is poor. After completing the material procurement procedure from MECD, tables shows clearly that, material does not reach proper time into the store department (within FY). Therefore, Management procedure is not effective to purchase foreign plan-material just in time. This troubles may relate to tendering, suppliers, evaluation, political or management. TGTDCL needs to address this matter. According to Manager (MPCS), MECD information, the approval of financial budget sometimes takes time and they cannot execute plan within financial year July to June. In addition, Material planner does not keep independency; financial persons sometimes arise questions irrespective of material plan and out of their professional jurisdiction. Here, user department sometimes send incomplete information regarding material requirements and description. MECD draws procurement plan manually based on the user information and based on their judgment. On the other hand, purchase department faces problems of tendering time and execution, supplier scarcity. Some of the tender can be non-responsive due to technically and financially nonresponsive according to PPR-2008 [9] and Tender committee decisions. Some of the Supplier cannot deliver product within time after getting purchase order. For instance, after 03 years gas connection binding open in 2013, the demand of residential gas customer was pile up. As a result, Supplier (BMTF, BSCIC) of residential gas instruments and materials such as regulator, lock wing cock, elbow and nipple was their beyond capacity. Finally, general stakeholder and shareholders did not get benefit due to material shortage affects ultimately customer services.

Total authorized capital of TGTDCL 2000.00 crore, Paid up capital 989.22 crore (as 30 June, 2014), annual gas sales revenue 7695.50 crore, fixed asset 1057.18 crore, administrative cost 370.38 crore, cost payment to national exchequer 615.41crore [sources 2013-14 annual report of TGTDCL]. TGTDCL performed execution of material procurement only 0.704% of gas sales revenue, 2.7% of authorized capital, 5.47% of Paid-up capital and 8.8% of government payment to national exchequer (2013-2014 FY annual report and sources MECD, TGTDCL) annually. Material Procurement planning can consider moderate, but execution level is poor. Management should consider the execution of material plan and no more delay of irrespective question arise from concerned department fulfilling proper customer services and respective shareholder wishes. As a material manager, one should consider initial capital cost of construction, safety and reliability, efficiency of operation, operating and maintenance cost, availability of spare parts, frequency extent and type of servicing, and environmental condition before purchase a material [8]. Here, some of the foreign materials spare parts conformity can secure significant money of TGTDCL.

PROPOSED MODEL FOR MATERIAL PLAN OF TGTDCL

Proper planning of material and its execution can save Titas Gas money as well as fulfill customer satisfaction. According to MECD material planning and Control Section (MPCS) of current situation, it is very difficult to execute Procurement Plan. TGTDCL needs to execute material plan professional way. Considering material in hand, prior given purchase order and uses, MPCS normally prepare material procurement plan according to the different department requirements. MPCS considers the practical situation and engineering point of view as well as financial matters what material needed to operate Titas Gas smoothly. Practical situation regarding material purchasing is crucial in Bangladeshi Government Company like TGTDCL. Here, Material planner should be initiative, intuitive and professional and handle different departments with care. The irrespective quarry from concerned department ultimately kills time and MECD cannot purchase proper material within the financial year. Therefore, it can be improved by the following proposed systems:

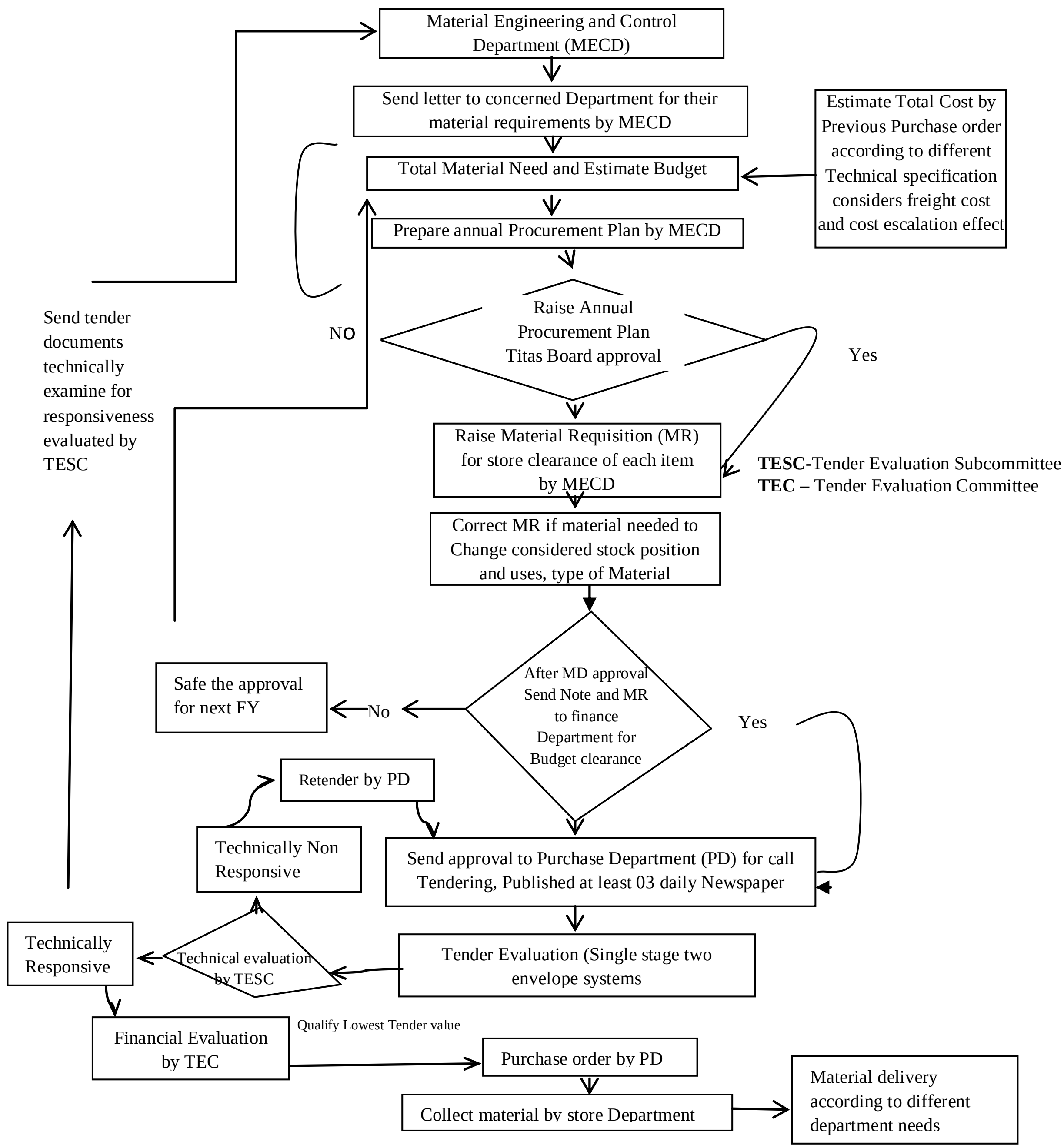

DISCUSSION OF PROBLEMS FINDING DIFFERENT SOLUTIONS AT TGTDCL:

The questions normally arise about purchase and inventory management systems about what proportion are in house production, local purchase and foreign purchase, financial/budget systems, handling communications between suppliers and company, type of technology adapted, ensuring supplier effectiveness in cost, timeliness and quality. TGTDCL runs a monopoly business at gas distribution sector due to government in nature. However, they should not forget regarding efficiency equivalent to international gas company and general public services. Most of the cases about the foreign purchasing at TGTDCL take long time due to bureaucratic and financial decision. Management should consider cost effective, trouble free, easy handling and high return on investment matters. Here, excellence, high quality network, effective maintenance plan, safe & reliable service, fit for purpose of network design, clear role and responsibilities, Technical training and development and last understanding market and customer service level are essential for a material planner. The material plan can do the best way based on previous consumption. Random decision about material purchasing of TGTDCL cannot satisfy customer, shareholder, employee and vision of a large company like TGTDCL. TGTDCL needs central repository interdepartmental and intercompany decision support system leaded by MECD. This central system can perform long range planning and forecasting by complying with the repair and maintenance staff, regulatory and safety requirements.

The inventory status records contain the status of all items in inventory, including on hand Inventory and schedule receipts. These records must keep up to date, with each receipt, disbursement, or withdrawal documents to maintain record integrity. Here, Problem of TGTDCL material planning are information gap and coordination, Store department contains records of inventory, and sometimes it differs with the material engineering & control department and purchase department after using user departments. It is a management control issues. Titas authority should address it with proper job staffing, guidelines, and training. It is a government & management policy to overlap role with three departments like purchase, store and MECD. Therefore, Communication and coordination are vital. Titas needs to enable the international standard, streamlined inventory and seamless dataflow conditions across the enterprise. The basic facts of finance are the time value of money, opportunity cost, cost of capital, expected return and risk, valuing the financial securities should consider before rejecting any budget of proposed material requisition from the finance section.

MECD of TGTDCL is responsible to monitor material demand and supply condition, communicate market and performance of materials. There are some unavoidable problems of management communication and hierarchy systems according to Bangladeshi culture. It is very difficult to break the systems. TGTDCL needs to accustom abide by Bangladeshi culture. To honor the culture, they need to develop systems for general public services. TGTDCL uses traditional method for purchasing instead of improving performance of entire supply chain of materials. However, the choice focuses on economic decision hinging provide maximum benefit at minimum cost. Hence, TGTDCL is a public limited government company; Management should consider public service as well as public safety. Enterprise Resource Planning (ERP) systems are extensions of material resources planning (MRP) systems that run on a single database in a client server environment. SAP (Systems, Applications and Products) in Data processing is currently the leading provider of ERP systems. Management can consider purchasing of modern supply chain management software like Enterprise resource planning, ERP (example, SAP) software. TGTDCL has significant meritorious Manpower. TGTDCL needs to develop labor by giving them robust training before purchasing this type of expensive software.

The developments of material planning should include the focus of demanding better and faster customer service; know globalization of the oil and gas business; inner company competition; and the availability of information technology to facilitate information exchange with Parents Company. Company's integration and cohesiveness will reduce costs if it leads to a more efficient system. Here, strong political and regulatory body's commitment and management people selection is a vital role to execute dynamic material management systems. Vertical integration of Parents Company can reduce cost and better customer service. TGTDCL communicate to Parents Company normally when problem arises. However, it is not effective. TGTDCL should develop communication systems with sister concern Company like PGCL, BGDCL, KGDCL, JGDCL, SGCL and BAPEX.

RECOMMENDATION AND CONCLUSION

Smooth cooperation's is vital for the Purchase, Store and Material Engineering and Control Department for proper asset data management and compliance. Change of management procedure regarding material planning at TGTDCL needs to emphasize improved material unit-coding system. This study shows that TGTDCL should reduce the bureaucratic barrier and improve professional conduct within the departmental jurisdiction. This paper demonstrates that that Service innovation is not given due importance at the TGTDCL. The reasons for not emphasizing services innovation needs further study. Transparency and accountability can play a vital role in improving management and expenditure of TGTDCL's gas distribution network. This study shows that that TGTDCL has lack of relevant trained people and deficiency regarding proper staff selection of work force on material planning control systems. Finally, TGTDCL can purchase Material Resource Management Software, ERP (SAP) with user module environment by giving robust and proper training and selecting of TGTDCL Personnel.

ACKNOWLEDGEMENT

I would like to thank TGTDCL authority to give me financial support and permission to publish this paper. I would like to thank Engr. Md. Najibul Haque, Manager-MPCS and Engr. Md abu Kaiser and Engr. Sumed Moni Chakma, Department of Material Engineering and Control, Engr. Md. Alauddin, Manager, T&QC (Member-Dead Stock Committee), Mechanical Engineering Department, Engr. Md. Anisul Haque, Manager-Operations Department (Member-Dead Stock Committee), TGTDCL who gave me valuable information. I convey plenty of thanks to Mr. Maksudul Haque, Manager-Store accounts (Member-Dead Stock Committee), Department of Accounting, TGTDCL giving me significant information.

REFERENCES

1) Dr.I.Selvaraj, 'Material management', I.R.M.S Sr. D.M.O (Selection Grade officer) (on study leave), Indian railways medical service.
2) A. K. M. Solayman Hoque1, S.K. Biswas and M. A.Wazed (2015) 'Relationship between inventory management and industries becoming sick, especially in third world countries', Journal of Mechanical Engineering, Mechanical Engineering Division, The Institution of Engineers, Bangladesh Vol. ME 45, No. 1, June 2015, Page 7-13.
3) Annual Report 2013-14, Titas Gas Transmission and Distribution Company Limited, Dhaka , www.titasgas.org.bd
4) Christopher M. Chima (2007), Supply- 'Chain Management Issues In the Oil and Gas Industry Journal of Business & Economics Research' – June 2007, Volume 5, Number 6, California State University, Dominguez Hills.
5) Professor Guillermo Gallego, 'Material Requirements Planning (MRP)', IEOR 4000: Production Management.
6) Volman, T, E, Berry, W.L., and Whybark, D.C. (1992), 'Manufacturing Planning and Control Systems', Third Edition, IRWIN, Burr Ridge, IL.

7) Dr Vassilis Moustakis (2000), 'Material requirements planning, Innoregio: Dissemination of innovation and knowledge management Technique', Associate Professor, Department production and management engineering, Technical University of Crete, January 2000.

8) Technical standards and specification manual for gas distribution systems- safety, design, construction, operation and maintenance of natural gas distribution systems, Alberta, sixth edition November 2010, government of Alberta.

9) Public Procurements Rules-2008, Public procurement act-2006, Bangladesh.

10) Gas Distribution Asset Management Plan, 2015-2025, Vector, Newzealand.

11) Planning practice guidance of onshore Oil and Gas, Department for communities and local government, July-2013, UK.

12) Ken Brown , Peter Moles, Kathryn Vagneur , Craig Robinson (2011) 'Finance for the Oil and Gas Industry', Heriot-Watt University, FO-A1-engb 1/2011 (1046).

13) AT Kearney (2002), 'Materials Management, A gold mine for upstream oil & gas', LLC Korea , Email insight@atkearney.com

International Conference on Petroleum Engineering 2016 (ICPE-2016)
Bangladesh University of Engineering & Technology (BUET)
Dhaka-1000, Bangladesh

ICPE (2016-004)

Development of a Gas Production Database for Gas Fields in Bangladesh

Md Ruhul Amin Foisal[1], Mohammad Mojammel Huque[1], Mahbuba Yeasmin[2], Md. Jahangir Kabir[3]

[1]Department of Petroleum and Mineral Resources Engineering, Bangladesh University of Engineering and Technology, Dhaka-1000, Bangladesh

[2]Department of Computer Science and Telecommunication Engineering, Noakhali Science and Technology University, Noakhali-3802, Bangladesh

[3]Data Management Division, Petrobangla, Dhaka-1000, Bangladesh

ABSTRACT

Database plays an important role for managing data with speed and accuracy in information technology. The aim of this project is to design a Gas Production Database to keep the gas production record of Bangladesh in an easy access form for authorized personnel only. This Database is designed to help minimize data entry errors and to make it easier to generate reports and visual presentation based on different requirement. Petrobangla is an organization for exploration and production of Natural Gas of Bangladesh but they do not have any database system. Currently the Data Management Division uses Microsoft Excel to store and keep track of the natural gas production of Bangladesh which is not a suitable application to store and retrieve large volume of data. To devolve a database system, "Microsoft Access 2013" application has been used. Microsoft Access 2013 is much easier to operate and develop a database system then other available data management applications. Initially tables are created to store daily production data, gas field, well and historical information. Relationship between tables has been designed based on the table and their data type and based on query. Query has been designed based on outcome requirement to generate reports and graphs. Finally, forms have been designed as a graphical user interface (GUI). Using this form, the user will interact with the database system. Reports are the outcome of this database system. This database can generate gas production report on daily, monthly, yearly basis or for a specific time period. Historical work over record according to well, chemical composition according to gas field can be generated. Graphical presentation of production history such as flowing well head pressure (FWHP) vs. time, Cumulative Production (Gp) vs. time, condensate production vs. time, water production vs. time for a time period or entire time period are also the outcome of this database system.

Keywords: Gas Production Database, RDBMS, Report, Data Management.

* Corresponding Author address
Email: ruhul.foisal@gmail.com

INTRODUCTION

In these days of information flows, the success of an organization depends on its ability to acquire strict and real-time data about its operations, to manage this data effectively, and to use it to analyze and guide its activities [8]. Thus, effective database design is becoming a successful element of strategy to support or make the projects and organizations run smoothly, especially for the oil gas industry [2]. As most petroleum studies are dependent on the analyses of discovery, development, production record, there are always extensive data needed for the researcher's study and development [6].

Presently it is an important issue to use the databases and database management systems to process large amount of gas production data for improving the data management division of petrobangla. As petrobangla has to handle a large amount of data they extremely need a data management system to improve work efficiency. The database contains records and tables for daily gas, condensate, water production and flowing well head pressure, well history, fields chemical composition, reserve according to field. The database is an essential tool for processing and analyzing this kind of massive amount of gas production data, which generated from the very beginning of the gas production up to present date and updated on daily basis [7].

The objective of this project is to design and implement a dynamic database system. The core of the system is a database which is used to store the gas production information of Bangladesh. The front-end of the system is a set of Graphical User Interface (GUI) applications which act as a bridge in between the end users and the system [3]. The main key points of this database are to reduce the number of errors in data entry, save time in adding, editing, and reporting gas production information, facilitate the ease sharing information between management, develop of well wise production record, well history record, well work over record with respect to time and improve of drilling record, work over record and field wise production record and gas field chemical composition record to analyze the wells data as it requires for the future study.

The production database should be able to store the gas production information, which normally includes the daily gas production data. The database will also support the following functions as shown in Table 1:

Table 1: Function of the database

Data input to the database	Possible outcome from the database

• Daily production of gas, condensate, water, FWHP according to well.
• New well if new one comes into production.
• New gas field if new gas field discovered.
• Well history.
• Chemical composition according to the gas field.
• Well work over record according to well.
• Reservoir pressure and Gp based on date.
• Gas field history document
	• Generation of production record on daily basis, monthly basis, yearly basis or for a specific time period or whole time period.
	• Historical work over record and drilling history according to well.
	• Chemical composition and its trend monitoring according to a gas field.
	• Analysis of production history such as
	    • FWHP vs. time,
	    • G_P vs. time,
	    • condensate production vs. time,
	    • water production vs. time

METHODOLOGY

Depending on different project or the scale of data, there are a plenty of processes for doing database design which will be carried out by the database designer. Most commonly used six stages in the design of database. Database design process steps are given following Table-2 [5].

Table 2: Database design process steps

Stage	Process
1. Requirement analysis	To document the data requirements of the users.
2. Conceptual design	To produce a conceptual schema of the database for achieving understanding of database structure, semantics, interrelationships and constraints.
3. Choosing a DBMS (Database Management Systems)	Establishing the best framework for implementing the produced schema.
4. Logical design (data model mapping)	To transform the generic, DBMS independent conceptual schema in the data model of the chosen DBMS.
5. Physical design	To choose the specific storage structures and access paths for the database files.
6. Implementation	To create the database, compile and execute DDL (Data Definition Language) statements.

a. Gas production database

The idea for the database came about due to the scale of the production data. Bangladesh has 26 gas fields and 21 of them are producing gas with about 102 wells [1]. The main focus is to keep all the production data on day basis in a single database so that production report and production graph can be generated any time needed. The database was designed using Microsoft Access 2013. This was chosen due to its relatively low cost, in comparison to more strong database-solutions, and the Access's ease of use. The database consists of fourteen tables for daily production record, well list, gas fields, companies, chemical composition, reserve, well history, well work over, user table, cumulative production and gas field documentation. The procedure of database design and implementation was illustrated by following Figure 1.

Relationship diagram is a way to represent data in a graphical form [4], in this case the Gas production database.

Figure 2 shows the relationship details of the database. Each relationship represented by a connecting line indicating with the sign “1” and “∞”. It represents the relationship status about how the tables are connected. The relationship explained in Table 3.

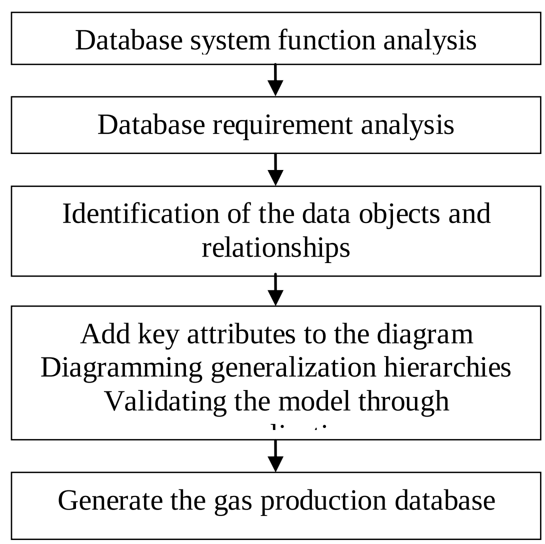

Figure 1: The procedure of the design and implementation of the database

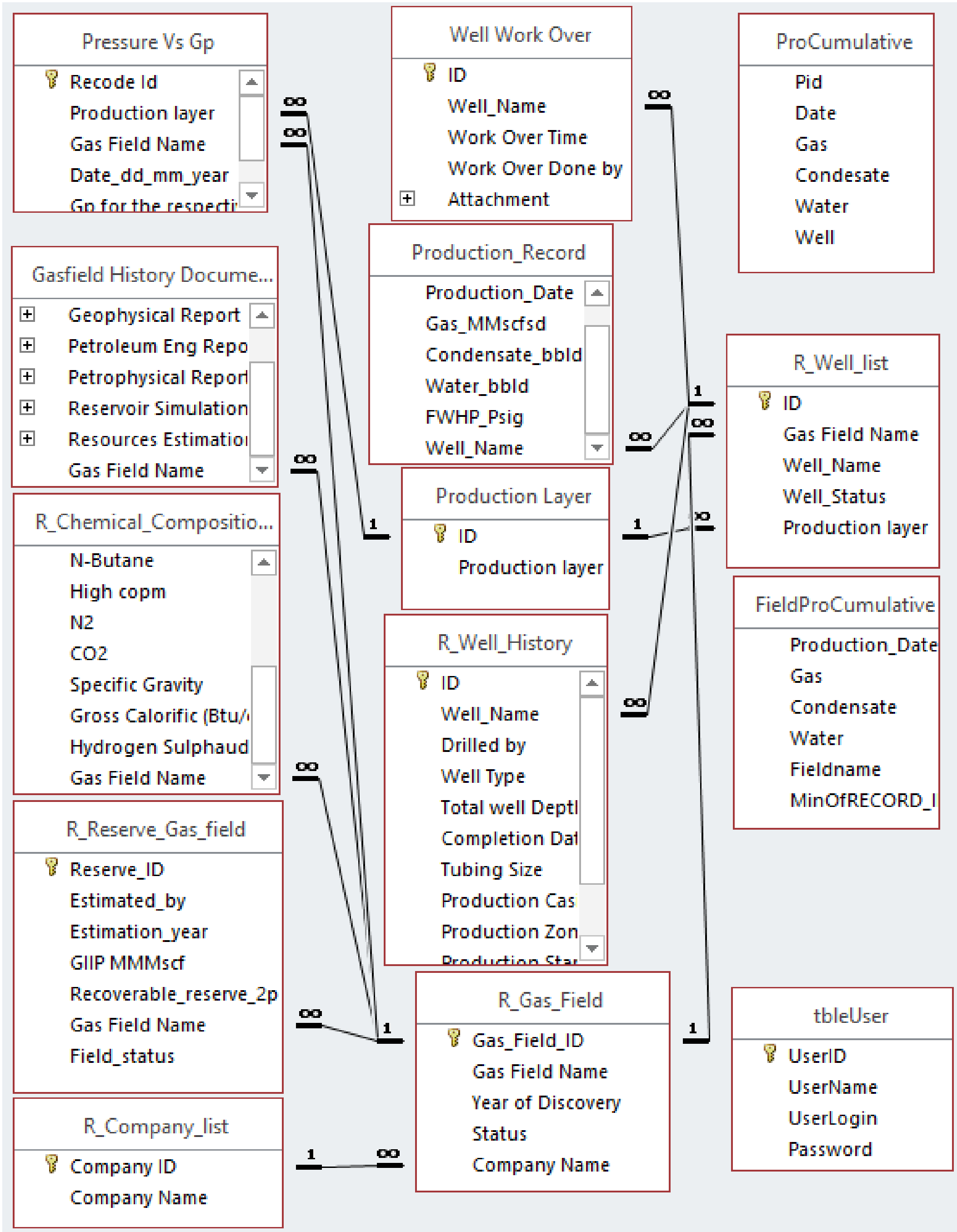

Figure 2: Simple relationship diagram of the gas production database

Table 3: Relationship explanation

Relationship	Express as	Explanation	Example
One to many	1 ---- ∞	Table “R_Cmpany_list” is connected to table “R_Gas_Field” using ‘one to many’ relationship.	Means there are many gas fields under one company from the company table
Many to One	∞-----1	Table “R_Reserve_Gas_field” Is connected to table “R_Gas_Field” using ‘many to one’ relationship.	Means there are Many reserve record can be estimated by different company for a gas field.
Many to many	∞---1---∞	Table “Gasfield History Documentation” and table “R_Chemical_Composition_Gasfield” are connected using many to many relationships through table “R_Gas_Field”.	Means there are many Historical document and many chemical composition data are linked to the respective gas field.

b. Query design

There are total 23 queries designed in this study to generate 18 data report and 24 graphical reports. All of the reports and graphs are completely dynamic and all of them will be generated based on dynamic criterion [5].

List of query criteria’s based on:

- Entire country production for specific date
- Entire country production for time period
- Specific well production for life time
- Specific well production for a time period
- Specific field production for life time
- Specific field production for a time period
- Cumulative production report for life time
- Chemical composition according to gas field
- Reserve according to gas field
- Well history well basis
- Well work over according to well
- Reservoir pressure vs. cumulative production graph for gas field
- Gas field documents

RESULT ANALYSIS

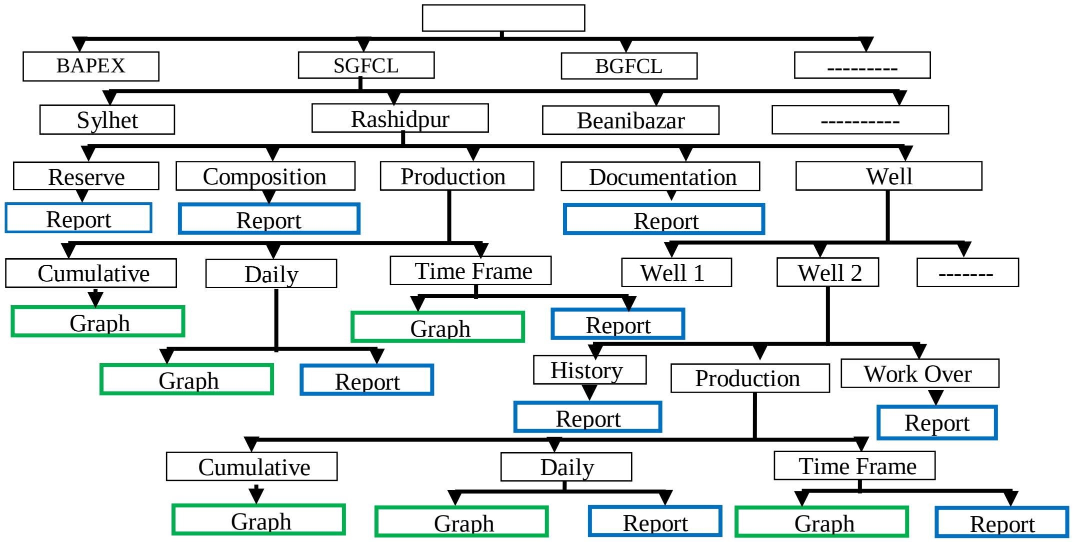

Figure 3: Production database tree

The overall improvements made by the database system will be analyzed of all the function that user wishes to have in the system is described. Figure 3 show the structure of report and graph generation using the database. After the data is fed to the system, the system will process data to generate output. The system processes the data that is fed into the system. The system will produce different kinds of reports as the outputs.

Example of a Specific field production report generation

This form is to generate report or graph based on a specific field. Here is a drop down list to select the required well. Figure 4 shows the 'specific field production' form. This form has two segments, one for report generation and the other one for graph generation. Using this form production report, report summary and summary well basis can be generated for a specific gas field for its entire life production.

Figure 4: Specific field production report generation form

Specific Field production Report

Production Report of **Rashidpur**

Production Date	Gas MMscfsd	Condensate bbld	Water bbld	FWHP Psig	Well Name	GasField Name	Company Name
9/1/1993	16.696	1.441	1.08	1573	RP 1	Rashidpur	SGFCL
9/2/1993	16.697	1.441	1.08	1573	RP 1	Rashidpur	SGFCL
.	.	.	.	.	.	.	.
.	.	.	.	.	.	.	.
9/27/1993	16.722	1.441	1.08	1573	RP 1	Rashidpur	SGFCL
9/28/1993	16.723	1.441	1.08	1573	RP 1	Rashidpur	SGFCL

This Report is Generated on Monday, November 21, 2016 Page 1 of 974

Figure 5: Field production report page template

Specific Field production Report

Production Report Summary of **Rashidpur**

	Gas MMscfs	Condensate bbl	Water bbl
Total	436475.6806	604456.94	570639.62

This Report is Generated on Monday, November 21, 2016 Page 1 of 1

Figure 6: Field production report summary for entire life

Figure 5 shows a segment of the production report a Rashidpur gas field. This report shows the daily basis production details of gas, condensate and water production on the basis of date. Figure 6 shows the total production of Rashidpur gas field for its entire life. This report contains the total production of gas, condensate and water for the specified gas field.

Figure 7 shows the production report summary of the specified gas field in the basis of per well production. This report shows there are seven well in the Rashidpur gas field and it shows the per well production summary of gas, condensate and water production over the life time.

Specific Field production Report

Production Report of **Rashidpur**

Well Name	Gas MMscfsd	Condensate bbld	Water bbld
RP 1	101170.098	122726.55	99763.73
RP 2	82374.811	113004.76	62671.24
RP 3	91409.553	129433.91	113048.43
RP 4	87417.3035	124131.46	91215.14
RP 5	25355.646	41431.14	59708.53
RP 6	8801.8143	14265.47	30398.28
RP 7	39946.4548	59463.65	113834.27
Total	436475.6806 MMscf	604456.94 bbl	570639.62 bbl
	436.4756806 Bcf	604.45694 MSTB	570.63962 MSTB

Figure 7: Field production report summary based on well for entire life

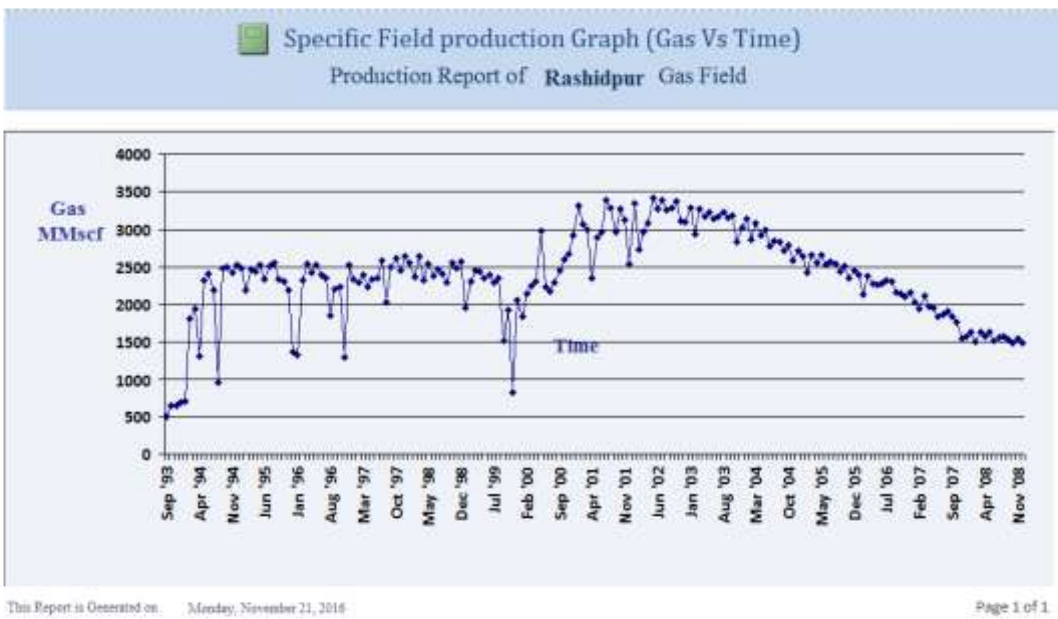

Figure 8: Field production graph (gas vs. time)

Figure 8, 9 and 10 shows the production graph of Rashidpur gas field for its entire life of gas vs. time, condensate vs. time and water vs. time respectively. Figure 8 and 9 shows the decrease in production of gas and condensate respectively over the time frame.

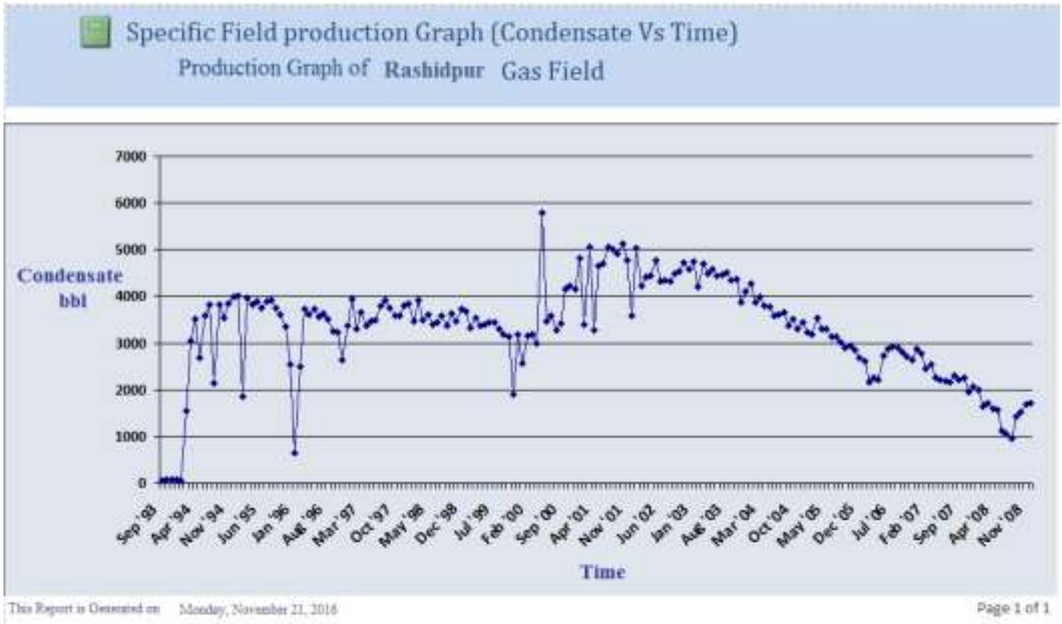

Figure 9: Field production graph (condensate vs. time)

Figure 10**:** Field production graph (water vs. time)

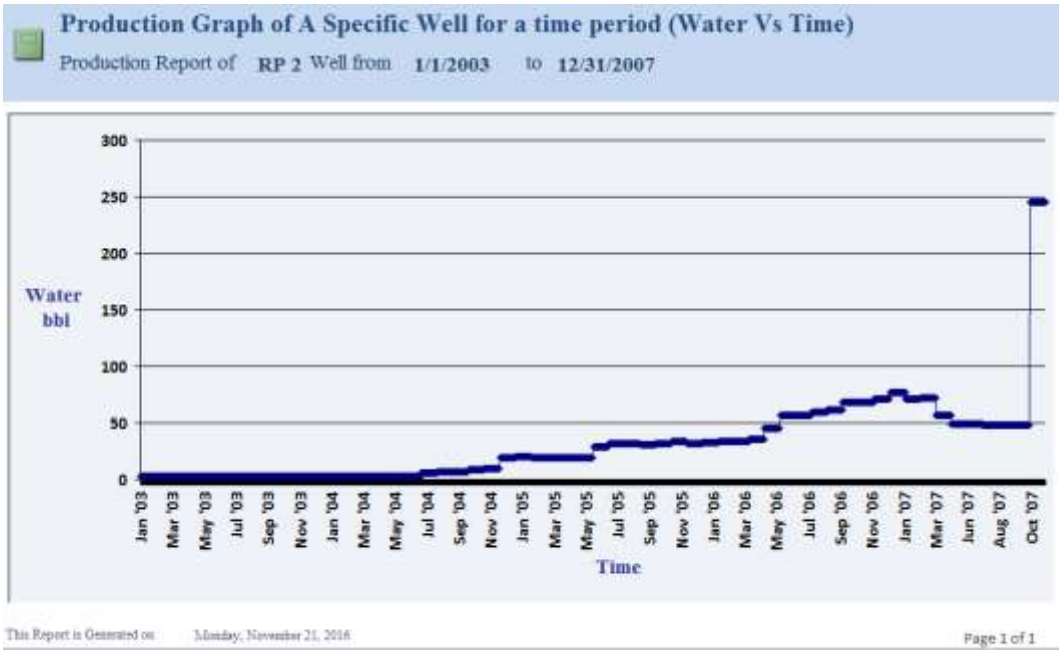

Figure 11: Water production of RP2 well of Rashidpur gas field from 1/1/2003 to 12/31/2007.

Figure 10 shows the rapid increase of water production after 2004 of Rashidpur gas field and a sharp decrease after 2007. And Figure 11 explain the reason behind the increase and decrease of water production. It shows the water production trend for the RP2 well from Rashidpur gas field. At the end of the 2007 this well shut down due to its excess water production. And because of it the total water production of the field dropped instantly which is found in figure 10.

This database will be a strong analyzing tool for analysis of production data. It will save time and help the personal to take the correct decision at required moment.

CONCLUSION

The purpose of this project was to design a simple user friendly natural gas production database for data management division of petrobangla to manage production record and keeping with a frame work and retrieve the stored information with required criteria. The database system has made it easier to manage daily natural gas production information. Entering and editing production information has been facilitated by a simple interface. Certain checkpoints in the data entry form have been set to verify contents before submission. This will help to reduce errors. Finally, the method to filter production data for creating reports has been made simpler. This project is appropriate for study reservoir engineering. The next step would be to employ Microsoft SharePoint to make this database accessible from anywhere through internet for authorized personal only.

NOMENCLATURE

BAPEX	= Bangladesh Petroleum Exploration and Production Company Limited.
bbld	= Barrels per day
BGFCL	= Bangladesh Gas Field Company Limited.
FWHP	= Flowing Well Head Pressure.
Gp	=Cummulative Gas Production

GUI = Graphical User Interface
MMscfd = Million standard cubic feet per day
MSTB = Thousand stock tank barrels
RDBMS = Relational Database Management System
RP = Rashidpur Gas Field
RP2 = Rashidpur well no 2
SGFL = *Sylhet Gas Fields Limited*

REFERENCES

1. Daily gas production report. 2016, Petrobangla. Available from: URL: http://petrobangla.org.bd/admin/attachment/webtable/255_upload_0.pdf.
2. Elmasri, R. and S. and Navathe, Fundamentals of Database Systems, ed. n. edition. 1994: Benjamin/Cummings.
3. Gray, J. and A. and Reuter, Transaction Processing: Concepts and Techniques. 1993: Morgan Kaufmann.
4. Joseph J. Adamski and and Kathy T. Finnegan, New Perspectives on Microsoft Access 2010. 2010, Grand valley state university, USA. : congagebain.com.
5. Joseph M. Hellerstein, et al., Adaptive Query Processing: Technology in Evolution, . Adaptive Query Processing, 1993. 23(2).
6. Korth, H. and A. and Silbershatz, Database System Concepts, ed. 2nd. 1991: McGraw Hill Inc.
7. Parthasarathy Ranganathan, Kourosh Gharachorloo, Sarita V. Adve, and Luiz Andre Barroso, Performance of Database Workloads on Shared-Memory Systems with Out-of-Order Processors. in Proceedings of the eighth international conference on Architectural support for programming languages and operating systems. 1998. Califonia, USA.
8. Ramakrishnan, R., Database Management Systems. 1998, Boston, Mass: WCB McGraw Hill.

International Conference on Petroleum Engineering 2016 (ICPE-2016)
Bangladesh University of Engineering & Technology (BUET)
Dhaka-1000, Bangladesh

ICPE (2016-012)

A Study on Friction Loss and Holdup Ratio in the Water Lubricated Pipeline Transportation of Heavy Oil

S. Rushd** *and* ***A. Rahman*
Department of Petroleum Engineering, Texas A&M University (Qatar), Doha, Qatar

ABSTRACT

Core Annular Flow (CAF) is an economically efficient and environmentally sustainable technology for transporting heavy oil and bitumen, especially compared with conventional methods, such as truck hauling, dilution and heating. In CAF, heavy oil forms the core of the flow and a water sheath encloses this core by forming a continuous layer on the pipe-wall. Power requirements are orders of magnitude lower than those associated with the flow of heavy oil alone. In fact, the CAF pressure loss is comparable to that for transporting only water. One of the major obstacles to the large scale implementation of this technology is the unavailability of a reliable model for the frictional pressure loss. In this work, a CFD based modeling methodology is validated and analyzed with respect to the measured values of pressure losses in a CAF pipeline. Another subject of interest in the field of CAF hydraulics is modeling the holdup, which simply refers to the *in situ* volume fraction. Most of the previous works did not focus on the underlying physics of the phenomenon. As a result, the available models do not take into account the process parameters like mass flow rate, viscosity and density. A new modeling approach is introduced in this work that addresses the actual physics of holdup. The current study helps to understand the hydrodynamics that govern friction losses in CAF pipelines.

Keywords: Core Annular Flow, Pressure loss, CFD model, Holdup, Pipeline transportation

INTRODUCTION

The reserves of non-conventional oils, mostly comprised of bitumen and heavy oil, represent one of the largest global petroleum resources (Nunez et al. 1998). The production of these dense and viscous oils demands extraordinary techniques that are not required to produce conventional petroleum deposits. The viscous oil is transported after extraction from a company's various production sites to its upgrading facilities. The non-conventional oil industry is keen to use pipeline transportation as it is a cost-effective technology (Nunez et al. 1998; Saniere et al. 2004).

* Corresponding Author address
Email: aziz.rahman@qatar.tamu.edu

Current research is on the water lubricated pipeline transportation of the non-conventional oils where an annular water-film separates the viscous oil-core from the pipe wall and, thereby, acts as a lubricant. This technique is sometimes referred to as Core Annular Flow (CAF). The most significant benefit of this flow system is that the annular water layer is found in the high shear region near pipe wall. As a result, the CAF involves much lower energy input (through the pumps) than if the viscous oil were transported alone at comparable process conditions (Arney et al. 1993; Rodriguez et al. 2009; Crivelaro et al. 2009).The ideal flow regime of CAF is presented schematically in Figure 1.

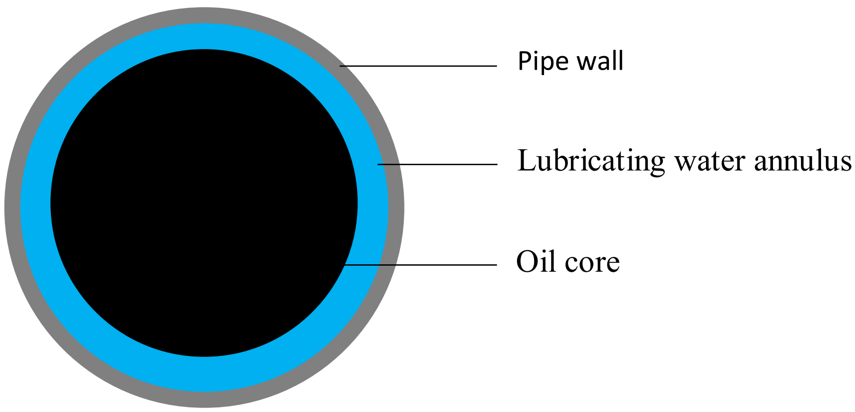

Fig 1: Hypothetical presentation of the flow regime involved in the ideal core annular flow

A technical challenge to the application of CAF is the unavailability of a reliable model to predict pressure loss on the basis of flow conditions. In this regard, a number of empirical, semi-mechanistic and numerical models have been proposed previously. Notable examples of such models include those of Arney et al. (1993), Ho and Li (1994), Rodriguez et al. (2009), Crivelaro et al. (2009) and Shi (2015). These can be classified as either single-fluid or two-fluid models (Rushd et al. 2012).

The single-fluid models typically take an empirical approach. The CAF hydrodynamics is modeled with respect to the transportation of an “equivalent” liquid (e.g., Arney et al. 1993, Rodriguez et al. 2009 and Shi 2015). These models are mostly system specific. Degree of uncertainty may vary appreciably when a model is applied for different flow systems (see, for example, Rodriguez et al. 2009). Compared to this kind of empirical models, the two-fluid models are more mechanistic. The governing equations for oil and water are solved here using computational fluid dynamics (CFD). The water annulus is usually assumed to be turbulent whereas the core (containing the viscous oil) is considered to be in laminar flow. Two examples of two-fluid models are Ho and Li (1994) and Crivelaro et al. (2009). Ho and Li (1994) suggested the shear in turbulent water annulus to be the primary source of pressure losses. The turbulence was modeled using Prandtl mixing-length model and the core-flow was considered to be laminar with constant velocity (i.e. plug flow). Extending this idea, Crivelaro et al. (2009) solved the governing equations numerically using a CFD code available in ANSYS CFX 10.0. They used the standard k-ε model for the turbulence in the water annulus. Their numerical simulations provided promising predictions of velocity profile, volume fraction and friction loss. Recently, Gupta et al. (2016) adopted a similar methodology to study the oil-water interface in a vertical CAF pipeline. Although encouraging, this modelling approach cannot be considered reliable until validated with actual measurements.

A significant input parameter for the CAF models is the "holdup" or *in situ* volume fraction. Oliemans (1986) and Arney et al. (1993) correlated the water holdup to the input water fraction. Rodriguez et al. (2009) correlated the oil holdup to the superficial velocities of the fluids. This is a convenient modeling approach; however, it does not address the actual physics of the phenomenon. The holdup in a CAF pipeline is likely to be dependent on the properties and the individual flow rates of water and oil. Although Rovinsky et al. (1997) demonstrated the dependency with a rigorous theoretical study, a realistic approach to model CAF holdup in a physically meaningful way is not available in open literature.

In the current work, the modelling approach proposed by Crivelaro et al. (2009) is validated using benchmark data of Arney et al. (1993). Its performance in predicting CAF friction loss is analyzed by comparing with other models. Also a new approach to model holdup is proposed that allows addressing the actual physics of the phenomenon by taking into account important process parameters, such as flow rate and fluid properties.

MODELING METHODOLOGY

The modeling methodology proposed by Crivelaro et al. (2009) requires solving the conservation equations of mass (continuity) and momentum numerically by using the commercial CFD code available in ANSYS CFX.

Mass conservation (continuity):

$$\frac{\partial(f_\alpha \rho_\alpha)}{\partial t} + \frac{\partial(f_\alpha \rho_\alpha U_{\alpha i})}{\partial x_i} = S_{MS\alpha} + \sum_{\beta=1}^{N_P} \varphi_{\alpha\beta} \quad \text{...........} \ (1)$$

Momentum conservation:

$$\frac{\partial(f_\alpha \rho_\alpha U_{\alpha i})}{\partial t} + f_\alpha \rho_\alpha U_{\alpha j} \frac{\partial U_{\alpha i}}{\partial x_j} = -f_\alpha \frac{\partial p_\alpha}{\partial x_i} + \frac{\partial}{\partial x_j}\left[f_\alpha \mu_\alpha \left(\frac{\partial U_{\alpha i}}{\partial x_j} - \tau_{\alpha ij}\right)\right] + \sum_{\beta=1}^{N_P} \varphi_{\alpha\beta}^{+} + S_{M\alpha} + M_\alpha \ldots\ldots \ (2)$$

Where α and β represent the phases (water and oil), x_i is the coordinate axis (x, y and z), f is the volume fraction, U_i is the velocity vector, N_P is the number of phases, p is the pressure, ρ is the fluid density, μ is the fluid viscosity and τ_{ij} are the components of the Reynolds stress tensor. Additionally, $S_{MS\alpha}$ is the user specified mass sources, $\varphi_{\alpha\beta}$ is the mass flow rate per unit volume from β to α, $S_{M\alpha}$ is the sum of body forces (buoyancy and rotational), M_α describes the interfacial forces (drag, lift, wall lubrication, virtual mass and interphase turbulent dispersion force), and $\varphi_{\alpha\beta}{}^{+}$ represents the momentum transfer induced by interphase mass transfer.

Some assumptions were necessary to simplify the model. Most important considerations are as follows:

i) The k-ε model is suitable for the Reynolds stresses (τ_{ij}) in the turbulent water annulus.
ii) Both phases (water and oil) are incompressible and isothermal.

iii) The Mixture model available in ANSYS CFX can be used to take into account the interphase transfers.
iv) The effect of buoyancy force is considered negligible, since the densities of oil and water are comparable.
v) The mass convergence criterion is considered to be 10^{-7} kg/s.

The geometry of the 3D computational domain was chosen to be a 0.0159 m diameter cylinder to match with that of the experimental pipe. A length of 1.2 m was considered sufficient for this study as the length independent flow field was found to develop beyond 0.5 m. The presented results of simulation were taken at 0.75 m.
The workbench platform of ANSYS CFX 13.0 was used to mesh the geometry. Unstructured meshes were generated for the numerical solutions. Based on the number of elements, the meshes tested in the current work can be classified as coarse (elements < 10^6), intermediate (10^6 < elements < 10^7) and fine (elements > 10^7). The total elements considered to be sufficient for grid independence was 36.2×10^7.

At the inlet, the viscous oil was considered to enter as a concentric core surrounded by water annulus. The mass flow rates of oil and water calculated from the experimental data were specified as the boundary conditions. Adapting the method suggested by Rushd et al. (2012), the diameter of the oil core (D_o) was calculated on the basis of the water holdup (H_w) and pipe diameter (D).

$D_o = D\sqrt{(1 - H_w)}$ …………..(3)

The oil core was set as a laminar flow and the water annulus was considered to be turbulent flow. The standard k-ε model with 5% turbulence intensity was selected for the annulus. The interphase transfer of oil and water under flow condition was modeled with the mixture model. An interfacial length scale of 1 mm was regarded as most suitable for this study. A constant pressure (relative pressure of 0 Pa) was set as the outlet boundary condition. No slip and smooth wall boundary conditions were specified for the pipe wall.

VALIDATION AND ANALYSIS

Numerical simulations were conducted for both transient and steady state. However, only the steady state results of volume fraction, velocity profile and pressure gradient are presented here.

The simulation results of volume fraction and velocity profile are presented for a specific data point. The flow conditions are available in Table 1. Fig. 2 and Fig. 3 demonstrate the volume fractions in the steady state solution. The fraction of water in the core and that of oil in the annulus was negligible. It is interesting to note from Fig. 2 that the oil core in the fully developed flow is not perfectly cylindrical. This is due to the development of wave on the oil core. Fig. 3 shows that the mixing zone is located over the interface. As expected, it is a very thin layer compared to the core and the annulus. These results agree quite well with experimental observations (Arney et al. 1993; Ho and Li 1994; Sotgia et al. 2008; Rodriguez et al. 2009; Strazza et al. 2011; Bannwart et al. 2012).

Table 1: Experimental flow conditions

Pipe's material of construction	Glass
Pipe's internal diameter (ID)	0.0159 m
Oil viscosity	2.7 Pa.s
Water viscosity	0.001 Pa.s
Oil density	989 kg/m^3
Water density	998 kg/m^3
Oil superficial velocity	0.64 m/s
Water superficial velocity	0.4 m/s
Water input fraction	0.38
Input ratio of volumetric flow rates (Q_w/Q_o)	0.63
Pressure gradient	1.43 kPa/m

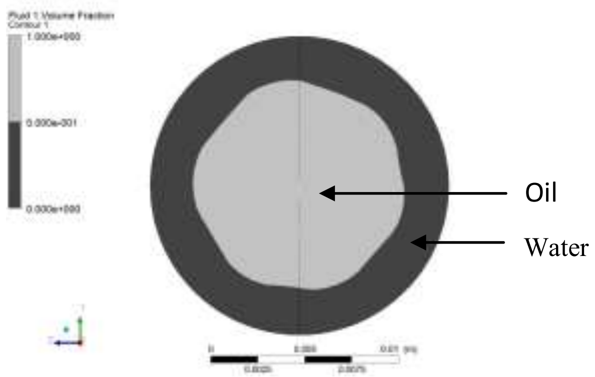

Fig 2: Cross sectional contour plot of oil and water volume fraction

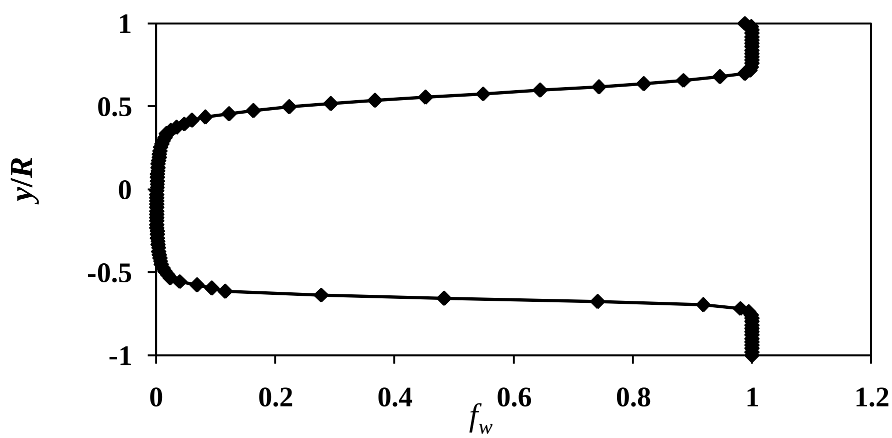

Fig 3: Volume fraction profile of water (*y* is the radial distance from the center, *R* is the pipe diameter and f_w is the water volume fraction)

Velocity profiles are shown with Fig. 4 and Fig. 5. As presented in Fig. 4, water velocity sharply rises to a maximum value at the oil-water interface and, then, it decreases to zero in the core. The reduced local velocity represents the depletion of water fraction from the interface to the core. The mixture velocity is demonstrated in Fig. 5. It is the typical profile in a CAF pipeline that has been observed in different experiments (Arney et al. 1993; Sotgia et al. 2008; Strazza et al. 2011; Bannwart et al. 2012; Shi 2015).

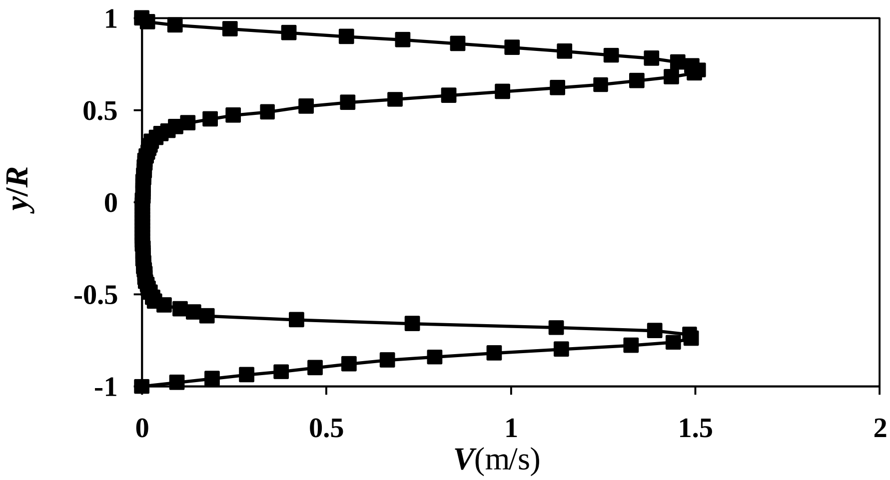

Fig 4: Cross sectional view of the water velocity profiles

The simulation results of pressure gradients are presented in Fig. 6 with respect to a pressure gradient ratio (PGR) and the water equivalent Reynolds number (Re_w). The PGR is the ratio between the simulation results and the measured values. The equivalent Re_w is calculated from the pipe diameter (D), average mixture velocity (V) and properties of water (ρ_w and μ_w).

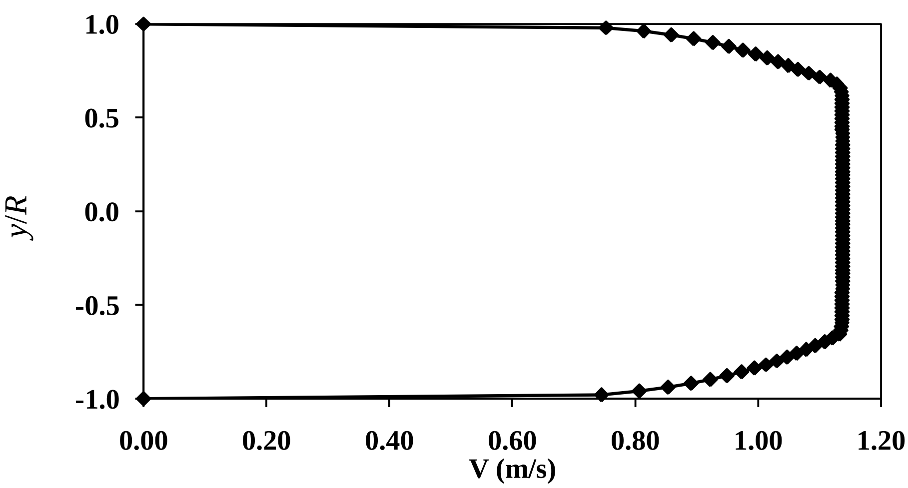

Figure 5. Mixture velocity profile

$$Pressure\ gradient\ ratio\ (PGR) = \frac{Simulation\ \ Result\ \ of\ Pressure\ \ Gradient\ \ (\frac{kPa}{m})}{Experimental\ \ \ Pressure\ \ Gradient\ \ (\frac{kPa}{m})} \text{ .... } (4)$$

$$Re_w = \frac{DV\rho_w}{\mu_w} \text{ .... } (5)$$

As observed from Fig. 6, the CFD modeling methodology presented in this work is capable of reproducing the experimental data within ±25%. The agreement is quite remarkable considering the limitations associated with both experiments and simulations.

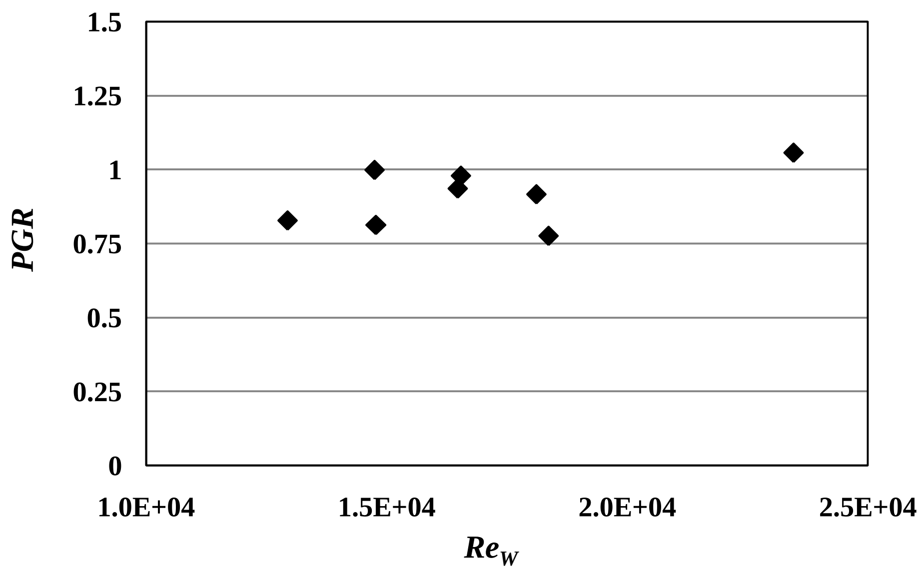

Fig 6: Simulation results of pressure gradients (PGR: Pressure Gradient Ratio; Re_w: Water equivalent Reynolds number)

For three different data points, the simulation results of pressure gradients are compared with the predictions of other models in Fig. 7. It should be noted that the selected data points are different than the ones presented in Fig. 6. The model predictions are presented in Fig. 7 as a function of corresponding measured values. The perfect agreement is presented by the diagonal. Lines representing ±25% error limits are also incorporated. The performance of the CFD simulation in predicting pressure losses is comparable to that of the model proposed by Arney et al. (1993). This model was developed on the basis of the experimental data used for the current study. Fig. 7 also shows that the uncertainty associated with other models in predicting pressure losses can be as high as 50%. That is, the CFD based model is capable of producing reliable predictions of a frictional pressure loss in a CAF pipeline.

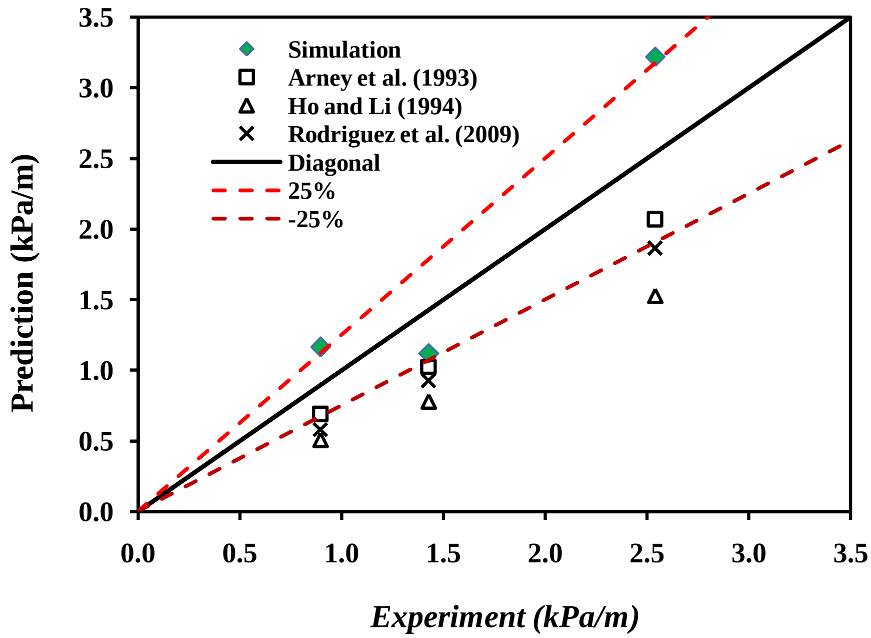

Fig 7: Comparative performance of different models in predicting CAF pressure gradients

NEW APPROACH TO MODEL HOLDUP

In general, holdup is an important feature of a multiphase flow system. It is a significant design parameter. Due to the different velocity profiles at the inlet and the fully developed flow section, the *in situ* volume fraction is considerably different than the input fraction. Differences in density and/or viscosity is considered to give rise to the holdup of a phase relative to the other (Shi 2015). The holdup of water and oil in a CAF pipeline can be defined as follows (Oliemans 1986).

$$H_w = \frac{A_w}{A} \text{ ……….. (6)}$$

$$H_o = \frac{A_o}{A} = 1 - H_w \text{ …………. (7)}$$

Where H_w is the water holdup, H_o the oil holdup; A is the pipe cross-sectional area, A_w and A_o are the cross-sectional areas occupied by water and oil, respectively.

In the field of CAF, the holdup is usually correlated to the input parameters. Examples of correlations for H_w are as follows.

$$H_w = C_w[1 + 0.35(1 - C_w)] \text{ ……… (8)}$$

$$U_o(1 - H_o) - 1.17U_wH_o - 0.02H_o^{1.79} = 0 \text{……………(9)}$$

Where U_o is the superficial velocity of oil and U_w is the superficial velocity of water. Eq. (8) was proposed by Arney et al. (1993) and Eq. (9) by Rodriguez et al. (2009). Recently, Shi 2015 modified Eq. (8) by including a complex function of Froude number (Fr), which signifies the ratio between the inertial force and the gravity force.

A careful examination reveals that the actual physics of holdup cannot be addressed properly following the methodology or basis of the existing correlations. This is because the controlling process variables were not included in these models. In the current work, the most important parameters like viscosity (μ), density (ρ) and flow rate (m) are included in modeling holdup with respect to a new dimensionless number, P^*.

$$P^* = \left(\frac{\mu_w}{\mu_o}\right)\left(\frac{\rho_w}{\rho_o}\right)\left(\frac{m_w}{m_o}\right) \ldots\ldots\ldots\ldots (10)$$

Holdup is presented here as follows:

$$t^* = \frac{R_o}{R} \ldots\ldots\ldots\ldots (11)$$

The ratio R_o/R is related to H_w according to Eq. (3).

The result of the proposed modeling approach is presented in Fig. 8. The trendline generated using MS Excel has a R^2 value of 0.99, which demonstrates a strong power law correlation to exist between t^* and P^*.

$$t^* = 0.126(P^*)^{-0.2} \ldots\ldots\ldots\ldots (12)$$

Eq (12) is proposed on the basis of the CAF data collected from Arney et al. (1993).

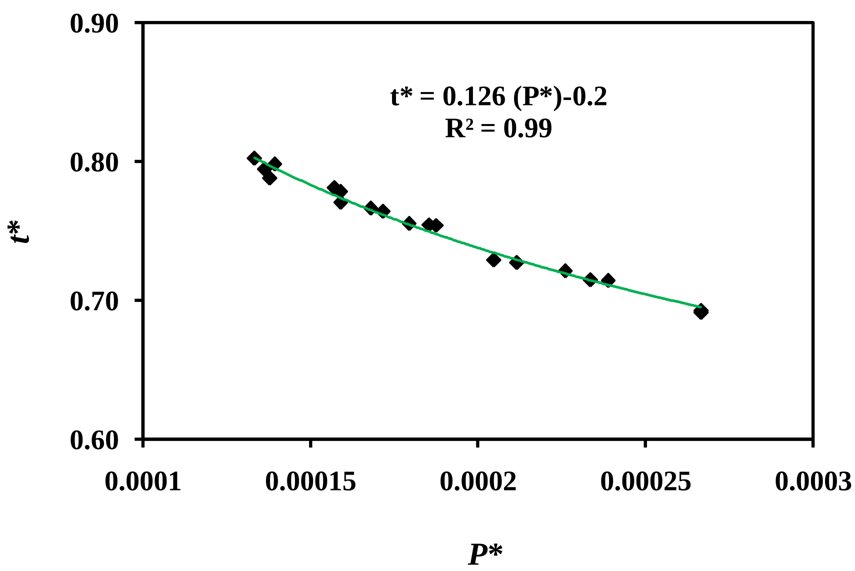

Fig 8: Presentation of new holdup model with experimental data points

CONCLUSIONS

The frictional pressure loss and water holdup for water lubricated pipeline transportation of heavy oil or bitumen were studied in the current work. The modified version of a previously proposed CFD based modeling approach was validated and implemented to predict friction losses. Reasonable agreement between experimental and simulation results was observed. A simplified model was developed for the water holdup in a CAF pipeline. Its performance in predicting holdup is promising. Although only one data source was used, the performance of the models were consistent for a variety of flow conditions which substantiates the utility of the models presented in the current work.

ACKNOWLEDGEMENT

The authors thankfully regard the kind assistance of Dr. Sanders (Associate Professor, Department of Chemical and Materials Engineering, University of Alberta, Edmonton, AB, Canada). Most of the simulation works were conducted in his laboratory.

NOMENCLATURE

A	Cross sectional area (m^2)
$\Delta P/L$	Pressure gradient (Pa/m)
D	Internal Diameter (m)
D_o	Diameter of oil core (m)
f	Volume fraction
Q	Flow rate (m^3/s)
R	Pipe radius (m)
Re	Reynolds number
U_i or $\boldsymbol{U}$	Velocity vector (m/s)
U	Superficial velocity (m/s)
V	Average velocity (m/s)
C	Input volume fraction
H	*In situ* volume fraction or holdup
m	Mass flow rate (kg/s)
y	Local distance from pipe's center to wall (m)
k	Turbulence kinetic energy (J/kg)
ε	Dissipation of the kinetic energy (J/kg.s)
μ	Viscosity (Pa.s)
ρ	Density (kg/m^3)
τ_{ij}	Reynolds stresses in the momentum conservation equation (Pa)
CAF	Core annular flow
CFD	Computational fluid dynamics
ID	Internal diameter

REFERENCES

Arney M. S., Bai R., Guevara E., Joseph D. D. and Liu K., 1993. Friction Factor and Holdup Studies for Lubricated Pipelining – I, Experiments and Correlations. *Int. J. Multiphase Flow,* **19 (6)**, 1061-76.

Bannwart, A. C., Rodriguez, O. M. H., Biazussi, J. L., Martins, F. N., Selli, M. F. and de Carvalho, C. H. M., 2012. Water-assisted flow of heavy oil in a vertical pipe: pilot-scale experiments. *International Journal of Chemical Reactor Engineering*, **10**, Article A32.

Crivelaro K. C. O., Damacena Y. T., Andrade T. H. F., Lima A. G. B. and Farias Neto S. R., 2009. Numerical simulation of heavy oil flows in pipes using the core-annular flow technique. *WIT Transactions on Engineering Sciences,* **63**, 193 – 203.

Gupta R., Turangan C. K. and Manica R., 2016. Oil-water core-annular flow in vertical pipes: A case study. *Canadian Journal of Chemical Engineering*, **94**, 980 – 987.

Ho W. S. and Li N. N., 1994. Core-Annular Flow of liquid membrane emulsion. *AIChE Journal*, **40 (12)**, 1961 – 1968.

Nunez G. A., Rivas H. J. and Joseph D. D., 1998. Drive to produce heavy crude prompts variety of transportation methods. *Oil & Gas Journal,* **96 (43)**, 59 – 63.

Oliemans, R. V. A. and Ooms, G., 1986. Core-Annular flow of oil and water through a pipeline. *Multiphase Science and Technology*, **2**, 427 – 476.

Rodriguez O. M. H., Bannwart A. C. and de Carvalho C. H. M., 2009. Pressure loss in core-annular flow: Modeling, experimental investigation and full-scale experiments. *Journal of Petroleum Science and Engineering,* **65**, 67 – 75.

Rovinshy J., Brauner N. and Maron D. M., 1997. Analytical solution for laminar two-phase flow in a fully eccentric core-annular configuration. *Int. J. Multiphase Flow*, **23 (3)**, 523 – 543.

Rushd S., Rahman M. A., Adane K. F. K. and Sanders R. S., 2012. Analysis of frictional pressure loss in the water lubricated pipeline transportation of heavy oil: A new simulation approach. World Heavy Oil Congress, Aberdeen, Scotland, September 2012.

Saniere A., Henaut I. and Argillier J. F., 2004. Pipeline transportation of heavy oils, a strategic, economic and technological challenge. *Oil & Gas Science and Technology – Rev. IFP*, **59**, 455 – 466.

Shi J., 2015. A study on high-viscosity oil-water two-phase flow in horizontal pipes. PhD Thesis, Cranfield University, Cranfield, UK.

Sotgia, G., Tartarini, P. and Stalio, E., 2008. Experimental analysis of flow regimes and pressure drop reduction in oil-water muxtures. *International Journal of Multiphase Flow*, **34(12)**, 1161-1174.

Strazza, D., Grassi, B., Demori, M., Ferrari, V. and Poesio, P., 2011. Core-annular flow in horizontal and slightly inclined pipes: Existence, pressure drops, and hold-up. *Chemical Engineering Science*, **66**, 2853 – 2863.

International Conference on Petroleum Engineering 2016 (ICPE-2016)
Bangladesh University of Engineering & Technology (BUET)
Dhaka-1000, Bangladesh

ICPE (2016-013)

Prediction of Choke Size for Single Gas Flow using Artificial Intelligence Techniques

[1]*Murtada A. Elhaj*[*] , [2]*Fatai Anifowose*, [3]*Abdulazeez Abdulraheem*, [4]*M. Enamul Hossain***

[1]Department of Process Engineering, Memorial University, St. John's, Canada
[2]Center for Petroleum and Minerals, Research Institute, King Fahd University of Petroleum & Minerals, Dhahran, Saudi Arabia
[3]Department of Petroleum Engineering, King Fahd University of Petroleum & Minerals, Dhahran, Saudi Arabia
[4]Department of Process Engineering, Memorial University, St. John's, Canada

ABSTRACT

The choke is an important element in the well production system. The main function of choke is to control flow. Studying the single gas flow through wellhead chokes is vital to the oil industry. This is not only important to ensure the accurate estimation of gas flow rate but also to keep equipment protected from damage and destruction due to high gas flow rate. It also has the potential to avoid sand problems. Many correlations were developed to describe the flow through chokes. The accuracy of these correlations is not high enough. This study aims to show the importance of Artificial Intelligence (AI) techniques as a practical engineering tool for predicting, estimating and selecting the optimal choke size. In this study, reviewing, evaluating and comparing the predictive performance of the available choke correlations in literature with five AI techniques will be considered.

More than 150 data points were used to develop five AI models for predicting and selecting the optimal choke size. The data were fed to the five AI techniques beginning with Artificial Neural Network (ANN), Fuzzy Logic (FL), Support Vector Machine (SVM), Functional Network (FN) and Decision Tree (DT) and the results were optimized for each technique. The new models were found to perform better than the correlation and give the lowest error, with a mean absolute percentage error of 0.15% for the choke size predictions. Because of these reduced errors, the proposed AI-based models can improve gas flow rate prediction through chokes and can help in the selection the optimal choke size.

The results of this research will encourage researchers and engineers to explore advanced machine learning techniques such as hybrids and ensembles for continued improvement of petroleum exploration and production.

Keywords: Choke size, AI techniques, Correlation.

* Corresponding Author address
Email: mae162@mun.ca

INTRODUCTION

The reason behind the use of AI is because of its effectiveness in addressing Petroleum Engineering problems successfully. Although some engineers and researchers believe that AI can't be trusted and call it a "Black Box." However, as stated by (Mohaghegh and Ameri (1995) and Mohaghegh (2000), "just because they are not immediately visible does not mean one can not examine what goes in those layers." They suggested to call it a "Transparent Box" instead of a "Black Box". , additional to that, the experiments and results gain from AI for more than decades say otherwise.

The pressure drop is an important factor influencing the pressurization of the formation and as a result the performance and productivity of the well. Wellhead choke which is a part of the wellhead assembly component is used to control the flow of oil and gas. Two types of chokes are available: adjustable and positive. The eventual goal of this paper is to create models to give better prediction the optimal choke size and comparisons between five AI techniques. Our approach, to do that, consists of these steps: firstly, gather relative data from a gas well and put it on a table so AI techniques can handle it. Secondly, include the result of one correlation in the table to guide and help the artificial models. Thirdly and lastly, use several AI techniques to develop the model and recommend the one with the lowest error.

Chokes are extensively used in Oil and Gas Industry and focused on limit and control mass flow and well potential. Those chokes are nozzles, fixed or adjustable orifices that can control pressure drop and restrict gas volume at certain flowing well head pressure condition. Choke can be classified as fixed diameter and adjusted diameter choke. The knowing of choke performance will help us understand the gas transient flow through chokes. It is useful for pipe or tank leakage detection and analysis as well. Choke performance is very important in petroleum industry because it can be used to detect the blockage in the pipe due to scaling or hydration.

Accurate prediction of multiphase flow through chokes is required for modern production design and optimization of oil well performance. Most of the Middle-East oil wells are uniquely characterized by high production rates. Several correlations that relate the choke size with other variables involved in the multi-phase flow phenomena have been proposed in the literature.

In this study, more than 150 data point from a gas field in North Africa were collected to develop an AI model that covers a wide range of field production data. These data include choke size, upstream tubing pressure, downstream tubing pressure, upstream tubing temperature, gas gravity and gas flow rates. Dataset summarized in Table 1.

Table 1: Summary of Dataset

Description	Maximum	Minimum
Rate (MMSCF/DAY)	17.17	2.17
Tubing Temp. (F)	564	535.2
Upstream Pressure (PSIG)	1840	520
Downstream Pressure (PSIG)	500	100
Gravity (@60 F)	0.632	0.588
Chock size (IN)	128	16

Five AI techniques were used in this study to improve prediction of the gas rate in chokes and same techniques also used due selecting the optimal choke size. All results were compared to each other and one correlation was used to compare with these results from models to see how accurate of the results got from models. These techniques were Artificial Neural Network (ANN), Fuzzy Logic (FL), Support Vector Machine (SVM), Functional Network (FN) and Decision Tree (DT). The empirical correlation used in this study was New Saudi Aramco Choke Correlation which presented by (Jairo Leal et al. 2013).

PREVIOUS STUDIES

In literature, mostly empirical equations were reported for estimating the oil and gas rates flowing through chokes and predicting the optimum choke size. The chokes are nozzles with fixed or adjustable orifices (Morris, 1996). The first significant study on multiphase flow through chokes was conducted by Tangren et al., (1949). He derived an equation that is applicable for critical flow only, with a volumetric gas-liquid ratio less than 1.

Gilbert (1954) developed an empirical correlation based on the liquid flow rate, the gas-liquid ratio, the choke diameter, and the upstream pressure. Gilbert's work was followed by several researchers making modifications to his formula.

The researchers included Baxendall (1957), Ros (1959), and Achong (1961). Ros (1961a) developed a new equation for subcritical flow through restrictions. Poetmann and Beck (1963) converted the Ros equation to oil field units and reduced it to a graphical form. Omana et al., (1969) conducted experimental field tests to study the multiphase flow of gas and liquid through small sized chokes in a vertical position.

Fortunati (1972) presented a formula for calculating the rates through wellhead chokes, covering both critical and subcritical flow fluids. For the isentropic flow of an ideal gas through a choke, the rate is related to the pressure ratio, Pup/P down, by (Szilas, 1975), his empirical equation applied only when the pressure ratio is equal to or greater that critical pressure. In this study, we will focus only on a study done by (Jairo Leal, et al. 2013). He and his colleague have developed an empirical model of dry gas flow through the choke. This model had been chosen as the empirical equation used to compare its results to AI models, the selection for this model was based on; the inputs are the same as for this study, the accuracy of this model compare to others and the model was recent developed.

Generally, we can say a good number of research has been carried out on the use of various Artificial Intelligence (AI) schemes to predict the characteristics of oil and gas flow through reservoirs and pipes using such schemes including Logistic Regression (LR), K-Nearest Neighbor (KNN), Functional Networks (FunNets), Support Vector Machines (SVM), Artificial Neural Networks (ANN), Probabilistic Networks (PN), Adaptive-Neuro Fuzzy Systems (ANFIS) and Decision Trees (DT).

PROBLEM DESCRIPTION

Since the optimum chokes size prediction is highly important not only to ensure the accurate estimation of gas flow rate but also to keep equipment protected from damage due to high gas flow rate. It also has the potential to avoid sand problems. First attempt to predict multiphase flow rate through chokes using AI was performed by Al-Khalifa (2009) where he used only Artificial Neural Network (NN). In this investigation, several techniques of Artificial Intelligence will be used to predict the optimum chokes size and a comparison of the results obtained from the different technique with an empirical correlation will be made.

BACKGROUND OF ARTIFICIAL INTELLIGENCE TECHNIQUES

Artificial Neural Network (ANN)

A Neural Network as defined by Dr. Hecht Nielsen is "a computing system made up of a number of simple, highly interconnected processing elements, which process information by its dynamic state response to external inputs. This definition reflects the basic structure of a Neural Network as that of a computer representation of a biological neuron (nerve cell) that is interconnected with other neurons (a brain). Mathematically, Neural Networks can be viewed as a multi-variable non-linear regression. Neural Networks are not programmed to find a solution, instead, they learn by example. Where most computer programs have the principles of chemistry and physics coded into the program itself as equations, Neural Networks do not. Neural Networks do not have any a priori knowledge coded into the program at all. Conventional programs apply the coded scientific principles in the program to the problem's inputs to calculate an answer. A Neural Network learns an empirical relationship between the inputs and the desired outputs.

The network is presented with different examples of inputs and outputs and relationships are learned after reviewing the examples over and over again, as many as ten million times. A Neural Network initially assumes a random relationship between all the inputs and the desired outputs. By comparing its first attempt at an answer to the desired output, it self-modifies this initial random relationship into a relationship that best fits the outputs. Mathematically, learning is the process by which a set of weights are found that produces the expected output when a net is presented within an input. You can train a neural network to perform a particular function by adjusting the values of the connections (weights) between elements (Jeirani, 2006).

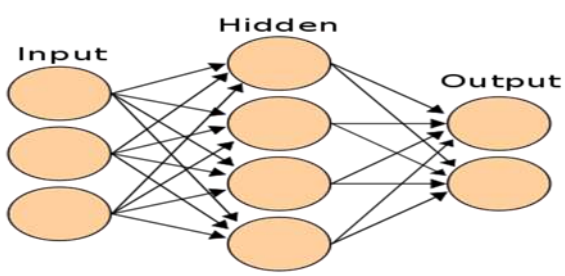

Figure 1. ANN structure.

Fuzzy Logic (FL)

Fuzzy logic is an extension of conventional Boolean logic (zeros and ones) developed to handle the concept of partial truth: truth values between "completely true" and "completely false". It was introduced by Dr. Lotfi Zadeh of UC/Berkeley in the 1960's as a means to model uncertainty (Zadeh, 1965). As a method for modeling, the Fuzzy Inference System (FIS) is the process of establishing formulated mapping from an input to an output using fuzzy logic. FIS involves the use of membership functions, logical operations, and a group of "If-Then" rules to create a matrix of rules between input sets and an output. It has been used in many petroleum applications such as permeability determination, stimulation candidate selection, production optimization and completion, and multilateral design.

Adaptive Neuro-Fuzzy Inference System (ANFIS) provides a technique for fuzzy modeling process to "learn" from datasets. This method is applied to construct FIS and tuning or adjusting the membership functions using back propagation algorithms along with least-square type functions to learn from datasets. A structure similar to neural networks is created to map inputs using input membership functions and associated parameters, and then through output membership functions and associated parameters to the outputs (Al-Shammari. 2011).

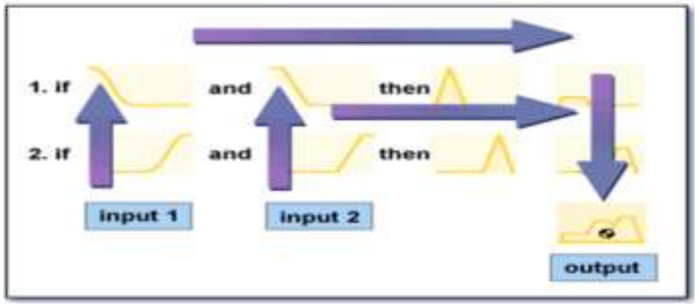

Figure 2. FL structure.

Support Vector Machine (SVM)

A Support Vector Machine (SVM) is a discriminative classifier formally defined by a separating hyperplane. In other words, given labeled training data (supervised learning), the algorithm outputs an optimal hyperplane which categorizes new examples. Support Vector Machines (SVMs) "also known as support vector networks, Vapnik, V. (1995)" are a popular machine learning method for clasification, regression, and other learning tasks. In machine learning, (SVM), are supervised learning models with associated learning algorithms that analyze data and recognize patterns, used for classification and regression analysis.

The SVM model was introduced by Vapnik (1995). Both classification and regression utilizations of the SVM have been systematically investigated by a number of researchers (Arabloo et al., 2013; Baylar et al., 2009; Chen et al., 2011; Cortes and Vapnik, 1995; Shmilovici, 2005; Obeyli, 2010; Vapnik, 1995; Yao et al., 2006). SVMs use the principle of the structural risk minimization (SRM) theory (Cortes and Vapnik, 1995). The SVM technique builds the input prototypes in a space with greater dimensions by employing a nonlinear mapping method. A linear pattern is then decided in this multi-dimensional feature space (Cortes and Vapnik, 1995; Pelckmans et al., 2002; Suykens and Vandewalle, 1999; Obeyli, 2010).

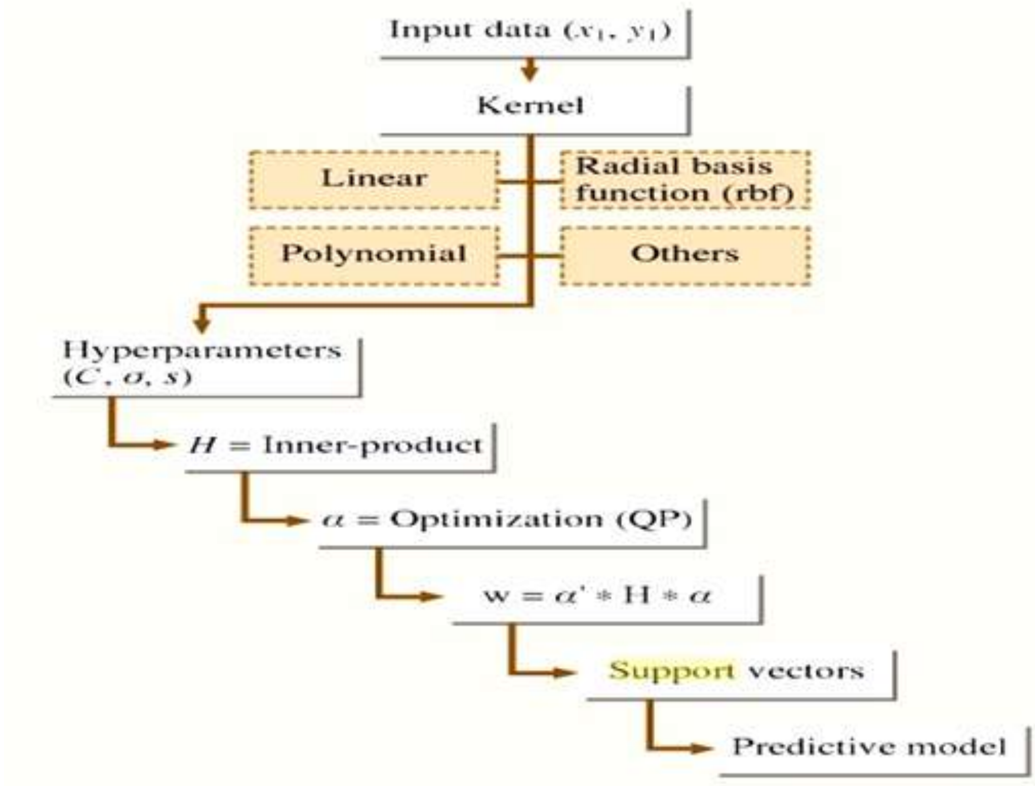

Figure 3. SVM structure.

Functional Network (FN)

FN was proposed as a new intelligence data-mining predictive model for solving numerous engineering problems such as predicting reservoir fluid (PVT) properties and rock mechanical parameter for hydrocarbon reservoirs (Castillo et al. 1993, 1999, 2002, 2005, 2008; El-Sebakhy et al. 2012). The most significant benefits of FN over ANN have been well documented by Anifowose and Abdulraheem (2011). The FN technique is a generalization of the standard ANN that deals with generalized functional models instead of sigmoidal standard types. In FN, the neuron functions that are associated with each neuron are not fixed but are learned from the available data. Hence, there is no need to include weights associated with links, because the neuron functions subsume the effect of the weights. FN allows neurons to be multi-argument, multivariate and different learned functions instead of fixed functions. Furthermore, FN allows converging neuron outputs, forcing them to be coincident. This leads to a system of functional equations, which requires some compatibility conditions on the neuron functions. Tarek et al. (2010) and Anifowose and Abdulraheem (2011) summarized the theory of FN algorithms and suggested appropriate ways of applying them.

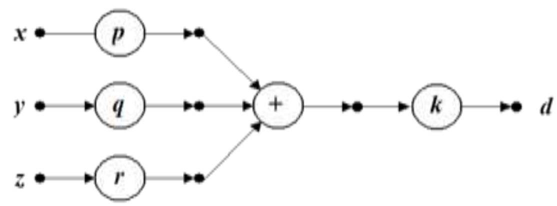

Figure 4. FN structure.

Decision Tree (DT)

Decision Tree (DT) analysis is one of most widely used data mining methods today. As illustrated in Figure 5, a decision tree (DT) is a flow-chart-like tree structure where each internal node denotes a test on an attribute variable, each branch represents an outcome of the test, and terminal nodes represent groups characterized by target variable. Moreover, DT is a hierarchical, sequential tree structure that recursively partitions the set of data into sub-branches. Each branch represents rules underlying the data.

DT analysis can be used in classification, prediction, and regression. A decision tree can be used to clarify and find an answer to a complex problem. The structure allows users to take a problem with multiple possible solutions and display it in a simple, easy-to-understand format that shows the relationship between different events or decisions. The furthest branches on the tree represent possible end results.

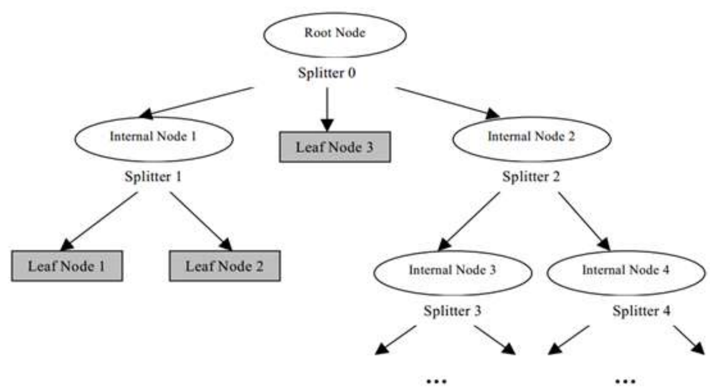

Figure 5. Decision Tree Structure

MODELS CONSTRUCTION

This section discusses how models were developed, the methodology, selecting the independent variable, model architecture, and optimization.

The artificial intelligence techniques used for prediction are:

1. Artificial Neural Networks (ANN)
2. Fuzzy Logic (FL)
3. Support Vector Machines (SVM)
4. Functional Networks (FN)
5. Decision Tree (DT)

The models build using the above techniques will be implemented using Matlab software. Statistical analysis will be carried out to compare between results obtained by the different techniques and methods.

Data Acquisition

In this study, more than 150 data points from a gas field in North Africa were collected to develop an AI model that covers a wide range of field production data. These data include choke size, upstream tubing pressure, downstream tubing pressure, upstream tubing temperature, gas gravity and gas flow rates. Dataset summarized in Table 1.

The independent variables were selected for gas flow through chokes based on New Saudi Aramco equation (Jairo et al., 2013) and the gas law equations. The New Saudi Aramco equation is a function of flow rate (Q), choke size (D_{64}), tuping tempretare (T), upstream pressure (D_{up}), downstream pressure (D_{down}) and gas gravity. These parameters were also in agreement with the parameters used in the literature.

Models Develop

The architecture of models used in this study was different and it depended on the type of the techniques. For example, the ANN model architecture in terms of the number of neurons, layers and the type of interconnection function were determined based on a trial and error process that was found to be the most successful criteria in developing the model. During development, the design started with a minimum number of neurons and was increased gradually while monitoring the performance for every case, using absolute average percent error, correlation coefficient in addition to other statistical and graphical analysis techniques, such as average percent error and standard deviation error. In addition to that, several learning functions were tested and monitored using the same approach in selecting the number of neurons. The model started with one hidden layer, which was increased until the optimum number was two for optimal choke size case (Figure 6). Different transfer functions were tested while changing the number of neurons but the best was the sigmoid. In the ANN model development, 60% of the data were used for training and 20% for testing and 20% for validation and it was block stratified data; this combination gave the best results for both gas flow rate prediction and selection of the optimal choke size.

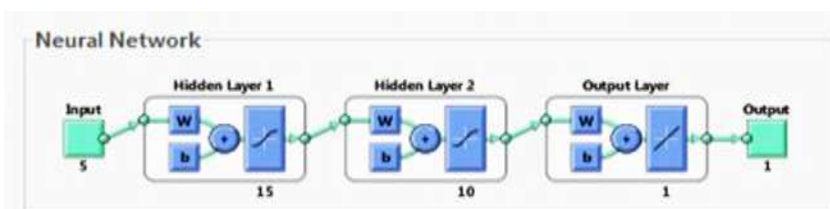

Figure 6. A number of neurons used in optimal choke size prediction.

Fuzzy Logic (FL) model architecture started first with setting the fuzzy set by excluding any odd or outfit data. The primary mechanism for doing this is a list of “if-then” statements called rules. The simplest membership functions were used to build this model in order to ensure simplicity since the data is of small size, using the scale proposed by Anifowose and Abdulraheem (2010). Of these, the simplest is the triangular membership function, and it has the function name *trimf*. This function is simply a collection of three points forming a triangle. We used the Seguno-type FIS and since there was only one output, *genfis2* used to generate an initial FIS for the *anfis* training. In the FL model development, the data was randomly stratified with 70% of the data used for training and the remaining 30% used for testing. This combination gave the best results.

The SVM model was designed with a randomly stratified dataset. 70% of the dataset was used for training and the remaining 30% used for testing. Blocked stratification of the dataset was tested as well but the random stratification gave the best results. All kernel functions (Polynomial, Gaussian Radial Basis, Exponential Radial Basis, Multi-Layer Perceptron and multiquadric) were tested with different values for C (regularization parameter). In the overall estimation, the Polynomial kernel function showed the best results with C = 25 for selecting the optimal choke size.

The design of the FN model started with a blocked stratification dataset but the random stratification gave better results. There are five available methods in FN which are 'FNESM', 'FNFSM', 'FNBEM', 'FNFBM' and 'FNBFM' also there are five available types of FN which are ‘Linear', 'Non-Linear(1)', 'Non-Linear(2)', 'Non-Linear(3)' and 'Non-Linear(4)'. For our cases “*method* 'FNBFM' *with type,* 'Non-Linear (1)'” gave the most accurate results. For the DT model, we used the “*gdi*” rule, which is the Gini diversity index for determining the criterion for choosing a tree split. The random stratification gave the best results.

OUTCOMES AND DISCUSSION

To show the effectiveness of the newly developed models compared to the existing correlations, the collected data were utilized to test one of the empirical correlations available in the literature, the Jairo equation.

Artificial Neural Network

The model architecture in terms of the number of neurons, layers and the type of connection function were determined based on trial and error process because it was the most successful criteria in developing the model. Different transfer functions were applied to both the input and output data like log-sigmoid and purelin.

It was found that the optimum number of layers is three layers with a different number of neurons. Figures (7 and 8) show some of the results obtained from the ANN along with the error distribution.

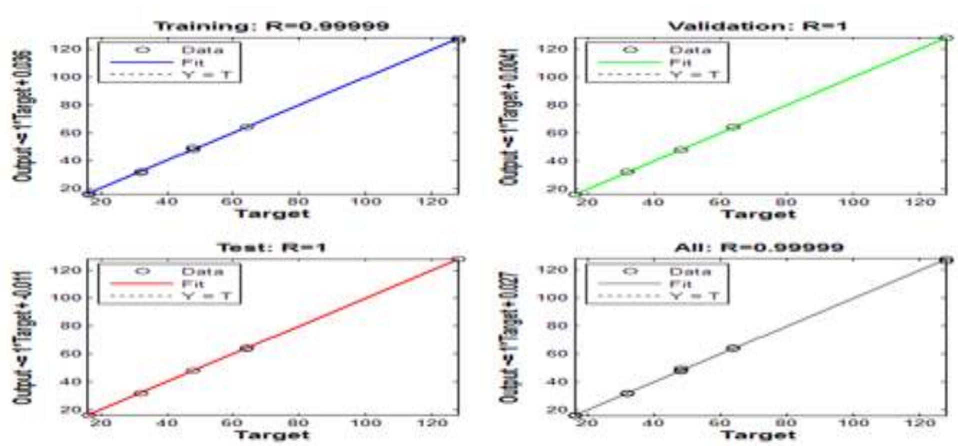

Figure 7. Crossplot of choke size prediction (ANN model).

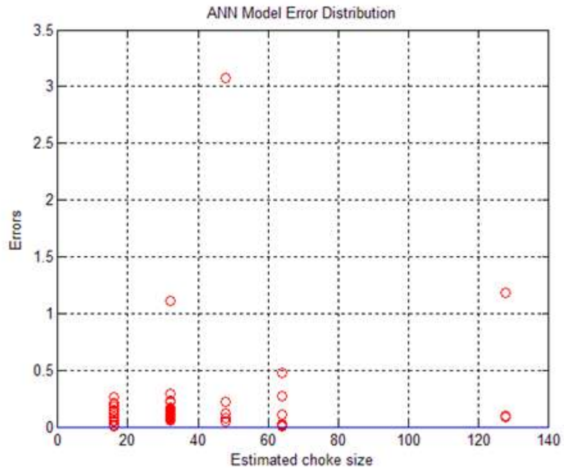

Figure 8. Error distribution for choke size (ANN model).

Fuzzy logic

Fuzzy logic is the second tool used in this study. It is of two types; grid partition, and sub-clustering. The simplest membership functions were used to build this model in order to ensure simplicity since the data is of small size, using the scale proposed by Anifowose and Abdulraheem (2010).

The simplest is the triangular membership function, and it has the function name trimf. This function is simply a collection of three points forming a triangle. We used the Seguno-type FIS and since there was only one output, genfis2 used to generate an initial FIS for the anfis training. Figures (9 and 10) show the results obtained from both training and testing data.

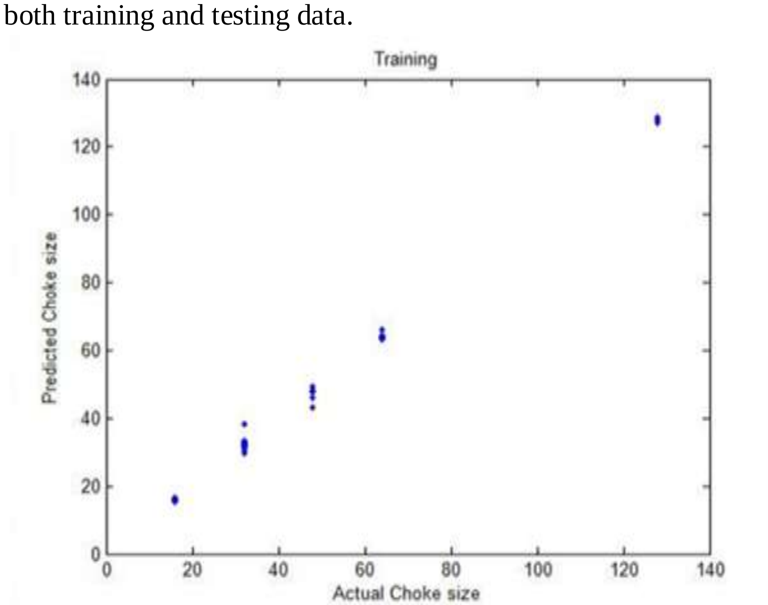

Figure 9. Cross plot of choke size prediction for the training set (FL model).

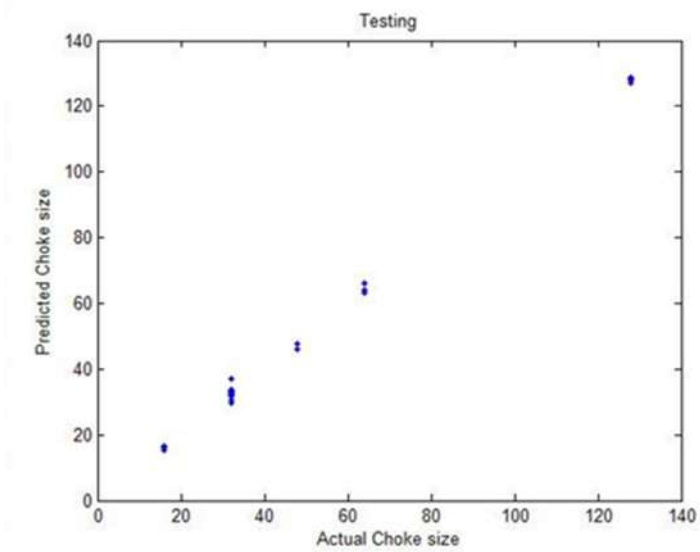

Figure 10. Cross plot of choke size prediction for testing set (FL model).

Support Vector Machines

Support Vector Machine (SVM) with different kernel functions was used. *kernel='poly'; %'gaussian'; 'polyhomog';'htrbf';'rbf'*. The SVM model was designed with a randomly stratified dataset. 70% of the dataset was used for training and the remaining 30% used for testing. Blocked stratification of the dataset was tested as well but the random stratification gave the best results.

In the overall estimation, the Polynomial kernel function showed the best results with C = 25 for selecting the optimal choke size. Figure (11 and 12) summarizes the results from the two techniques.

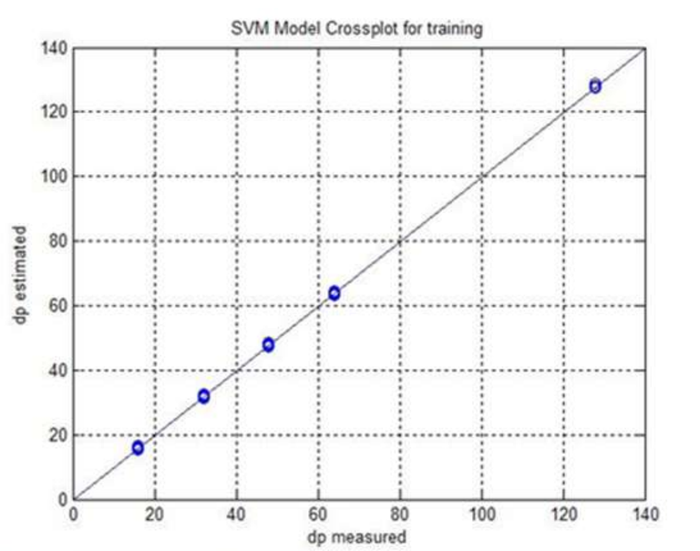

Figure 11. Cross plot of choke size prediction for the training set (SVM model).

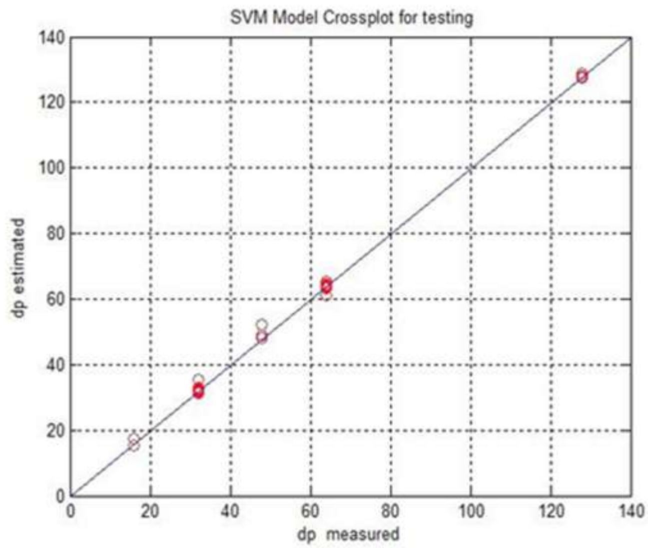

Figure 12. Cross plot of choke size prediction for testing set (SVM model).

Functional Network

Functional Network (FN) was applied using 70% of the data for training and 30% for testing. The design of the FN model started with a blocked stratification dataset but the random stratification gave better results. There are five available methods in FN which are 'FNESM', 'FNFSM', 'FNBEM', 'FNFBM' and 'FNBFM' also there are five available types of FN which are 'Linear', 'Non-Linear(1)', 'Non-Linear(2)', 'Non-Linear(3)' and 'Non-Linear(4)'. Figures (13 and 14) illustrate the testing and training date for this method.

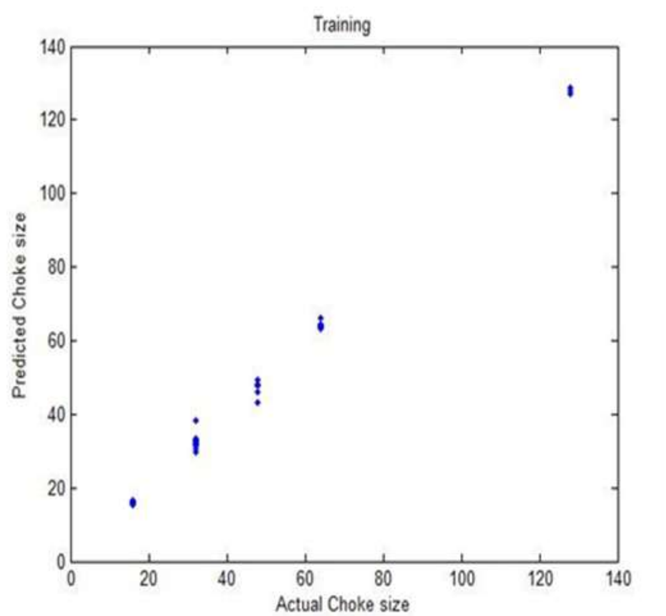

Figure 13. Cross plot of choke size prediction for the training set (FN model).

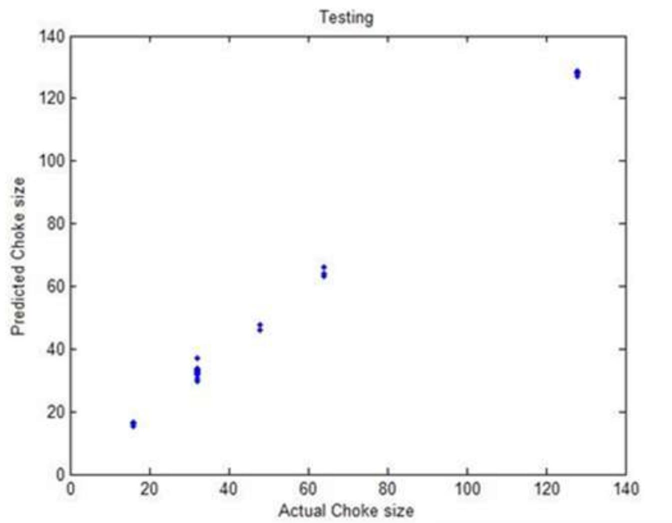

Figure 14. Cross plot of choke size prediction for testing set (FN model).

Decision Tree

"*gdi*" rule was used for this method, which is the Gini diversity index for determining the criterion for choosing a tree split. The random stratification gave the best results. Figures (15 and 16) show testing and training plots for this technique.

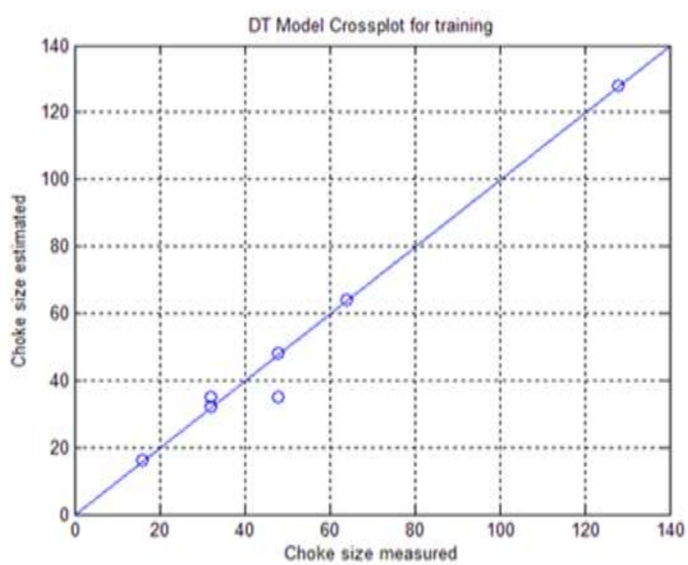

Figure 15 Cross-plot of choke size prediction for the training set (DT model).

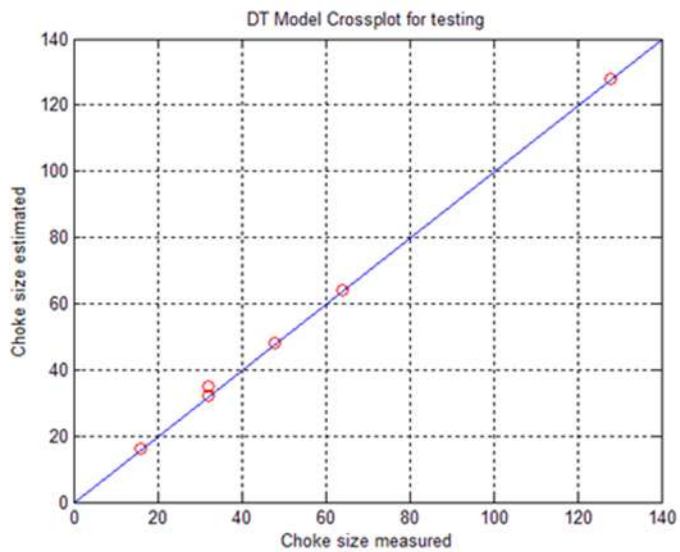

Figure 16. Cross plot of choke size prediction for testing set (DT model).

As a summary of the work that had been studied in this paper; Figures 7 through 16 show the results of the five models for training and testing while Table 2 shows the results for each model in comparison to those obtained from Jairo correlation. The graphical analysis technique was used by plotting the measured against the estimated values over a straight line of 45˚ drawn between them, as can be seen in figures 7 through16. The closer the points to this line are, the closer the unity between them and hence the higher the correlation is. The histograms, a well-known technique for data analysis, were used to visualize the errors for each model and compare them to the correlation errors (Figure 17).

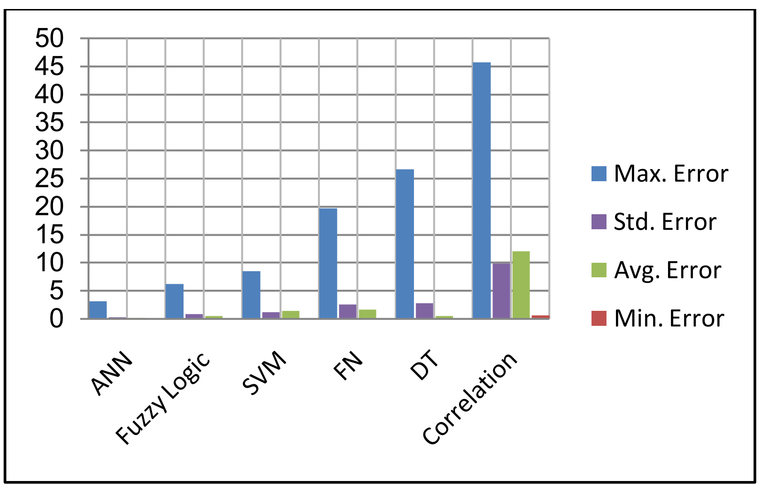

Figure 17 Histogram plot of errors in the prediction of choke size.

Table 2: Comparison between the five developed models and correlation for the selection of optimal choke size

Method	Max. Error	Min. Error	STDE	AAPE
ANN	**3.07093695**	**6.90057E-05**	**0.269305**	**0.151346**
Fuzzy Logic	6.148816558	0.000266674	0.790991	0.492274
SVM	8.415386504	0.053512976	1.197223	1.352805
FN	19.6298209	0.005426756	2.517911	1.574891
DT	26.66666667	0	2.717453	0.48218
Correlation	45.77263409	0.552200428	9.788648	11.96172

CONCLUSIONS

The proposed optimal choke size selection models showed good agreement between the measured and estimated values. This is evident from the AAPE values of (0.15%, 0.48%, 0.49%, 1.35% and 1.57% for ANN, DT, FL, SVM and FN, respectively. The results are far better than that given by the empirical correlation (Table 2).

ANN gave the best results for prediction of the optimal choke size (1.5% for AAPE and 0.27% for STDE).

Five models for choke size prediction were developed using five Artificial Intelligence techniques, viz., Artificial Neural Network (ANN), Fuzzy Logic (FL), Support Vector Machine (SVM), Functional Network (FN), and Decision Tree (DT). Several statistical and graphical techniques were made to check the accuracy of the new models and to compare them with the correlation. In general, the new models have outperformed the empirical correlation, and have provided the lowest error. Artificial Neural Network gave the best results for the prediction of choke size.

NOMENCLATURE

Q	Flow Rate
D_{64}	Choke Size
T	Tubing Temperature
D_{up}	Upstream Pressure
D_{down}	Downstream Pressure

REFERENCES

Abdul-Majeed, G., and Abual-Soof, N.: "Estimation of Oil and Gas Surface Tension," Journal of Petroleum Science and Engineering, April 2000, pp. 197-200.

Abdul-Majeed, G.H.: "Correlation Developed to Predict Two-Phase Flow through Wellhead Chokes," Paper SPE 15839, May 1986.

Al-Attar, H.. "Performance of wellhead chokes during sub-critical flow of gas condensates". J. Petrol. Sci. Eng. 2008, 60 (3-4), 205—212.

Al-Attar, H.: "Performance of Wellhead Chokes during Subcritical Flow of Gas Condensates," Journal of Petroleum Science and Engineering, August 2007, pp. 205-212.

Al-Attar, H.H., and Abdul-Majeed, G.H.: "Revised Bean Performance Equation for East Bagdad Oil Wells," Paper SPE 13742 presented at 1987 Middle East Oil Show and Conference, Bahrain, 11-14 March.

Al-Rumah, M., and Al-Bizanti, M.: "New Choke Correlation for Sabriyah Field Kuwait," Paper SPE 105103 presented at the 2007 Middle East Oil and Gas Show and Conference, Bahrain, 11-14 March.

Al-Towailib, A.I., and Al-Marhoun, M.A.: "New Correlation for Two-phase Flow through Chokes," M.S. Thesis, King Fahd University of Petroleum and Minerals, Dhahran, Saudi Arabia (1992).

Arabloo, M., Shokrollahi, A., Gharagheizi, F., Mohammadi, A.H., Toward "a predictive model for estimating dew point pressure in gas condensate systems". Fuel Process. Technol. 2013,116, 317—324.

Ashford, F.E. "An evaluation of critical multiphase flow performance through wellhead chokes". J. Petrol. Technol. 1974, 26 (8), 843—850.

Ashford, F.E., and Pierce, P.E.: "Determining Multiphase Pressure Drops and Flow Capacities in Downhole Safety Valves," Journal of Petroleum Technology, September 1975, pp. 45-52.

Bahadori, A.. "Estimation of flow coefficient for subsonic natural gas flow through orifice-type chokes using a simple method". J. Nat. Gas Sci. Eng. 9, 2012b, 39—44.

Bahadori, A. "A simple predictive tool to estimate flow coefficient for subsonic natural gas flow through nozzle-type chokes". J. Nat. Gas Sci. Eng. 2012, 7, 1—6.

Balan, B., Mohaghegh, S., & Ameri, S. (1995). State-Of-The-Art in Permeability Determination from Well Log Data: Part 1- A Comparative Study, Model Development. In *SPE Eastern Regional Meeting*. Society of Petroleum Engineers.

Baylar, A., Hanbay, D., Batan, M., "Application of least-square support vector machines in the prediction of aeration performance of plunging overfall jets from weirs". Exp. Syst. Appl. 36 (4), 2009, 8368—8374.

El-Gibaly, A.M. and Nashawi, I.S.: "Prediction of Two-Phase Flow through Chokes for Middle East Oil Wells," Paper SPE 36274 presented at the 1996 Abu Dhabi International Petroleum Exhibition and Conference, Abu Dhabi, U.A.E., 13-16 October.

Fortunati, F.: “Two-phase Flow through Wellhead Chokes,” Paper SPE 3472 presented at the 1972 SPE European Meeting, Amsterdam, The Netherlands, 16-18 May.

Freeman, J.A., and David, M.S.: “Neural Networks: Algorithms, Applications, and Programming Techniques,” Addison- Wesley Publishing Company, (1991).

Ghareeb, M. and Shedid, A.S.: “A New Correlation for Calculating Wellhead Production Considering Influences of Temperature GOR, and Water Cut for Artificially Lifted Wells,” Paper IPTC 11101 presented at the 2007 International Petroleum Technology Conference, Dubai, U.A.E., 4-6 December.

Gilbert, W.E.: “Flowing and Gas-Lift Well Performance,” API Drilling and Production Practices (1954) 143.

Guo, B., Bemani, A.S. and Ghalambor, A.: “Application of Sachdeva’s Choke Flow Model in Southwest Louisiana Gas Condensate Wells,” Paper SPE 75507 presented at the 2002 SPE Gas Technology Symposium, Calgary Alberta, Canada, 30 April - 2 May.

Leal J., Al-Dammen M., Villegas R., Bolarinwa S, Aziz A et al. "A New Analytical Model to Predict Gas Rate Volume Measurement Through Well Head Chokes" International Petroleum Technology Conference, Publisher: International Petroleum Technology Conference, 2013.

Mohaghegh, S., (2000). "Virtual-Intelligence Applications in Petroleum Engineering: Part 1—Artificial Neural Networks". Journal of Petroleum Technology, 52(09), 64–73.

Nokleberg, L., Sontvedt, T., “Erosion in choke valves-oil and gas industry applications”. Wear 186—187 (part 2), 1995, 401—412.

Omana, R., Houssier C., Brown K.E., et al.: “Multiphase Flow through Chokes,” Paper SPE 2682 presented at the 1969 SPE Annual Meeting, Denver, Colorado, 28 September - 1 October.

Osman, M.E., and Dokla, M.E.: “Gas Condensate Flow through Chokes,” Paper SPE 20988, presented at the 1990 European Petroleum Conference, The Hague, The Netherlands, 21-24 October.

Pelckmans, K., et al., 2002. LS-SVMlab: A matlab/c Toolbox for Least Squares Support Vector Machines. Tutorial. KULeuven-ESAT, Leuven, Belgium.

Perry, R.H.A.G.D., 1984. Perry's Chemical Engineer's Handbook, sixth ed. McGraw-Hill.

Poetmann, F.H., and Beck, R.L.: “New Charts Developed to Predict Gas-Liquid Flow through Chokes,” World Oil, March 1963, pp. 95-101.

Rodriguez, R., et al., 2013. A new analytical model to predict gas rate volume measurement through wellhead chokes. 6th International Petroleum Technology Conference. 2013, International Petroleum Technology Conference, Beijing, China.

Ros, N.C.J.: "An Analysis of Critical Simultaneous Gas-liquid Flow through a Restriction and its Application to Flow Metering," Appl. Sci. Res., 1960, pp. 374.

Ros, N.C.J.: "Simultaneous Flow of Gas and Liquid as Encountered in Well Tubing," Journal of Petroleum Technology, October 1961b, pp. 1037.

Ros, N.C.J.: Letter to Editor "Flow meter Formula for Critical Gas-Liquid Flow through a Restriction," Appl. Sci. Res., 1961a, pp. 295.

Sachdev, A.R., Schmidt, Z., Brill J.P. et al.: "Two-phase Flow through Chokes," Paper SPE 15657 presented at the 1986 SPE Annual Technical Conference and Exhibition, New Orleans, Louisiana, 5-8 October.

Shmilovici, A., 2005. "Support vector machines. In: Maimon, O., Rokach, L. (Eds.), Data Mining and Knowledge Discovery Handbook". Springer, US, pp. 257—276.

Surbey, D.W., Kelkar, B.G. and Brill, J.P.: "Study of Multiphase Critical Flow through Wellhead Chokes," SPE Production Engineering Journal, May 1989, pp. 142-146.

Suykens, J.A.K., Gestel, T.V., Brabanter, J.D., Moor, B.D., Vandewalle, J., "Least Squares Support Vector Machines". World Scientific Pub. Co., Singapore, 2002.

Tangren, R.F., Dodge, C.H. and Seifert, H.S.: "Compressibility Effects in Two-phase Flow," Journal of Applied Physics, July 1949, pp. 637-645.

Ubeyli, E.D., Least squares support vector machine employing model-based methods coefficients for analysis of EEG signals. Expert Syst. Appl. 37 (1), 2010, 233—239.

Wang, H., Hu, D. "Comparison of SVM and LS-SVM for regression". In: International Conference on Neural Networks and Brain. IEEE, Beijing, China, 2005, pp. 279—283.

Xavier-de-Souza, S., Suykens, J.A.K., Vandewalle, J., Bolle, D., "Coupled simulated annealing". Syst. Man Cybern. Part B: Cybern. IEEE Trans. 2010, 40 (2), 320—335.

Yao, J., Zhao, S., Fan, L., "An enhanced support vector machine model for intrusion detection". In: Wang, G.-Y., Peters, J., Skowron, A., Yao, Y. (Eds.), Rough Sets and Knowledge Technology. Lecture Notes in Computer Science. Springer, Berlin Heidelberg, 2006, pp. 538—543.

International Conference on Petroleum Engineering 2016 (ICPE-2016)
Bangladesh University of Engineering & Technology (BUET)
Dhaka-1000, Bangladesh

ICPE (2016-020)

Experimental Investigation of Multiphase Pressure and Temperature Loss Using High Pressure Flow Loop

Mohamed Abdalla Odan, Faraj Ben Rajeb, Syed Hasnain Haider Zaidi, Amer Aborig, Yan Zhang, Imtiaz Syed, Aziz Rahman
Faculty of Engineering & Applied Science
Memorial University of Newfoundland
St. John's, NL, Canada A1B 3X5

ABSTRACT

Multiphase flow is a multi-component flow which occurs in many industrial processes including those involved in the pharmaceutical, food, processing, and petroleum industries. Oil and gas exploration, production and transportation in arctic and offshore conditions are technically very challenging. In addition to the technical challenges involved in arctic operations, there are several environmental challenges posed by offshore operations. One of the operational challenges of hydrocarbon transmission through flow lines in offshore and arctic environments is the formation of hydrates. This imposes a severe flow assurance challenge in offshore operations. Hydrates can form during untreated water flow through a pipeline with high pressure in cold weather. This untreated water can characterize by their multiphase nature and therefore require flow assurance analysis and evaluation during each design stage of offshore project. The main goal of this study is to conduct experiments to understand how multiphase flow affects the formation of hydrates in flow lines. From the preliminary experimental results in the Multiphase Hydrate Flow loop at Memorial University of Newfoundland, we have observed that two-phase gas-liquid flow produces higher pressure in the flow lines compared to single- phase flow. Moreover, due to turbulence in the bends of the flow lines, there is an approximately 1°C local temperature increase in bends. In the future work related to this study, a parametric study will be presented to attempt to understand how multiphase hydrodynamic and pipe length scale (diameter) will affect the hydrate induction time. This study will also help to minimize flow assurance challenges in offshore flow lines and provide improved design conditions.

Key words: multiphase flow, carbon dioxide, pressure and temperature.

* Corresponding Author address
Email: mao274@mun.ca

1. INTRODUCTION

1.1. Literature Review

In the present work, flow phenomena of multiphase flows in a pipeline are studied. In the offshore oil and gas industry, one of the biggest challenges is to overcome flow assurance issues. This research investigates the fluid mechanics in a horizontal pilot scale experimental setup. Moreover, the fluid dynamics for different pipe angles are analyzed by studying the pressure drop and friction factor of different two-phase flows in relation to the liquid flow rate. The friction factor is a very important parameter for the extraction of oil from wells. The different frictional effects are the most significant input in the pressure drop between the oil reservoir in the ground and the oil platform. The total pressure drop is composed of the hydraulic pressure drop, the friction pressure drop and pressure drop through the fittings, instruments, and elbows in the pipe system. These pressure effects have an important influence on the output of the oil well and must be determined as accurately as possible to ensure economic feasibility of the oil production. If the pressure drop of a multiphase flow through a pipe is accurately known; the oil extraction can be optimized. The analysis of the different pressure phenomena in oil reservoirs and well- bores is important to forecast the effect of the pressure drop along the length of the pipeline. In particular, a large pressure drop has to be overcome if the permeability of the formation is poor. Therefore, the pressure drop in the well should be limited. In order to do so, the pressure drop and its causes have to be known as accurately as possible [1, 2]. Through this study of the pressure drop, oil industry is supported in avoiding problems such as those described above.

For a flow with a high Reynolds number shows a turbulent flow pattern. For turbulent flow, the friction factor depends on the wall roughness. At low flow rates a laminar sub layer exists on the pipe wall suppressing the influence of the pipe wall on the friction. At high flow rates this sub layer exists as well, but it is thin compared to laminar flow and the pipe roughness is significant [3]. This study helps to understand how the friction factor changes at different flow regimes in horizontal pipe sections, thereby optimizing the flow behavior in pipelines.

When considering the production of oil and gas (hydrocarbon fluids) from offshore gas systems, flow assurance is an important issue [4]. In particular, flow assurance is a major challenge in offshore and deep-water operations in the oil and gas industry. In a survey of 110 oil companies, the flow assurance was listed as the major technical problem in offshore energy development [3]. Understanding the arise of hydrate blockages in pipelines is crucial for the prevention of this important safety issue. Flow assurance covers the following topics in multiphase hydrocarbon production systems:

- Hydrates: The formation of ice and snow particles in high pressure, low temperature flow
- Waxes/asphaltenes: The deposition of solids in the pipeline, thereby reducing the flow capacity through the pipeline
- Slugging: The phenomenon caused by fluxes of the gas and liquid interface and liquid sweep-out by gas inertial effects
- Erosion: Wear of the pipe work and pipeline wall due to solid particles such as sand or liquid impingement
- Corrosion: Wear of the pipeline resulting in the reduction of wall thickness due to the chemical composition of the produced fluids
- Emulsion: Oil and water mixture at around 40-60% water cut that causes excessive pressure drop
- Scaling: Solid build-up, especially on the wellbore tubing, due to the chemical composition of produced water [3].

Production facilities, especially offshore wells and offshore transmission lines, may be operated under conditions where hydrate formation is favorable. Gas hydrate formation occurs when neutral gas molecules are surrounded by water molecules. These cages are known as “clathrates” [5]. Gas hydrates are similar in appearance to ice. Both materials have crystalline structures with similar characteristics. The important difference between ice and natural gas hydrates is the guest molecule that is an integral part of its structure [3, 6, 7]. Examples of typical hydrate forming gases include nitrogen, hydrogen sulfide (H_2S), carbon dioxide (CO_2), and light hydrocarbons (such as methane up to heptanes) [5]. Depending on the pressure, the gas composition, and gas hydrates can form at temperatures of up to 30 °C (86 °F) where gas co-exists with water [5, 8].

1.2. Objectives

The objectives of this project are:

- Develop an experimental setup for studying multiphase flow.
- Investigate of operations conditions such as pressure and temperature on multiphase pressure loss.
- Effect of CO_2 on pressure loss in a pipeline system.

2. EXPERIMENTAL SET-UP

The flow loop is a 20.574 m pipe (test section) open cycle system. The liquid can be pumped from the tank through 19.05 mm PVC pipe. Transparent PVC pipes are used to facilitate visualization. Currently, two-phase flow can be created by mixing the gas flow from the gas cylinder or air through airline and the liquid from the liquid line. Instrumentation includes eight pressure and temperature sensors, and flow meters for the gas and liquid pipes to measure the individual gas and liquid flow rate. The air injection pipe is also provided to run the pump. Manual control valves are installed in the liquid to facilitate control of the flow conditions and generate different flow regimes. The control of the flow loop is implemented through a fully integrated online computer system, which also handles the data acquisition. Figure 1 gives the lay out of the test section.

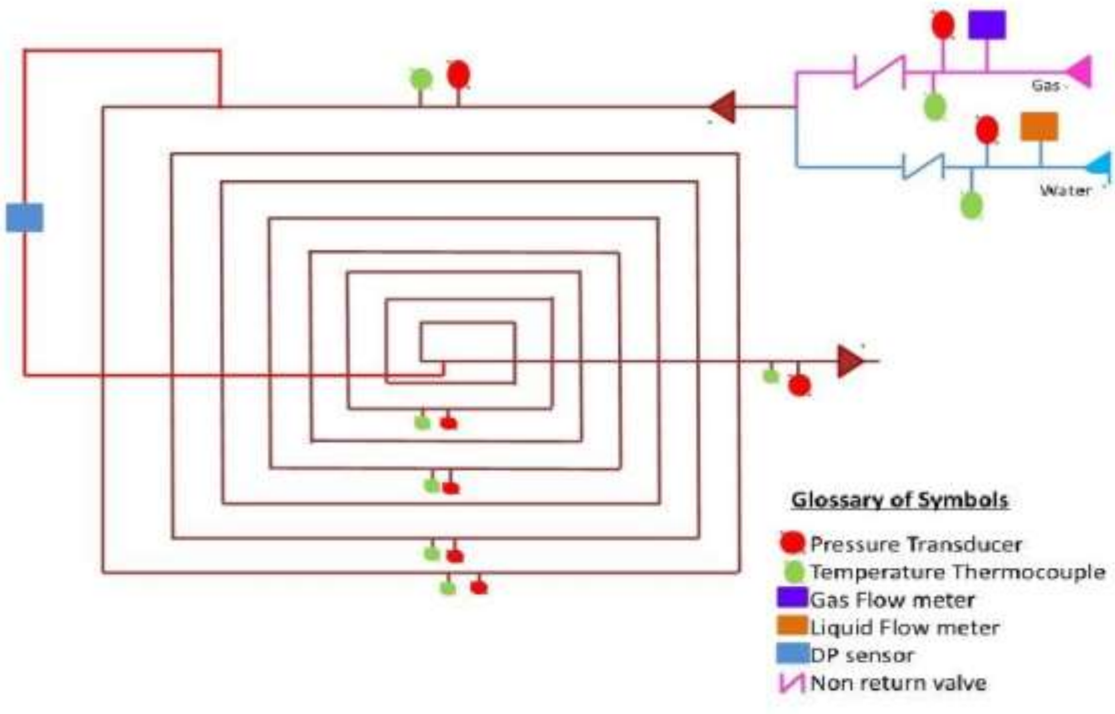

Figure 1: Experimental set-up of the test section of flow loop.

3. RESULTS AND DISCUSSIONS

3.1. Single Phase Experiments

Once the experimental setup was ready experiments for single phase (that was liquid) was conducted. Water is used as liquid medium and strategy was selected to keep increase the liquid flow rate from 0.25 L/S till 0.28 L/S and observe the behavior of pressure and temperature as shown in figure 2 and 3 respectively and data record for pressure and temperature data points are given below in Table 1and 2 respectively.

Table 1: Data points of pressure for single phase flow.

Liquid Flow rate (Q_L) (L/S)	Location of Pressure Sensors						
	Inlet 1.06 m	2.92 m	5.06 m	9.09 m	15.83 m	20.96 m	Outlet 25.22 m
	P1 (kPa)	P2 (kPa)	P3 (kPa)	P4 (kPa)	P5 (kPa)	P6 (kPa)	P7 (kPa)
0.25 (L/S)	113.280	109.626	92.3208	83.633	72.188	48.883	25.717
0.26 (L/S)	133.482	127.621	107.76506	97.078	84.322	58.743	31.853
0.27(L/S)	150.926	146.237	126.449	115.762	99.973	66.120	32.819
0.28(L/S)	164.715	155.100	138.998	125.829	106.317	72.188	39.713

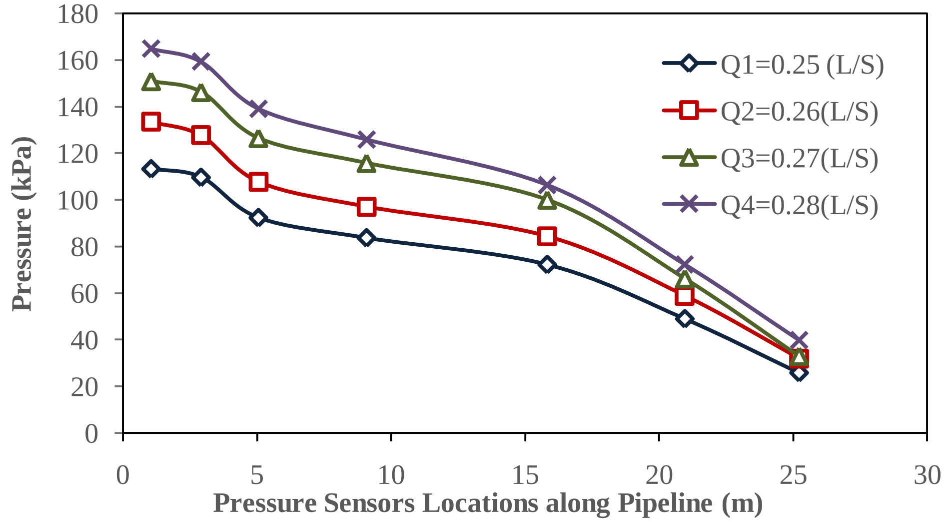

Figure 2: Pressure profile for single phase flow.

Figure 2 show us that we can rise the local pressure through the loop pipeline by increasing water flow rate. Also, we can observe the decline of pressure for the same flow rate as the flow reach far points in the loop. This can match the basics of Bernoulli equation for pipeline flow.

Table 2: Data points of temperature for single phase flow.

Liquid flow rate $Q_{L,}$ (L/S)	0.28 (L/S)	0.27 (L/S)	0.26 (L/S)
Location	T (°C)	T (°C)	T (°C)
Inlet 0.96 m	19.75	19.71	19.69
3.67 m	19.78	19.76	19.73
7.73 m	19.96	19.94	19.9
13.59 m	20.06	20.03	19.98
18.95 m	20.09	20.05	20.02
22.70 m	20.23	20.21	20.2
Outlet 23.67 m	20.77	20.68	20.58

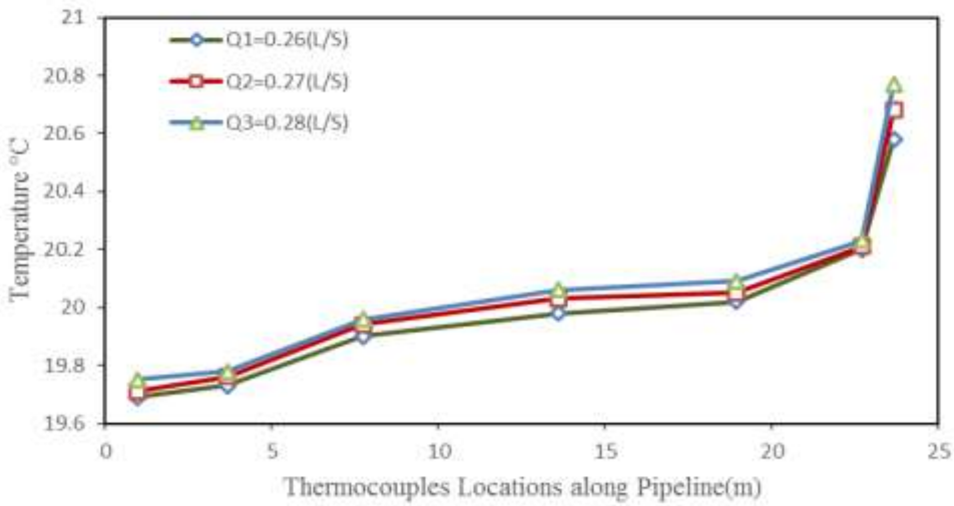

Figure 3: Temperature profile for single phase flow.

Figure 3 explains the temperature distribution along with pipeline loop at chosen locations for the same flow conditions as a Figure 2 There is a gradual rise in temperature as the flow go during the tube. This occurs due to the friction effects on water. The sharp rise of temperature at last meter of the loop because of sudden change of flow direction.

3.2. Two Phase Flow

Similarly, experiments conducted for two phase flow taking water as liquid phase and air as gas phase. The strategy that was obtained for conducting experiments including for each test run keep the liquid flow at constant rate and increasing the flow rate of gas for first test and obtain three data points. Change the flow rate of liquid for second test and repeat the same process.

Results for first case (TEST-1) where liquid phase was kept constant at 0.553 (L/S) and gas flow rate was kept on increasing is shown in Table 3.

Table 3: Data for two phase flow at liquid flow rate is constant.

Pump inlet air pressure = 68.9476 kPa and liquid flow rate = 0.553 (L/S)							
Gas flow rate Q_g (L/S)	Location of Pressure Sensors						
	Inlet 1.06 m	2.92 m	5.06 m	9.09 m	15.83 m	20.96 m	Outlet 25.22 m
	P1 (kPa)	P2 (kPa)	P3 (kPa)	P4 (kPa)	P5 (kPa)	P6 (kPa)	P7 (kPa)
3.903(L/S)	191	185	173	152	125	86	47
5.177(L/S)	230	226	200	183	149	107	59
6.880(L/S)	278	265	244	224	181	130	78

The graphical representation of the experiments in shown in Figure 4.

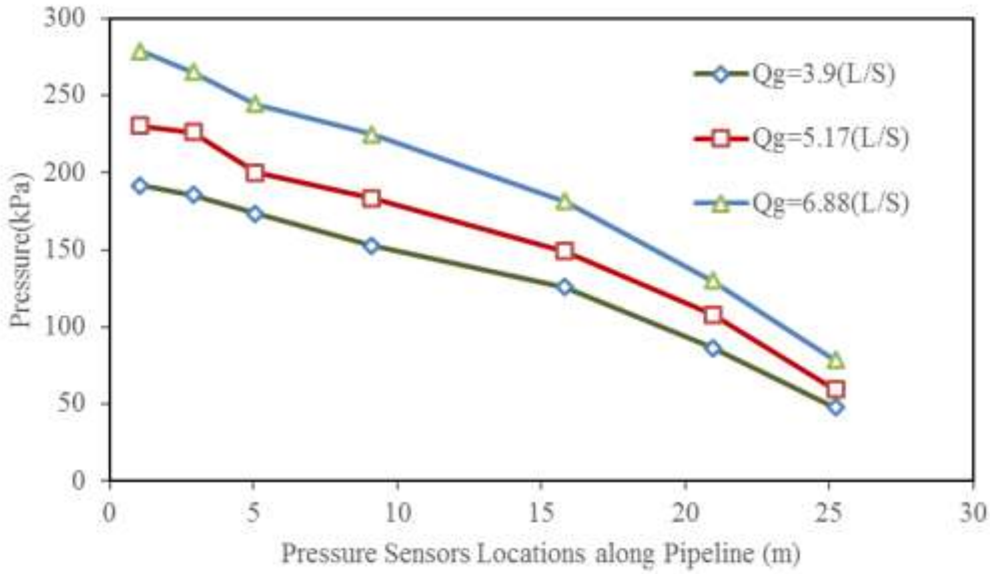

Figure 4: Results for Two phases flow TEST-1

The Results for first case (TEST-2) where liquid phase was kept constant at 0.362 (L/S) and gas flow rate was kept on increasing is shown in Table 4.

Table 4: Data for two phase flow at liquid flow rate is constant.

Pump Inlet Air pressure = 68 kPa and liquid flow rate = 0.362 (L/S)							
Gas flow rate Q_g (L/S)	Location of Pressure Sensors						
	Inlet 1.06 m	2.92 m	5.06 m	9.09 m	15.83 m	20.96 m	Outlet 25.22 m
	P1 (kPa)	P2 (kPa)	P3 (kPa)	P4 (kPa)	P5 (kPa)	P6 (kPa)	P7 (kPa)
2.831(L/S)	105	101	86	77	65	41	19
4.511(L/S)	165	156	139	124	101	69	35
6.371(L/S)	186	179	157	142	116	81	46

The graphical representation of the experiments in shown in figure 5.

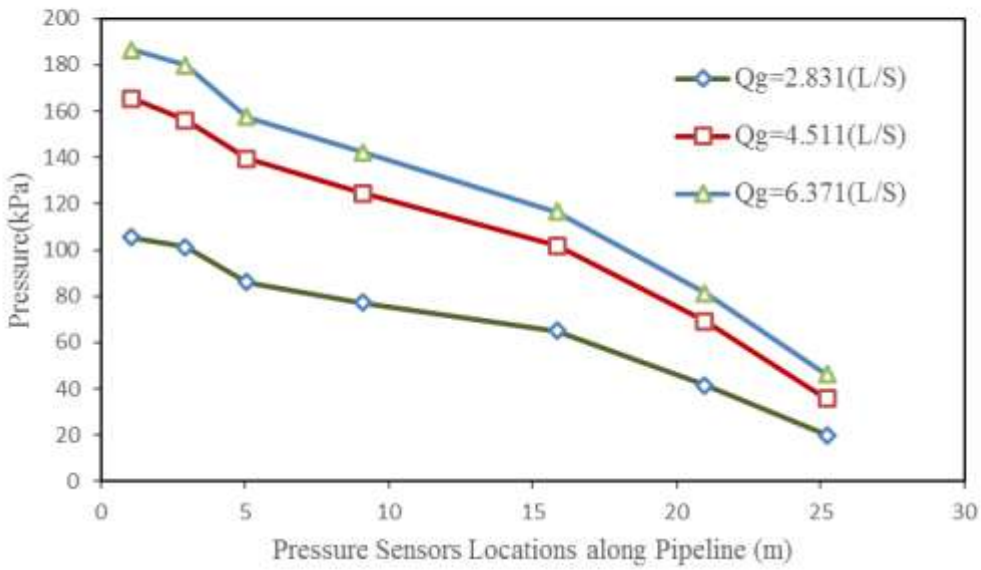

Figure 5: Results for Two phase flow TEST-2.

Figures 4 and 5 for the two-phase flow (Air & Water) give us the same trend for pressure drop as one phase flow, but two phase flow can result in pressure higher than one phase flow. The two figures show us that increasing liquid and gas flow simultaneously can result in high loop pressure.

Table 5: Data for two phase flow at different liquid flow rate

liquid flow rate Q_L, (L/S)	Gas flow rate Qg (L/S)	Pressure P4 (kPa)	Pressure P6 (kPa)	Differential Pressure ΔP, (kPa)
0.553(L/S)	3.90	152.92	86.39	66.39
	5.17	183.60	107.97	76.43
	6.88	224.97	130.17	94.80
0.36(L/S)	2.83	77.15	41.43	35.72
	4.51	124.51	69.15	55.36
	6.37	142.23	81.42	60.81

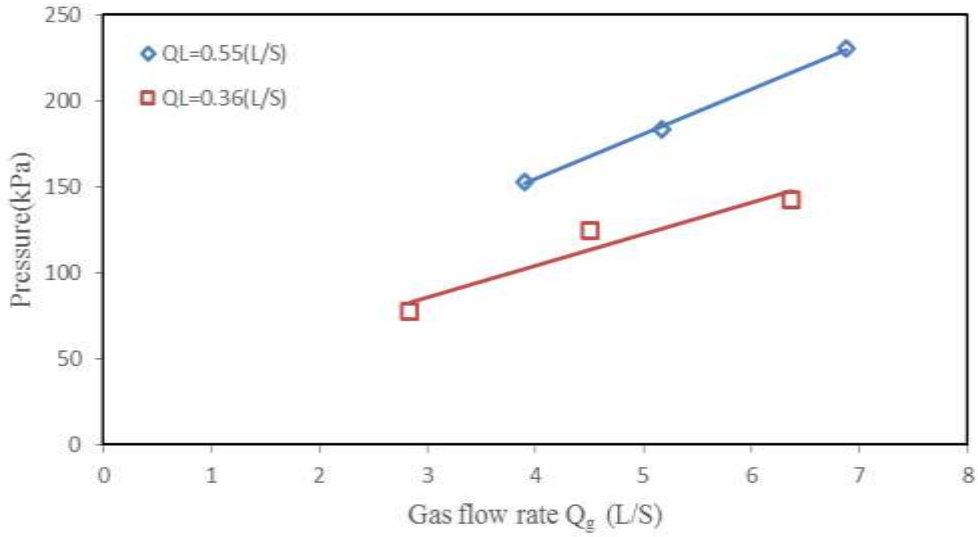

Figure 6: Effect of increasing Liquid & Gas flow rates on Loop Pressure at 9, 20m locations.

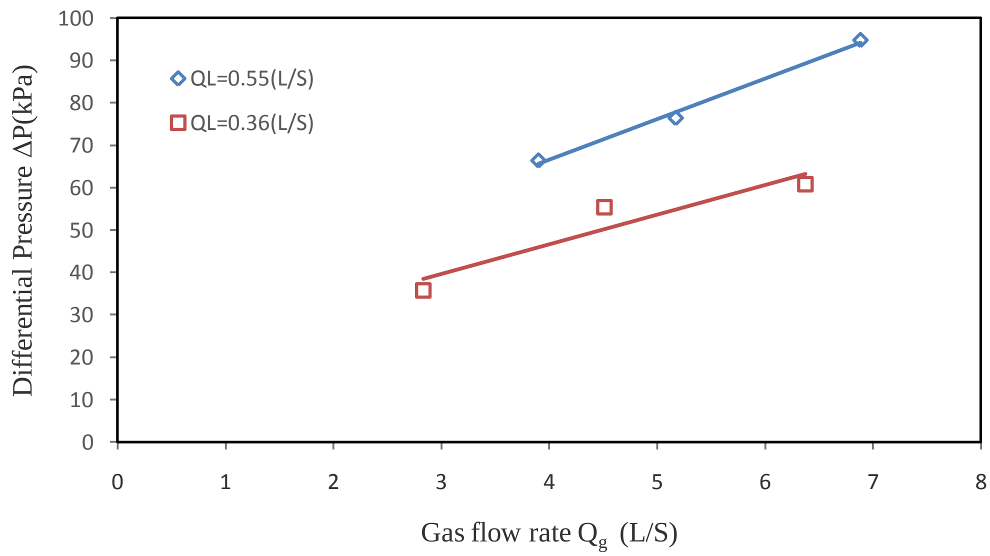

Figure 7: Effect of increasing Liquid & Gas flow rates on differential Pressure (P_4-P_6).

Figures 6 and 7 indicate the result that we obtain from figures 4, 5. And Figure 7 explain relationship between gas flow rate and differential pressure for two locations on the loop.

3.3. Pressure Comparison at Using (CO2 - Water) & (Air –Water) as Second Phase Flow.

Table 6: (CO_2 - Water) & (Air –Water) results comparison

Gas Flow Rate Qg (mL/S)	CO_2 differential pressure (ΔP) kPa	Air differential pressure (ΔP) kPa
6.970	42.333	92.941
6.994	65.638	168.163
7.027	75.773	175.609
7.0367	112.108	183.676

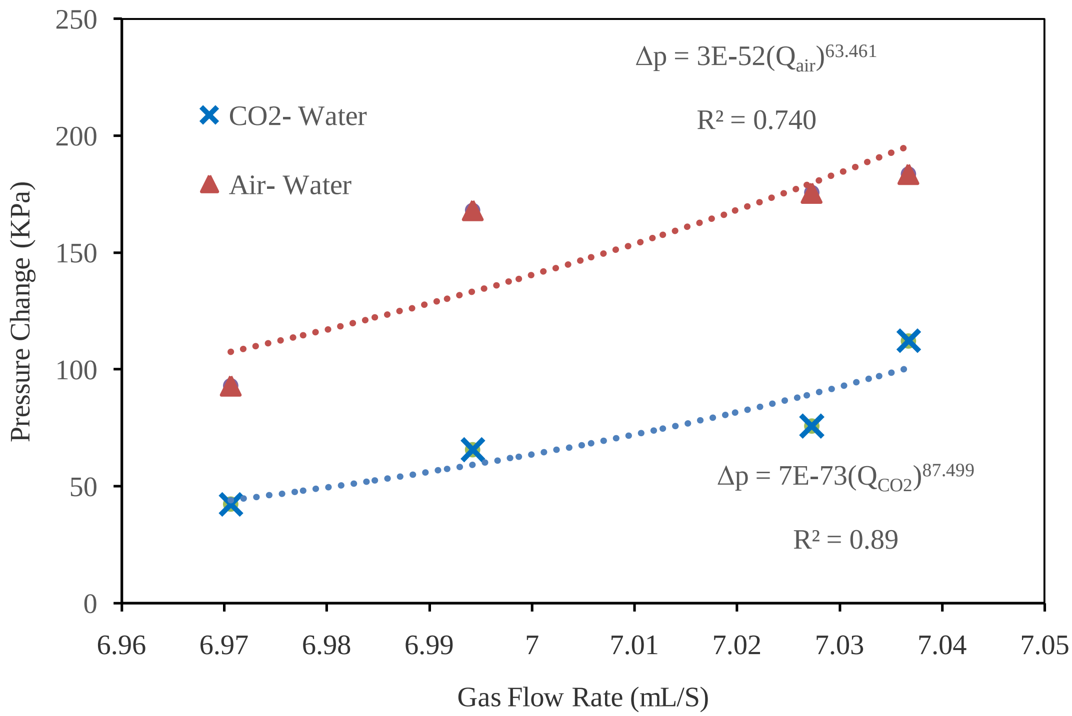

Figure 8: Pressure drop comparison (CO_2 - Water) & (Air –Water) along Pipeline.

The comparison between using (CO_2 - Water) & (Air –Water) as a second phase in the loop in Figure 8 to explain that we can get high pressure from using Air for the same gas flow rates when we use CO_2.

3.4. Temperature Comparison at Using (CO2 - Water) & (Air –Water) as Second Phase Flow.

Table 7: (CO_2 - Water) & (Air –Water) results comparison.

CO_2 Gas Flow Rate (mL/S)	Air Gas Flow Rate (L/S)	Temperature Drop (CO_2 - Water), °C	Temperature Drop (Air –Water), °C
6.97	2.826	0.11	0.4
6.99	3.832	0.17	0.4
7.02	6.678	0.15	0.41
7.03	8.075	0.22	0.5

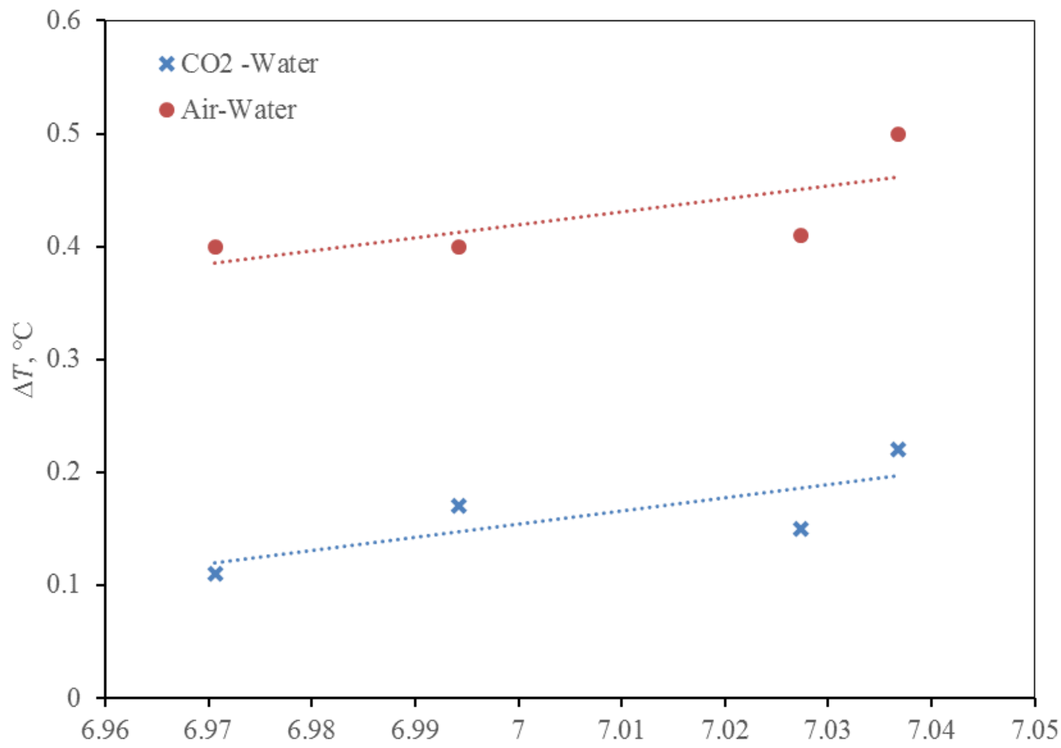

Figure 9: Temperature drop comparison (CO_2 - Water) & (Air –Water) along Pipeline.

Different gas flow rates have been used for (CO_2 - Water) & (Air –Water) in Figure 9 and the comparing is about the effecting of using the two gases on loop temperature. It’s clearly that the using of Air result in differential temperature higher than using of CO_2.

4. Conclusions and Recommendations

- A multiphase flow loop has been developed and experiments conducted initially for single phase, then for two phase. Calibration of sensors has been already done. This flow loop is a lab scale experimental facility to study the multiphase flow and as well as hydrate induction process.
- Experiments for single phase (water) was conducted. Strategy was selected to keep increase the liquid flow rate from 0.25 L/S till 0.28 L/S and the behavior of pressure and temperature has observed.
- In the same way, experiments conducted for two phase flow taking (water and air). Thus, CO_2 has used with water for other experiments. Pressure and temperature has recorded at different location on the loop.
- The trends of single phase and two phase flow indicates decrease in pressure or increase in pressure drop with length, which is a good indication that pressure in decreasing over length due to a long profile and a lot of elbows, However temperature profile is not much affected because the experiments was conducted at room temperature that do not effect temperature.
- Using CO_2 or Air as a second phase in the loop can result in different values of differential pressure and temperature.
- To study the hydrate formulation processing flow loop needs to place in a cold room which will be our plane in future work.
- Flow Regimes in Horizontal Pipes sholud be Investigated, and friction influence in pressure loss shuld be considered.

REFERENCERS

H. Asheim, J. Kolnes and P. A. Oudeman, Flow Ressistance Correlation for Complete Wellbore, Jornal of Petroleum Science and Engineering, 8, 97-104,1992.

R. S. Schulkes, T. Rinde and O. H. Utvik, Pipe Flow with Radial Inflow: Experimental and Modeling Work, Jornal of Fluids Engineering, 121, 106-111, 1999.

G. W. Govier and K. Aziz, The Flow of Complex Mixtures in pipes, New York: Van Nostrand Reinhold Ltd., 1972.

A. C. Metha and U. C. Klomp, An Industry Perspective on the State of the Art of Hydrates Management, paper 4001 presented at the 2005 Fifth International Conference on Gas Hydrates, Trondheim, June 13-16.

L. W. Clark, L. M. Frostman, SPE and J. Anderson, Low-Dosage Hydrate Inhibitors (LDHI): Advances in Flow Assurance Technology for Offshore Gas Production Systems, International Petroleum Technology Conference, Doha, Qatar, 21-23 November 2005.

R. Corfield, Close encounters with crystalline gas, Chemistry in Britian, 22, May 2002.

Y. F. Makogon, Hydrates of Natural Gas, Tulsa, Oklahoma: PennWell Publishing Co., 1981.

Y. Taitel and A. E. Dukler, A model for predicting flow regime transitions in horizontal and near horizontal gas-liquid flow, AIChE Journal, Volume 22, Issue 1, pages 47-55, January 1976.

T. Knott, Holding hydrates at bay, Offshore Engineer (Feb. 2001) 29.

O. Bratland, Pipe Flow 1 - Single-phase Flow Assurance, Ove Bratland, 2013.

O. Bratland, Pipe Flow 2 - Multi-Phase Flow Assurance, Bratland Ove, 2013.

International Conference on Petroleum Engineering 2016 (ICPE-2016)
Bangladesh University of Engineering & Technology (BUET)
Dhaka-1000, Bangladesh

ICPE (2016-027)

Compressed Biogas from Maize Waste

Sadia Saberin[a]*, Rupack Ranjan Halder[a], Ijaz Hossain PhD[a], Md. Abdur Rouf, PhD[b], Taposhi Rabeya[b], Ajay Kanti Mondal[b], Shahed Israil Kan[c]

[a]Department of Chemical Engineering, Bangladesh University of Engineering and Technology, Dhaka, Bangladesh.

[b]Institute of Fuel Research and Development, Bangladesh Council of Scientific and Industrial Research, Dhaka, Bangladesh.

[c]Chicks & Feeds Limited, Dhaka, Bangladesh

ABSTRACT

Maize (Zea mays) has burgeoning demand as energy crop for biogas production and is considered to have the highest yield potential of field crops. In Bangladesh, about 27.5 lakh tons of maize is grown in 2015-2016 to meet the food demand and the needs of poultry feed sector. The maize stover is left over and has little economic value besides lying in the fields or some being used as fuel. Rotting of plants gives off methane which is a contributor to green house gas. But if it is utilized in a process, it can be converted into useful feedstock to produce biogas and the solid content of the sludge can also be used as fertilizer. This research was aimed at compressed biogas (CBG) production from maize plant by anaerobic digestion process. Several experiments were performed in variable condition where anaerobic digestion of maize stover was observed with cow dung and without cow dung. Methane production was observed for 60~100 days in batch digester at 33°C. Startup and retention time of anaerobic digestion was longer and biogas yield was lower in normal condition. To increase specific biogas yield, two types of pretreatment processes were performed. One treatment was done with dirty water and the other with sodium hydroxide. These effects are briefly discussed with characteristic graphs. Maximum yield of biogas and approximate CBG was found 0.271m^3/kg and 0.1195kg with cow dung. Methane content of produced biogas was (55~70) % which can be converted to CBG consisting ≥97% methane. It would be a successful attempt if maize waste is implemented for producing CBG as an alternative source of CNG in Bangladesh as a renewable source of energy to mitigate the emerging energy crisis.

Keywords: CBG, maize stover, anaerobic digestion, biogas, water scrubber, desulphurization, compression, energy crisis.

* Corresponding Author address
Email: tsaberin@gmail.com

1. INTRODUCTION

Sustainable energy is the form of energy obtained from non-exhaustible resources which includes renewable energy sources, such as hydroelectricity, solar energy, wind energy, wave power, geothermal energy, bioenergy, tidal power and also technologies designed to improve energy efficiency. Technologies are being promoted in the energy transition from fossil fuels to ecologically sustainable systems, which support 100% renewable energy. Renewable energy sources are clean, eco friendly, sustainable and a suitable substitute for fossil fuels.

Renewable energy is derived from natural processes such as biomass from energy crop, animal manure, solid waste, biogas from organic waste, biodiesel from vegetable oil etc. Energy is an attribute of all biological systems from the biosphere to the smallest living organism. Within an organism it is responsible for growth and development of a biological cell or biological organism. Energy is stored by cells in the structures of molecules of substances such as carbohydrates, lipids and proteins which release energy when reacted with oxygen in respiration.

Anaerobic digestion is completely natural and biological process. The main objective of this thesis is to study the scope and possibilities of anaerobic digestibility of maize waste on producing biogas in Bangladesh. It also incorporates thorough study on physical, biological characteristic of maize. The demand of maize is increasing day by day not only as food but also energy crop. Because of its increasing demand and availability, it can be a good source of renewable energy to meet the existing crisis in Bangladesh.

2. DEMAND OF MAIZE IN BANGLADESH

Maize is one of the oldest and most important crops in the world. It is the highest yielding grain crop having multiple uses. It is revealed that area, production, and yield of maize is increasing for maize in each year. Its position is 1^{st} among the cereals in terms of yield [(maize: 7 tonnes/ha; wheat: 3.5 tonnes/ha and rice: 4tonnes/ha) (2016)] but in terms of area and production, it ranks 2nd just after rice and relegating wheat to third. Major maize growing districts are Chuadanga, Dinajpur, Bogra, Lalmonirhat and manikganj based on intensity of maize area.

Demand for maize is increasing day by day in the world as well as in Bangladesh due to its diversified uses. Farmers are switching to maize cultivation in increasing numbers because of better prices of the cereal and high demand by feed and flour mills. Areas under maize cultivation rose 9 percent to 4.09 lakh acres in 2010-11, according to data from Bangladesh Bureau of Statistics. Maize output rose to 27.5 lakh tonnes in 2015-16 from the year 2010-11 while the output was around 10.18 lakh tonnes, according to BBS data. Having lower cultivation cost amd being more profitable than rice, are reasons that attracted farmers to maize, a key ingredient of poultry and other feeds.

Crop duration*:* The average crop duration of maize was found 157 days. The highest crop duration was also found in Lalmonirhat (168 days) followed by Dinajpur (163 days), Bogra (151 days), and Chuadanga (147 days)

Harvesting time*:* Maize is harvested from 3rd week to 4th week of March to 3rd week to 4th week of May or 1 week of June. Another season of maize seed sowing on 3 weeks of October and it continued upto the last week of December.

3. ANAEROBIC DIGESTION

Anaerobic microorganisms digest the organic materials in the absence of oxygen, to produce methane and carbon dioxide contains small amount of hydrogen sulfide (H_2S) and ammonia (NH_3), as well as trace amounts of other gases as end-products. Many microorganisms affect anaerobic digestion, including acetic acid-forming bacteria (acetogens) and methane-forming archaea (methanogens). These organisms promote a number of chemical processes in converting the biomass to biogas.
Intermediate end products are primarily alcohols, aldehydes, and organic acids, plus carbon dioxide. In the presence of specialized methanogens, the intermediates are converted to the end products of methane, carbon dioxide and trace levels of hydrogen sulfide.

In an anaerobic system, the majority of the chemical energy contained within the starting material is released by methanogenic bacteria as methane.

The equation for fuel production from anaerobic digestion7 is as follows:

$$C_xH_yO_z + (x–y/4–z/2)H_2O \rightarrow (x/2 – y/8 + z/4)CO_2 + (x/2 + y/8 – z/4)CH_4$$

Anaerobic digestion can be better explained in four stages. Such as: hydrolysis, acidogenesis, acetogenesis and methanogenesis.

3.1 Hydrolysis

In most cases, biomass is made up of large organic polymers. The process of breaking these chains and dissolving the smaller molecules into solution is called hydrolysis. Therefore, hydrolysis of these high-molecular-weight polymeric components is the necessary first step in anaerobic digestion. Through hydrolysis the complex organic molecules are broken down into simple sugars, amino acids, and fatty acids.

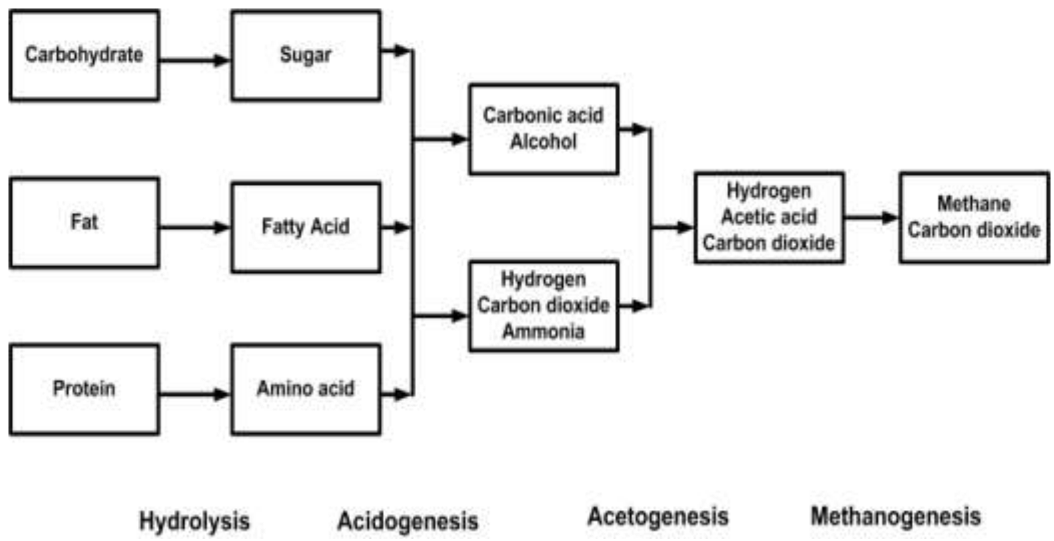

Figure 1. Simplified process diagram of anaerobic digestion process

3.2 Acidogenesis

In this stage those sugar molecules, fatty acids and amino acids broken down further into alcohols and volatile fatty acids with by-products of carbon dioxide, ammonia and hydrogen sulfide.

3.3 Acetogenesis

In this stage those volatile fatty acids and alcohols are converted again, this time into hydrogen, carbon dioxide, and acetic acid.

3.4 Methanogenesis

In this stage, methanogens use the intermediate products of the preceding stages and convert them into methane, carbon dioxide, and water. Methanogenesis is sensitive to both high and low pHs and occurs between pH 6.5 and pH 8. The remaining, indigestible material the microbes cannot use and any dead bacterial remains constitute the digestate.

4. BIOGAS

Biogas is a product of bio-methanation process when fermentable organic materials such as cattle dung, kitchens waste, poultry droppings, night soil wastes, agricultural wastes etc. are subjected to anaerobic digestion in the presence of methanogenic bacteria. The digested slurry from biogas plants is available for its utilization as bio/organic manure in agriculture, horticulture and pisciculture as a substitute/supplement to chemical fertilizers. Bio-methanation process of converting biomass into gaseous fuel is superior and a sustainable process that can be processed in biogas plants. Biogas plants provide three-in-one solution of gaseous fuel generation, organic manure production and wet biomass waste disposal/management.

The composition of biogas varies depending upon the origin of the anaerobic digestion process and the type of feedstock. Normally methane content varies from (50~75) %. Carbon dioxide content varies between (25~50) %. There is a trace amount of hydrogen sulfide, hydrogen, oxygen and nitrogen. Biogas can be further treated to increase the methane content according to the demand and use.

4.1 Compressed Biogas (CBG)

After separating impurities such as moisture, carbon dioxide and hydrogen sulfide and generating pure methane from biogas, it is filtered, compressed and filled in a gas bottle i.e. a CNG bio-methane (purified biogas) which is nearly same as CNG. It can be used for all applications for which CNG are used.

Purified biogas (bio-methane) has a high calorific value in comparison to raw biogas. CNG quality of Compressed Biogas (CBG) is used as vehicular fuel in addition to meeting stationary & motive power, electricity generation thermal application etc. The purity of biogas is more than 95% Methane and compressed to 200~250 bar pressure for filling in cylinders. The purified biogas is filled in CNG cylinder and supplied to mid-day meal scheme, mess, hotel, industries etc. for various purposes such as cooking & heating etc. Calorific value of purified biogas is equivalent / similar to CNG.

5. BIOGAS PURIFICATION AND BOTTLING

Biogas is purified of all impurities and moisture. Pure methane gas is than compressed. This process has two parts. First part deals in separating impurities such as moisture, carbon dioxide and hydrogen sulfide and generating pure methane from biogas. Second part deals in filtering, compressing and filling Methane in a gas bottle i.e. a CNG dispenser making it suitable as an IC engine fuel.

5.1 Purification

Biogas can be extracted to pure and high calorific value fuel methane from low calorific fuel biogas to make it an IC Engine suitable fuel. Once pure Methane is available in suitable quality and quantity it finds a wide range of applications from running an oil engine, driving a motor car engine to operating a gas turbine for rural power generation. Biogas generated from the digester is allowed to flow through moisture traps. This process drains out the moisture present in the gas. Then sulfides are removed. Treated gas is pressurized with the help of a primary compressor. The pressurized clean gas is than passed through a physical separation device. The physical separation device is a specially designed modern high pressure combined directional flow device for cleaning biogas of it high impurities.

A number of gas upgrading technologies have been developed for the treatment of biogas however not all of them are recommended for the application with biogas because of the price and/or environmental concerns.

5.1.1 Hydrogen sulfide removal

Hydrogen sulfide must be removed in order to avoid corrosion. The most common methods for hydrogen sulfide removal are:

- Air/oxygen dosing to digester biogas

- Iron chloride dosing to digester slurry
- Iron oxide
- Activated carbon-water scrubbing
- NaOH scrubbing

Biological desulphurization of biogas can be performed by micro-organisms. Most of the sulfide oxidizing microorganisms belongs to the family of *Thiobacillus* and it is essential to add stoichiometric amounts of oxygen to the biogas.

5.1.1.1 Air/oxygen dosing to biogas

Digester is the simplest method of desulphurization. It consists in addition of oxygen or air (2 to 6% air in biogas) directly in the digester or in a storage tank serving at the same time as gas holder. Measures of safety have to be taken to avoid overdosing of air because biogas in air is explosive in the range of 6 to 12% depending on the methane content. In large digestion plants, there is often a combined procedure of water scrubbing and biological desulphurization.

5.1.1.2 Iron chloride dosing to digester slurry

It consists in feeding iron chloride directly to the digester slurry or in a pre-storage tank. It reacts with produced hydrogen sulfide to form iron sulfide salt (particles). This method is very effective in reducing high H_2S level but less effective to attain low and stable levels such as for vehicle fuel demands.

5.1.1.3 Iron oxide

Iron oxide (or hydroxide) also reacts with H_2S. The reaction is slightly endothermic (minimal temperature of 12°C) and the biogas should not be too dry since the reaction needs water. The iron sulfide formed can be oxidized with air so that the iron oxide is recovered. This process is highly exothermic. Usually an installation has two reaction beds. While the first one is desulfurizing the biogas, the second is regenerated with air. Iron oxide wood chips or iron oxide pellets can be used.

5.1.1.4 Activated carbon

Activated carbon is also used to adsorb sulfide. H_2S has to be converted before into sulfur and water, in presence of air which is added to the biogas.

5.1.2 Carbon dioxide removal

Removal of carbon dioxide enhances the energy of the gas either to reach vehicle fuel standard or natural quality gas. Four different methods are used commercially to achieve it:

- Water scrubbing
- Polyethylene glycol scrubbing
- Carbon molecular sieves

- Membranes separation

5.1.2.1 Water scrubbers

It is used to remove carbon dioxide and hydrogen sulfide, since these gases have higher water solubility than methane. The absorption process is purely physical. The water used can be regenerated and recirculated.

5.1.2.2 Polyethylene glycol scrubbing

It is a physical process like water scrubbing. The difference is that carbon dioxide and hydrogen sulfide are more soluble in this solvent and therefore smaller quantities of scrubbing media are required. In addition, water and halogenated hydrocarbons are also removed when scrubbing biogas with polyethylene glycol. This scrubbing is always done with recirculation.

5.1.2.3 Carbon molecular sieves

Molecules are adsorbed in the cavities of the molecular sieve but not irreversibly bound. The selectivity of adsorption is achieved by different mesh sizes and or application of different gas pressure. When the pressure is released the compounds from the biogas are desorbed.

5.1.2.4 Membrane Separation

There are two basic gas purification membrane systems. One is the high pressure gas separation which uses gas on both sides of the membrane. The membranes (made of acetate-cellulose) separate the small polar molecules such as carbon dioxide, moisture and hydrogen sulfide. In the low-pressure gas liquid adsorption separation, the essential element is a hydrophobic micro porous membrane separating the gaseous from the liquid phase. The molecules from the gas stream, flowing in one direction which is able to diffuse through the membrane will be absorbed on the other side by the liquid flowing in counter current.

5.2 Bottling

It employs with bottling this clean methane gas into a standard CNG bottle. The cleaned methane gas is than taken into a 3-Stage high-pressure compressor. The compressor compresses the gas from

a. atmospheric to 10 kg/cm^2 in stage I

b. 10 kg/cm^2 to 60 kg/cm^2 in stage II

c. 60 kg/cm^2 to 250 kg/cm^2 in stage III

This pressure is considered suitable to fill up a CNG bottle rack. This CNG bottle rack can than be connected to a standard CNG dispenser unit which is ready to be used as fuel in a motor car, or run a gas turbine or any CNG converted internal combustion engine connected to an alternator to produce electricity.

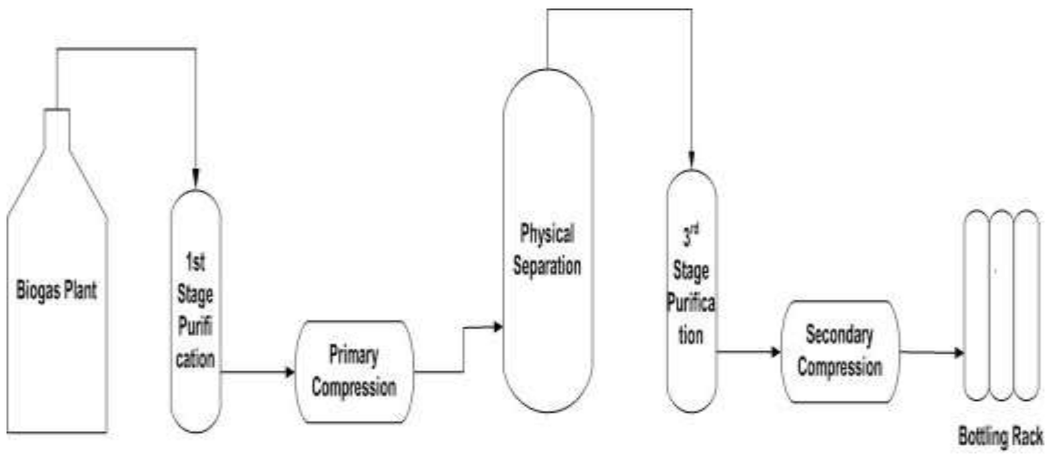

Figure 2. A simplified process flow diagram of biogas purification and bottling plant

6. USE OF DIGESTATE

Anaerobic digestion draws carbon, hydrogen and oxygen from the feedstock. Essential plant nutrients (N, P, and K) remain largely in the digestate. The use of digestate depends on its quality as well as the type of plant producing it. Depending on local regulations and conditions, strict limits exist for the total annual application of nitrogen, co-substrate and heavy metals introduced into the soil. Large scale commercial AD plants may find it worthwhile to further process the digestate to increase its value to markets. The digestate have to be dewatered and separated into two fractions: the fiber and the liquor. It leads to a reduction in application costs and permitting much better for land nutrient deficiencies. The fiber is bulky and contains a low level of plant nutrients which can be used as a soil conditioner and as a low grade fertilizer. Further processing of the fiber can produce good quality compost. The liquor (liquid effluent) contains a large proportion of nutrients and can be used as a fertilizer. A wider market has yet to be fully developed such has use in hydroponic systems or to grow aquatic weeds or fish. Many AD plants also reuse the liquor in their process.

7. CO-DIGESTION

Co-digestion is a process whereby energy-rich organic waste materials (e.g. Fats, Oils, and Grease (FOG) and/or food scraps) are added to dairy or wastewater digesters with excess capacity. In addition to diverting food waste and FOG from landfills and the public sewer lines, these high-energy materials have at least three times the methane production potential (e.g. biogas) of biosolids and manure.

There are several advantages to co-digestion of animal manures and slurries with others organic wastes. The primary advantage is the enhancement of the biogas yield per m^3 of reactor with consequent financial benefits for the plant operator. Solid wastes are converted into pumpable slurries when mixed with liquid manure. This can result in easier handling both in the digestion process and afterwards. Co-digestion results in more efficient digestion of certain organic materials. This may also be due to other synergistic effects of the mixed digestion process. In Denmark, these plants are now competing with each other for access to high biogas generating potential wastes coming from sources other than farms.

8. INCREASING BIODEGRADABILITY OF MAIZE

Maize stover is lignocellulosic biomass. The complex structure of lignocellulosic biomass provides a primary protective barrier that prevents cell destruction by chemical or biological methods, leading to lower digestion rate and biogas yield. This is the main reason why corn stover is usually not used alone as sole feedstock for biogas production. Pretreatment prior to anaerobic digestion has been proven to be one of simple and effective methods to improve biodegradability and biogas production of lignocellulosic materials. The physical structure and chemical compositions of lignocellulosic materials could be altered through various pretreatments which render the compositions in lignocellulosic materials more accessible and more readily biodegradable to anaerobic microorganisms. There are a number of methods available for the pretreatment of crop residues, such as size reduction, steam explosion, fungi biodegradation, ammonification, acidic and alkaline treatment. Compared to other pretreatment methods, chemical pretreatment method has advantages in terms of easiness, fastness, and effectiveness.

White rot fungi use a variety of mechanisms to accomplish the complete degradation of lignin and a wide variety of environmental pollutants. Both oxidative and reductive reactions are required for the metabolism of both lignin and environmental pollutants. The fungi secrete a family of peroxidases to catalyze both direct and indirect oxidation of chemicals. The peroxidases can also catalyze reductions using electron donors to generate reductive radicals. Lignin is highly oxidized so it is difficult to oxidize further. Lignin is a complex heteropolymer with no stereochemical regularity, due at least in part to the free radical mechanism of synthesis. Lignin biodegradation must therefore involve a nonspecific and nonstereoselective mechanism.

Acids and alkalis are mostly used chemicals for pretreatment. Compare to acidic pretreatment, alkaline method has practical advantages, especially when such pretreatment is to be followed by anaerobic digestion. The feedstock pretreated by acid has low pH due to remaining acids. Neutralization is required prior to anaerobic digestion. This would significantly increase pretreatment cost. However, the alkali remaining after pretreatment is still useful since the anaerobic digestion of lignocellulosic feedstock generally requires alkalinity addition for pH control. This makes alkali pretreatment method more attractive to practical application.

Compared to conventional pretreatment of alkali solution, solid state NaOH pretreatment is simpler, more cost-effective and more environmentally friendly. The chemical compositions, chemical structures and physical characteristics of lignocellulosic biomass would be changed during alkali pretreatment process, due to the complex physical and chemical roles of alkali. The changes include fiber swelling, decrease of the association of lignin with carbohydrate and some degradation and solubilization of lignin and carbohydrate. These changes work together to contribute to the improvement on biodegradability. The biodegradability of the NaOH-treated corn stover was improved through complex physical and chemical roles of NaOH. 6% NaOH-treated corn stover achieved higher TS and VS reduction as compared to the untreated stover for all loading rates. As a result more biogas produced for the same amount of substrate digested. This might be due to the improved availability and balance of the nutrients with NaOH-treated corn stover, which enhanced the biological conversion rate.

9. MATERIALS AND METHODS

9.1 Procedure

Several laboratory based experiments were performed to observe the biogas production potential and yield from maize stover in different condiotions. Pretreatment of raw material (maize) was performed such as: chopping, blending to smaller size (0.5~3) mm.Weight of maize was measured. Weight of cow dung was measured. 100 mL of inoculums was taken from previous biogas plant. Weighted maize, cow dung and inocolum are fed to a glass bottle and 840 mL water was added to it. Mixture was stirred to ensure proper mixing. pH of the mixture was measured. The glass bottle was sealed after that and it was connected with two other glass bottles (to store the produced biogas by siphoning). Temperature was maintained to 34°C. The slurry was allowed to be sealed for 70 to 100 days. Volume of produced gas was measured from time to time. Average temperature was maintained in the range of 32~34℃. Average pH was maintained at 6~8.

Figure 3. Experimental set-up of a producing biogas from maize stover

Page 1 of Table

Table 1. Table containing raw materials and solution used in every experiment

Name of the Expermient	**Raw materials**	**Solution**
Experiment 01	**(with cow dung)** Weight of cow dung = 175 g Weight of stem = 28g Weight of green leaves = 11g Weight of inoculum = 100 mL Water = 840 mL	Stem (2%)+ Green leaves (1%)+ Cow dung (3%)+ Inoculum(10%)+ Water(84%)= 1000mL
Experiment 02	**(Without cow dung)** Weight of stem = 28g Weight of green leaves = 11g Weight of inoculum = 100 mL Water = 840 mL Weight of $NaHCO_3$ = 10.03	Solution: Stem (2%) + Green leaves (1%) + Inoculum (10%) + Water (84%) = 1000 mL
Experiment 03	**(Treated with dirty water for 26 days)** Pretreatment solution: 700mL drain water+ 100mL inoculum + maize Weight of stem = 28g Weight of green leaves = 11g Water = 200 mL	Dirty water solution [Stem (2%) + Green leaves (1%)+ {drain water + inoculum (700mL)}] + Water (20%) = 1000 mL

Page 2 of Table:

Name of the Expermient	**Raw materials**	**Solution**
Experiment 04	**(with cow dung)** Weight of cow dung = 58.8 g Weight of dry leaves = 28g Weight of green leaves = 28.5g Weight of inoculum = 100 mL Water = 840mL	Dry leaves (2.5%) + Green leaves (2.5%) +Cow dung (1%) + Inoculum(10%) + Water(84%) =1000 mL
Experiment 05	**(with cow dung)** Weight of cow dung = 117.65 g Weight of stem = 42.8g Weight of green leaves = 11.38g Weight of inoculum = 100 mL	Stem (3%)+ Green leaves (1%)+ Cow dung (2%)+ Inoculum (10%)+ Water(84%)= 1000mL

	Water = 840 mL	
Experiment 06	**(with cow dung treated with NaOH)** Pretreatment: Maize and 3.6g NaOH (6% NaOH of dry matter) Weight of cow dung = 117.65 g Weight of stem = 57.06g Weight of green leaves = 22.77g Weight of inoculum = 100 mL Water = 820 mL	Stem(4%)+ Green leaves (2%)+ Cow dung (2%)+ Inoculum (10%)+ Water(82%)= 1000mL

10. RESULT

Maize stover (waste) has been used to experiment for biogas production by anaerobic digestion process. Composition of produced biogas was experimented in a gas chromatographer. Anaerobic digestibility of maize stover was observed through different experiments and its influence with different parameter. In those experiments amount of produced gas was recorded with time in a routine way. Hydraulic retention time was around 60~90 days in each experiment.

The highest methane yield was achieved from maize stover with cow dung. Performance of yield of methane was lower from maize stover without cow dung. Important factor for yield of methane depends on particle size. Particle size was 0.5-3mm. Temperature of digestion is another important factor. Room temperature was maintained at 34˚C. Reason for the increase in methane yield could be the predecomposition of lignin which improves the availability of nutrient for the methanogenic metabolism.

In each experiment, flame test rest was positive and the produces biogas was flammable. Methane content in biogas was found 55- 70%, carbon dioxide in the range of 45 to 30% and negligible amount of hydrogen sulfide or ammonia. After performing purification and compression approximate amount of CBG found was approximately 0.1195kg from 1 kg of maize.

10.1 Physical Interpretation of Characteristic Curves

10.1.1 Cumulative Biogas Production Curve

This curve is generated by plotting total amount of biogas produced as ordinate against no of days as abscissa. With no of days the amount of produced gas always increases, so this curve always has a positive slope. Initially the slope is smaller, when biogas only starts to generate. It is known as start up period. Normally these start up periods varied from 5-15 days. Then the growth rate increases faster. It is known as growth phase, where there are maximum amount of microorganism and their continuous growth increases the production of biogas. This stage varied between 15~80 days depends on several factors including nutrient, pH, temperature etc. After this stage, microorganism starts to die due to insufficient nutrient or environment and biogas production becomes slower or negligible.

10.1.2 Differential Curve of Biogas Production

This curve represents the growth rate per day of a digester. This curve is drawn by plotting growth rate per day as ordinate against no of days as abscissa. Initially biogas production is slower, so the curve has smaller slope which means gradual increase of microorganism. It varied 5-15 days same as cumulative biogas production curve. Then when microorganism starts growing exponentially, curve faces a very sharp increase which demonstrates maximum growth of microorganism and biogas generation as well. This phase varied 15-80 days like the cumulative curve. Then after maximum growth microorganism starts to die and biogas production gets slower and at one point it stops when there will be no more conversion of biogas and all microorganism responsible for biogas generation die out. As a result the slope becomes zero or negative.

There are some deviations from these phenomena in experiment 02, 03, 04. The reasons responsible for this might be unfavorable condition (insufficient nutrient, temperature, pH, inhibition etc.) for the microbial growth which caused death to a large number of microorganisms. After couple of days when the condition changed there is growth in biogas production.

10.1.3 Yield of Biogas

This curve is drawn by plotting yield of produced biogas per gram of total solid against no of days. As production of biogas increased over time, yield also increased in the same manner. It always has positive slope. This curve is quite similar to cumulative curve. Initially curve increased slowly and then it faces sharp increase and then again it became slow as the production rate decreases.

10.2 Influence of pH

pH of the slurry should be maintained between 6.5~7.8 which is required for methanogenic bacteria which reduce carbon dioxide and hydrogen to methane. If pH becomes lower than 5.5, the slurry becomes acidic where methanogenic bacteria does not grow and there will be no methane production. Acidogenesis step will be dominant resulting in the production of carbon dioxide and hydrogen instead of methane. So cow dung was used to maintain that buffer and the required pH. In experiment 02, 03 and 06 cow dung was not used, sodium bicarbonate was used to maintain the buffer.

10.3 Influence of Percentage of Cow Dung and Maize Stover

The influence of percentage of maize stover and cow dung on methane yield can be observed from experiment 01. It has the largest yield compared to other percentage having percentage of 3% maize with 3% cow dung.

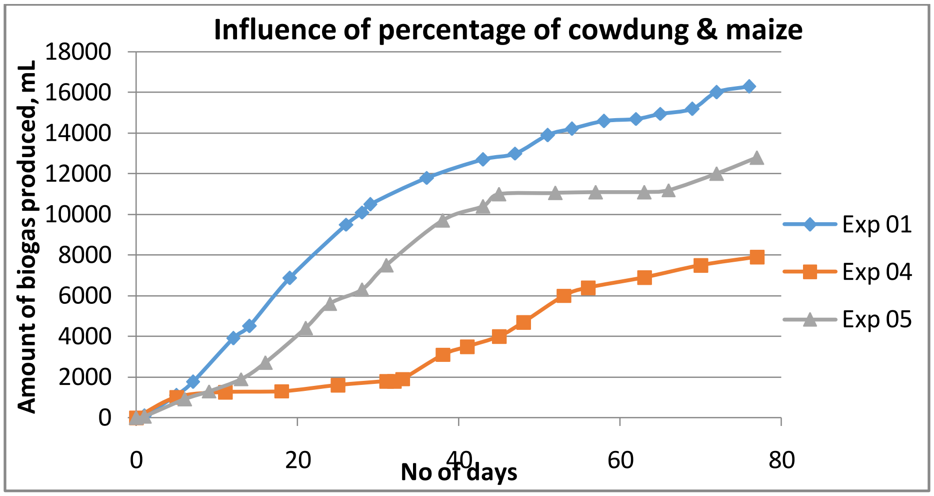

Figure 4. Graphical representation of influence of percentage of cow dung & maize stover

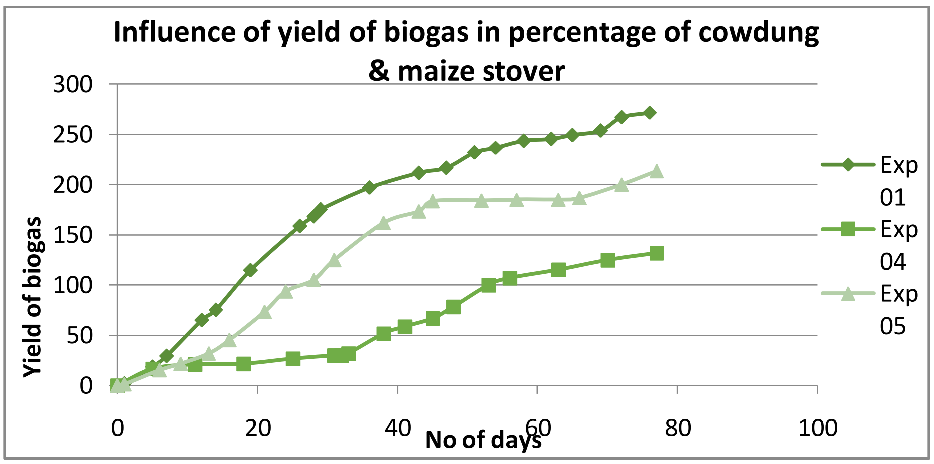

Figure 5. Graphical representation of influence of yield of biogas in percentage of cow dung & maize stover.

Yield of biogas was lower if the percentage of maize stover or cow dung is increased or decreased. According to Zscheischler et al. at dry matter content of maize at 30-35% give maximum biogas yield. Medium yield was obtained from 5% maize leaves (2.5% green leaves+2.5% dry leaves) in experiment 04 & 4% maize stover (3% stem+1% green leaves) in experiment 05. Amount of produced biogas was 6900mL & 11100 mL in 63 days whereas yield was 138mL/g & 277.50mL/g in experiment 04 & experiment 05 respectively. This comparison is shown in Figure 4 and 5.

10.4 Influence of Cow Dung in Biogas Production

When maize stover is used for biogas production without cow dung, delivers lower amount of production rate. In experiment no 02 and where the same 3% maize stover was used without cow dung. It had the yield of 166.67 mL/g and amount of biogas produced was 5000

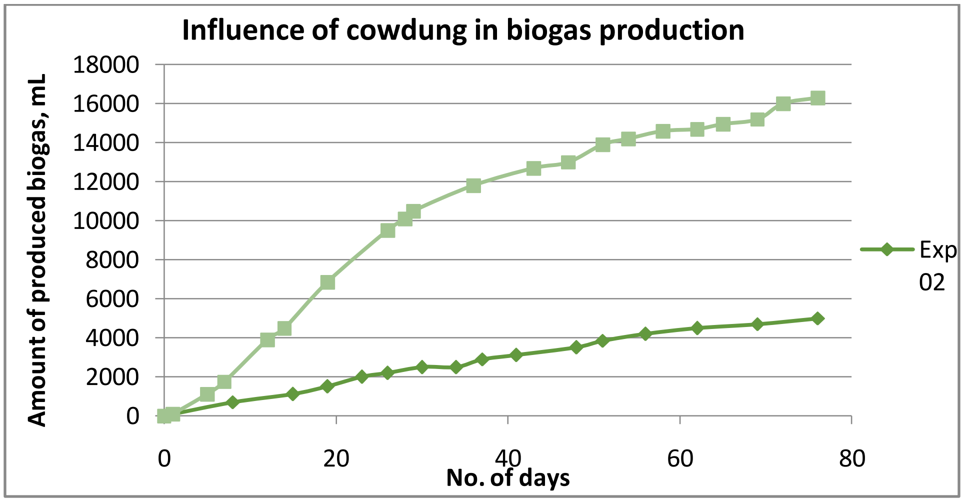

Figure 6. Graphical representation of influence of cow dung in Biogas production.

.

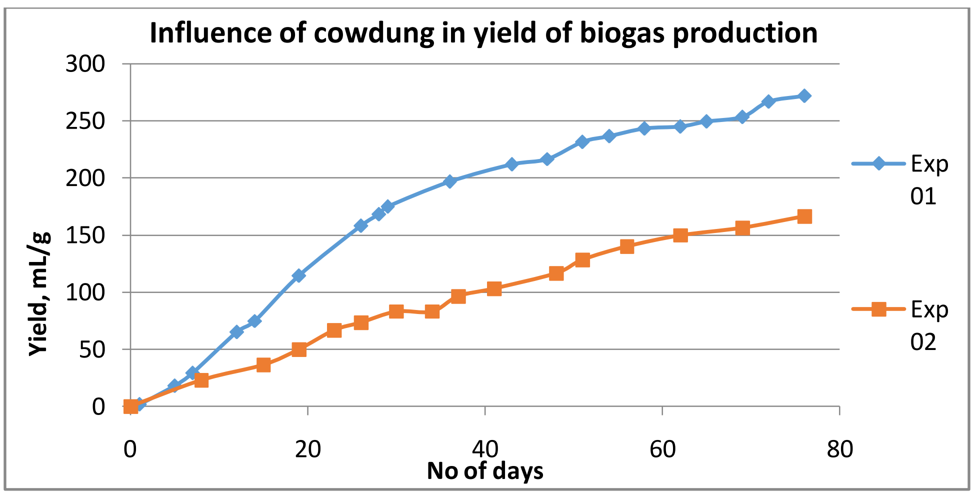

Figure 7. Graphical representation of influence of cow dung in yield of biogas production

mL in 76 days whereas the amount was 271.67mL/g and 16300 mL with cow dung in experiment 01. It is shown graphically in Figure 6 and 7.

10.5 Influence of Pretreatment of Maize Stover

Influence of pretreatment of maize stover on biogas yield has also been studied. A plant cell wall usually consists of polysaccharides (cellulose, hemicelluloses), lignin, tannins, lipids, cutins, and suberin. Among these cell wall components, lignin is likely to be the most recalcitrant and its decomposition is usually found to be the rate-limiting step. Influence of pretreatment process or by dirty water (white rot fungus) and

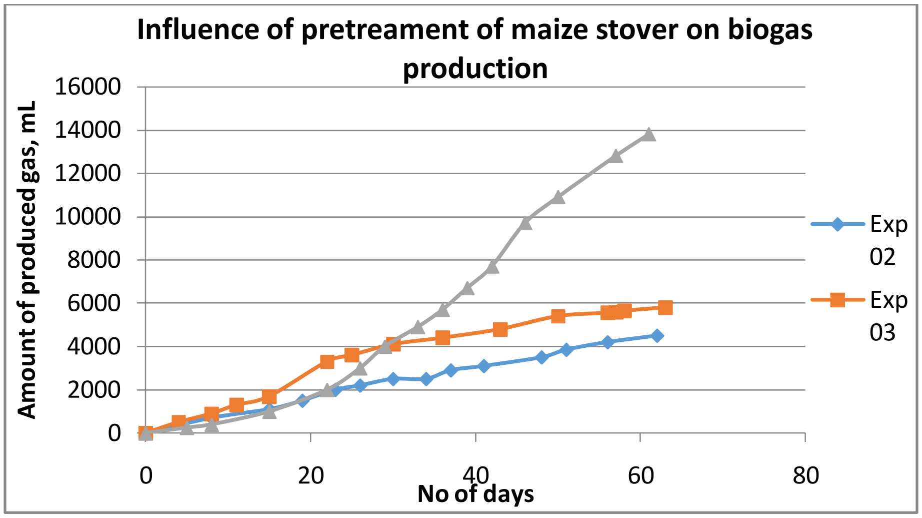

Figure 8. Graphical representation of influence of pretreatment of maize on biogas production

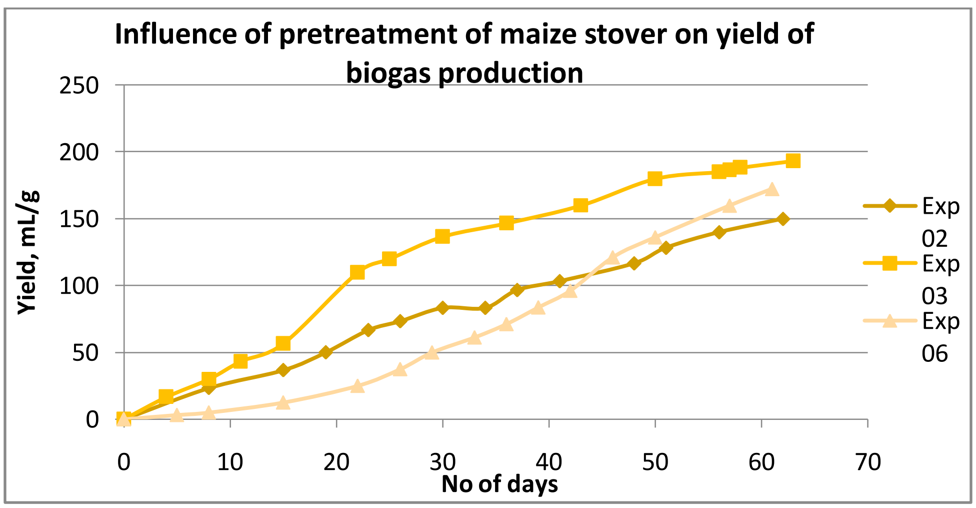

Figure 9. Graphical representation of influence of pretreatment of maize stover on yield of biogas production

sodium hydroxide has been studied in experiment 03 and 06 respectively. These pretreatment significantly influenced the overall biogas production and the yield. Amount of biogas production rate was faster increased,
the amount of produced biogas increased and also the yield as well. These effects of can be observed from experiment 03 and 06 thoroughly. A comparative study of the effect of pretreatment by graphical representation between experiment no 02(no substance used for digestion), 03(pretreated with dirty water) and 06(pretreated with sodium hydroxide) can be obtained from the Figure 8 and 9.

10.6 Overall Result Comparison

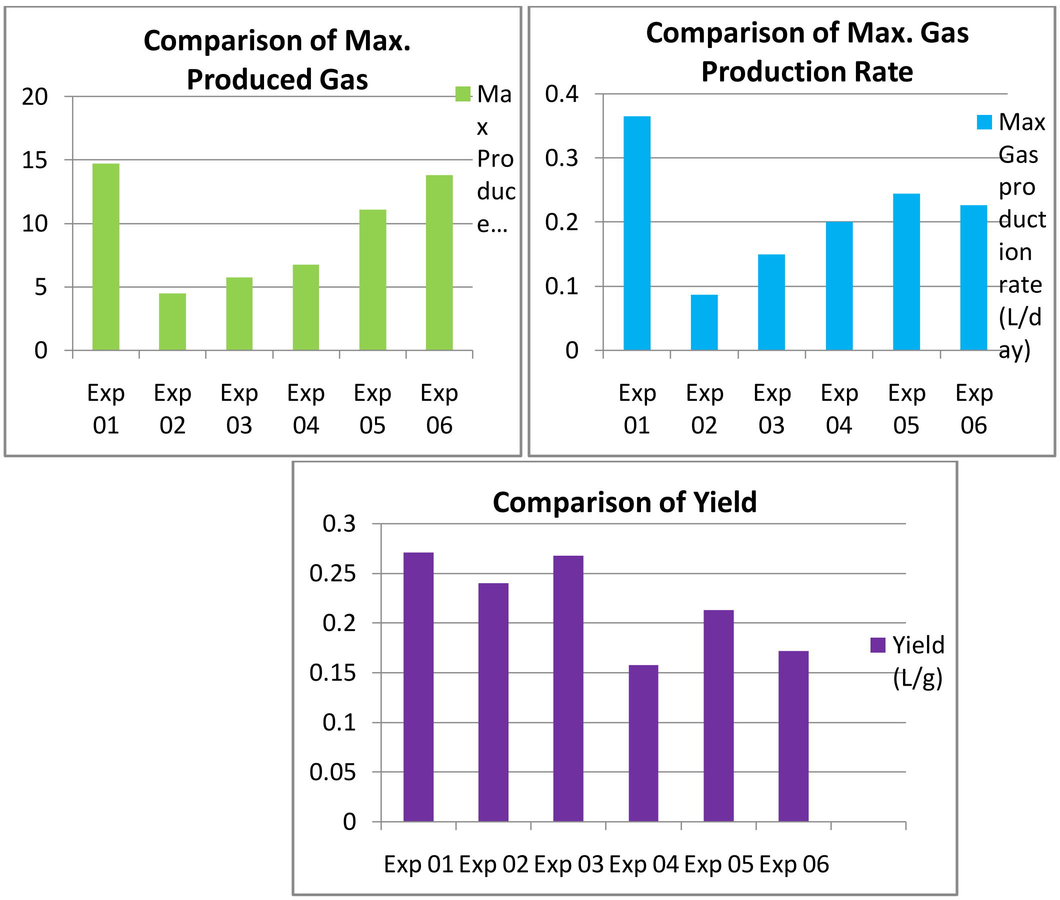

Figure 10. Bar charts comparing overall result obtained from six biogas plant

Amount of biogas produced in 60~90 days, maximum biogas production rate and maximum yield obtained from six experiments are compared in three bar charts in Figure 10. Results can be easily interpreted from these bar charts. Experiment 1 has the maximum biogas production with maximum biogas production rate and yield whereas experiment 5 and 6 also has a good potential of biogas production rate and yield with a shorter retention time.

11. ENERGY CONVERSION

Energy conversion is measured from the ratio of produced energy obtained from methane and energy of the raw material. Calorific value of maize is 3500 kCal/kg (14650 J/g), cow dung 3290 kCal/kg (13771.28 J/g) and methane 39820 kJ/m^3. Energy of raw material, biogas and energy conversion is as follows

Table 2. Table showing energy conversion of experiments.

Name of the expeeriment	**Experiment No. 1**	**Experiment No. 2**	**Experiment No. 3**	**Experiment No. 4**	**Experiment No. 5**	**Experiment No. 6**
Energy in, J	2995974	586000	586000	1637476	2413928	2789700
Energy out, J	389400	136400	168053	214789	316011	340699
Energy conversion, %	13	23.27	28.68	13.12	13.09	12.21

12. CONCLUSION

The objective of this research is to study on the potential of compressed biogas production from maize waste in Bangladesh. Producing compressed biogas from energy crop like maize has been proved to be an efficient, environment friendly and a renewable source of energy all over the world. Maize has privilege of being utilized as food and fuel and therefore it is also called as agronomic crop. It has a significant potential to biogas yield and the digestate can also be used as fertilizer. The performance of anaerobic digestibility of maize has been evaluated in terms of methane yield, production rate of biogas and cumulative amount of produced gas. Compressed biogas (CBG) from maize can be an effectual alternative to CNG whereas around 40000 MMCF of CNG is consumed as vehicle fuel in Bangladesh per year. Biogas from maize stover is also used as fuel for electricity generation in many countries including Germany, Denmark where a good percentage of their energy comes from this source. India is also producing CBG from biowaste. Demand of maize is increasing day by day and the meteorological condition of Bangladesh is favorable for anaerobic digestion. Compressed biogas production from maize can be optimized by controlling several parameters. A properly coordinated movement could result in complete conversion of vehicles from fossil-based fuel to sustainable biomethane from biomass like maize. If it can be implemented in large scale, a substantial amount of energy can be added to the existing energy sources to meet the increasing demand of energy in Bangladesh.

REFERENCES

Reaz Ahmad (2016). Amazing Growth In Maize Output. http://www.thedailystar.net/frontpage/amazing-growth-maize-output-1289713.

Monlruzzaman, M. S. Rahman, M. K. Karim and Q.M Alam (March 2009). Agro-Economic Analysis of Maize Production in Bangladesh: A Farm Level Study. *ISSN 0258-7122 Bangladesh J. Agril. Res. 34(1): 15 - 24.*

Sohel Parvez (2015) Growers switch to maize farming. http://archive.thedailystar.net/newDesign/news-details.php?nid=230331

Nick Barker and Louise Evans, AEAT (2009). National Non-Food Crops Centre. Evaluation of Opportunities for Converting Indigenous UK Wastes to Fuels and Energy (Report). *NNFCC 09-012*

Beychok, M. (1967). Aqueous Wastes from Petroleum and Petrochemical Plants. *John Wiley & Sons, LCCN 67019834. (September 26, 2016)*

An Outline of Anaerobic Digestion Technology. http://www.esru.strath.ac.uk/EandE/Web_sites/06-07/Biomass/HTML/anaerobic_digestion.htm
Sleat, R. & Mah, R. (2006). Hydrolytic Bacteria in Anaerobic digestion of biomass

Martin, A.D. (2007). Understanding Anaerobic Digestion, Presentation to the Environmental Services Association. *esauk.org. Retrieved 22.10.07.*

Biogas (CBG) Purification and Bottling. http://www.environmentalengineering.in/Biogas.htm

Biogas Generation, Purification And Bottling Development In India – A case study. http://mnre.gov.in/file-manager/UserFiles/case-study-Biogas-Generation_Purification_and_Bottling-Development-In-India.pdf
Biogas upgrading and utilization.

http://www.novaenergie.ch/iea-bioenergy- task37/dokumente/biogas%20upgrading.pdf
Fablen Monnet. (2003). Introduction anaerobic digestion to organic waste. http://www.remade.org.uk/media/9102/an%20introduction%20to%20anaerobic%20digestion%20nov%202003.pdf

Sun, Y.; Lin, L.; Pang, C.; Deng, H.; Peng, H.; Li, J.; He, B.; Liu (2007). S. Energy Fuels. *21, 2386–2389.*
Pavlostathis, S. G.; Gossett, J. M. *Biotechnol. Bioeng.* 1985, *27*, 334– 344.

Chen, H.; Liu, L.; Yang, Z.; Li, Z. *Biomass Bioenergy* 2005, *28*, 411–417.

Curreli, N.; Fadda, M. B.; Rescigno, A.; Rinaldi, A. C.; Soddu, G.; Sollai, F.; Vaccargiu, S.; Sanjust, E.; Rinaldi, A. *Process Biochem*. 1997, *32*, 665–670.

Muller, H. W.; Tro¨sch, W. Appl. Microbiol. Biotechnol. *1986, 24, 180–185*

Pavlostathis, S. G.; Gossett, J. M. Biotechnol. Bioeng. *1985, 27, 334– 344.*

Bumpus JA, Tien M, Wright DS, Aust AD. Oxidation of persistent environmental pollutants by white rot fungus. *Science 228:1434-1436 (1985)*.

Bumpus JA, Aust SD, Biodegradation of environmental pollutants by the white rot fungus Phanerochaete chrysosproium: involvement of the lignin degradating system. *Bioessays 6:166-170 (1986).*

Aust SD. Degradation of environmental pollutants. *Microb Ecol 20:197-209 (1990)*.

Crawford RL. The chemical structure of lignin and tye use of various lignin preparations for microbial studies In: Lignin Biodegradation and Transformation. *New York:John Wiley and Sons*, *1981;7-19.*

Pavlostathis, S. G.; Gossett, J. M. Biotechnol. *Bioeng. 1985, 27, 345–354.*

Lignin and carbon transformation in roots of maize and mixed perennial biofuel crops, Fritzie Ann Rivas Iowa State University , Ames, Iowa 2012

Calorific value of Different Fuels. http://www.ces.iisc.ernet.in/energy/paper/alternative/calorific.html
Fuels **-** Higher Calorific Values. http://www.engineeringtoolbox.com/fuels-higher-calorific-values-d_169.html

International Conference on Petroleum Engineering 2016 (ICPE-2016)
Bangladesh University of Engineering & Technology (BUET)
Dhaka-1000, Bangladesh

ICPE (2016-032)

Modeling Liquid Loading of Gas Wells and its Remediation

M. Aldousari[1], G. M. Hashmi[1], N. Tamim[1], Farhana Akter[2], and A. R. Hasan[1],
[1]Texas A&M University,
[1]Bangladesh University of Engineering and Technology

ABSTRACT

Liquid loading is often a problem for mature gas wells due to declining reservoir energy. It is the inability of a producing gas to remove its coproduced liquids from the wellbore. Due to declining reservoir energy, the liquid starts to accumulate in the well leading to a change in the fluid flow regime from annular two-phase flow to churn (or slug) flow. This transition from annular to churn or slug flow initiates the process of liquid loading. Currently, liquid loading is predominantly premised on diagnosing the problem at the wellhead-flow conditions. This study reveals that the problem may start well in advance of its effects being felt at the wellhead.

The remedial efforts needed to keep the well flowing are severely impacted by the stage at which liquid loading is diagnosed. Earlier diagnosis with the help of proposed coupled wellbore-reservoir modeling can prove instrumental in cutting costs of remediation. To this effect, the study also presents a model for the design of plunger lift for such wells. The model allows for an efficient design of plunger lift by incorporating physics of fluid flow in the wellbore. Because the dimensions and trajectory of the wellbore have such profound impact on the operability of plunger lift, operators can use this model by just providing the known input parameters to determine the design variables, target casing pressure and duration for the plunger cycle.

Keywords: annular flow, casing pressure, liquid loading, plunger lift, slug flow.

INTRODUCTION

With depletion of gas reservoirs, the removal of produced liquid from the wellbores becomes less efficient. This inefficiency gives rise to liquid accumulation in the wellbore, a phenomenon known as liquid loading. The consequent increase in bottomhole flowing pressure significantly reduces gas production. Reduced gas production further exacerbates the problem because reduced gas velocity allows for greater liquid accumulation in the wellbore initiating a vicious circle. The problem of liquid loading has spawned intense investigation and numerous publications in the field. Where many have studied the force balance on the liquid droplets, others have carried out experiments in laboratory to shed light on the matter.

* Corresponding Author address
Email:rashid.hasan@tamu.edu

The subject matter can be traced back to the pioneering work of Turner et al. (1969), who proposed the first critical rate-calculation procedure to predict liquid loading. Their critical velocity model is based on the force balance of the largest droplet and the upward gas flow. This work was followed by others, notably Coleman et al. (1991) and Nosseir et al. (2000), who matched field data by making adjustments to the critical velocity model with Nosseir et al. (2000) proposing two models, one each for laminar and highly turbulent flow regime. Zhou and Yuan (2010) focused on liquid holdup as the determining mechanism for liquid loading. They proposed models based on threshold liquid-holdup value. All these models, however, based their work on the original Turner et al. (1969) model. The classic work though, limited by technology at the time, used simplistic assumptions in their approach. This was pointed out by Sutton et al. (2010), who showed that the use of wellhead conditions to calculate liquid loading may give grossly inaccurate results especially in cases such as wells with multiple tubing sizes or tapered string, or if the tubing is set much higher than the perforation depth.

More recently, pipe-flow experiments carried out by several researchers have shed considerable light on the mechanism of liquid loading. van't Westende et al. (2007) conducted multiphase flow experiments and concluded that liquid-loading resulted due to film-flow reversal as opposed to the droplet flow reversal as claimed by many of their predecessors. Veeken et al. (2010) confirmed this finding by modeling the process with a transient multiphase flow simulator. Alamu (2012) linked this film reversal to the transition from annular flow. Similar observation was made by Yuan et al. (2013) in their experiments. To visually understand these different works in perspective, Fig. 1 demostrates a comparison between the transition from annular-flow pattern predicted by these works in literature. As can be seen, some of these (on the right) have a more conservative criterion than the others.

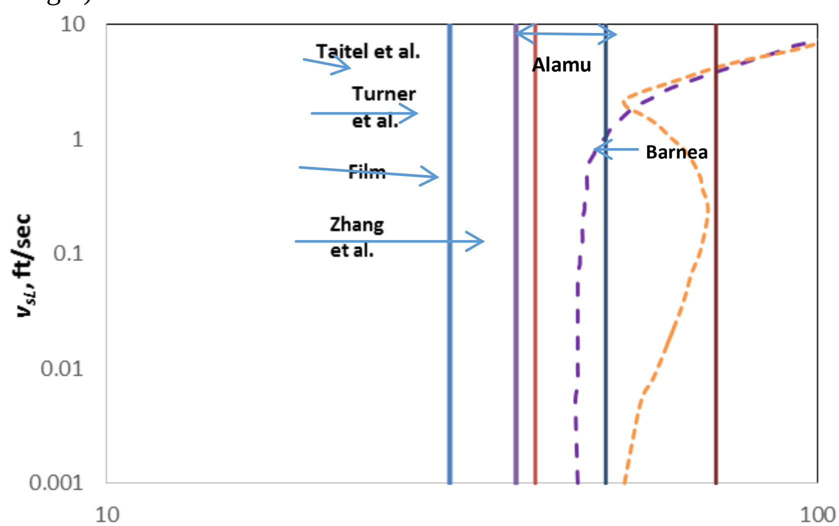

Fig. 1 – Estimates of transition from annular flow by various models.

In the last decade, many studies have coupled reservoir/wellbore modeling to gain understanding of the instrinsic problem at hand. Dousi et al. (2006) proposed analytical reservoir/wellbore simulation to forecast gas production under the liquid-loading condition. Hu et al. (2010) performed reservoir/wellbore coupled flow simulations in transient mode to predict intermittent production cycle. Zhang et al. (2009, 2010) carried out transient reservoir/wellbore simulation to predict the flowing-bottomhole-pressure oscillation in the near wellbore region, owing to liquid accumulation at the bottom. Jackson et al. (2011) performed similar simulations for horizontal wells in tight gas reservoirs. The same robust coupling of reservoir/wellbore was used by Agrawal and Sharma (2013), who studied the impact of liquid loading on the productivity of hydraulically fractured shale-gas wells. Most recently, Riza et al. (2015) explored various mechnaisms of liquid loading predicting gas-well performance under liquid loading conditions.

The problem of liquid loading can ultimately result in the death of the well. One of the many methods used to combat this issue involves a plunger. Plunger lift is a method that uses the energy of the gas/liquid well in a more efficient way by allowing a free piston to travel up and down the tubing in a cycle. Owing to the relatively low capital cost needed for the system, it has become a favorable option for many small-scale operators. Several authors have addressed the modeling of plunger-lift installations. Among these, Foss and Gaul (1965); Lea (1982); Chava et al. (2008, 2010); Tang and Liang (2008); and Luo and Kelkar (2014) are some of the more notable works. More recently, Hashmi et al. (2016) presented a mechanistic model for the design of plunger lift system. Their work focused on the physics of fluid flow and energy balance in the system by developing an expression for the minimum casing pressure needed for sustained production.

In this work we present a coupled reservoir-wellbore model that allows forecasting as well as prognosis of the liquid loading process for a given wellbore-reservoir system. We use a simple pseudo-steady reservoir being produced by a single well in the center to represent the system. History matching allows rough approximation of the real system for forecasting purposes. This allows an operator to estimate possibility of liquid loading initiation well in advance of diagnosis at wellhead. It also allows the operator to estimate the productive life without intervention, of the well after loading initiation. We also discuss the use of plunger lift as an inexpensive way to produce the well for a sufficiently long time to be a profitable proposition.

MODEL DEVELOPMENT

The onset of liquid loading is governed by both reservoir and wellbore dynamics. Therefore, the proposed modeling consists of both the systems.

Reservoir System

The reservoir is assumed to be a circular one with a well in the centre. Pseudosteady state flow conditions are assumed for the fluid flow in the reservoir. With known reservoir dimensions and saturation, initial gas-in-place, G_i, is calculated.

$$G_i = 43,560 \frac{A\, h\, \phi \left(1 - s_{wi}\right)}{B_{gi}} \tag{1}$$

$$B_{gi} = 0.0283 \frac{T Z_i}{p_i} \tag{2}$$

The empirical Vogel's two-phase inflow relationship is used to describe gas flow into the wellbore.

$$q_g = q_{g,\max} \left(1 - 0.2 \frac{p_{wf}}{p_r} - 0.8 \left[\frac{p_{wf}}{p_r} \right]^2 \right) \tag{3}$$

$$q_{g,\max} = \frac{1}{1.8} \frac{p_r^2 k_g h}{1424 \mu_g ZT \ln\left(0.472 \frac{r_e}{r_w}\right)} \quad (4)$$

For water flow, pseudosteady state radial flow relation is followed.

$$q_w = \frac{k_w h \left(p_r - p_{wf}\right)}{141.2 B_w \mu_w \ln\left(0.472 \frac{r_e}{r_w}\right)} \quad (5)$$

It should be noted that Vogel's relationship needs a special tuning for more accurate results in gas/water production.

Gas-water flow in porous media is a complicated subject due to reservoir heterogeneity and the nature of the two fluids, both being in different physical states. Many researchers proposed several correlations to describe gas-water relative permeability. Two of those correlations are given below:

Wyllie geometric model

$$k_{rw} = \left(S^*\right)^4 \quad (6)$$

$$k_{rg} = \left(1 - S^*\right)^2 \left(1 - S^{*2}\right) \quad (7)$$

Boatman's correlation is similar to Wyllie

$$k_{rw} = \left(S^*\right)^{1.5} S_w^3 \quad (8)$$

$$k_{rg} = \left(1 - S^*\right)\left(1 - S^{*0.25} S_w^{0.5}\right)^{0.5} \quad (9)$$

In both correlations:

$$S^* = \frac{S_w - S_{wi}}{1 - S_{wi} - S_{gr}} \quad (10)$$

Residual gas saturation is needed to use the two proposed correlations. Agarwal (1967) proposed a relationship to calculate final gas saturation in the reservoir based on initial gas saturation. The following correlation is the result of fitting 300 experimental data for common rock classifications.

$$S_{gr} = 0.1813 S_{gi} + 0.096071 \quad (11)$$

Once the gas flow rate is estimated using Eq. 3, it can be used as a starting point. Applying material balance on the reservoir in light of the known gas flow rate, provides the approach to successively obtain the declining average reservoir pressure through material balance.

$$\frac{\bar{p}_n}{\bar{Z}_n} = \frac{p_i}{Z_i}\left(1 - \frac{G_{pn}}{G_i}\right) \quad (12)$$

$$G_{pn} = \sum q_n \quad (13)$$

where the subscript n refers to each time step.

Wellbore System

The reservoir model is connected to the wellbore model with a seamless computational approach. The wellbore model can be discretized into any segments for multiple phase flow pressure drop calculations along the wellbore. Our approach is to estimate fluid pressure in the entire wellbore to determine conditions that can lead to liquid loading at any point in the wellbore.

The general, momentum-balance equation for multiphase compressible fluids involving hydrostatic, kinetic, and frictional pressure heads is expressed by

$$\Delta p = \frac{g}{g_c}\rho_m dz + \rho_m \frac{\Delta v_m^2}{2g_c} + \frac{2f_m \rho_m v_m^2 dz}{g_c d} \tag{14}$$

The in-situ gas velocity can be expressed as the sum of the bubble-rise velocity (v_∞) and the channel center mixture velocity (C_o v_m) (Hasan and Kabir, 2002). Therefore, the gas void fraction can be expressed by

$$f_g = \frac{v_{sg}}{C_o v_m + v_\infty} \tag{15}$$

The flow parameter (C_o) depends on flow regime, well deviation, and flow direction.

A robust heat transfer model is needed to accurately estimate wellbore-fluid properties. For high-pressure/high-temperature gas reservoir, temperature change influences gas velocity considerably. These temperature changes are accounted using the temperature model below (Hasan et al. 2009).

$$T_f = T_{ei} + \frac{1 - e^{(z-z_j)L_R}}{L_R}\left[g_G \sin\theta + \varphi_T + \frac{g\sin\theta}{c_p}\right] + e^{(z-z_j)L_R}\left(T_{fj} - T_{eij}\right) \tag{16}$$

Transition from Annular Flow

As gas velocity declines, it reaches a value, termed the critical liquid loading velocity, below which gas stream cannot drag the liquid droplets in the wellbore upward. We surmise that this inability to drag liquid droplets leads to the onset of liquid loading. This critical liquid loading velocity can be calculated as proposed by Taitel et al. (1980) in their work.

$$v_{gc} = 3.1\left[\frac{g\left(\rho_l - \rho_g\right)\sigma}{\rho_g^2}\right]^{0.25} \tag{17}$$

To demonstrate the physical phenomenon that occurs during liquid loading, Fig. 2a and 2b illustrate the flow pattern, liquid holdup, and the pressure-gradient profile of a generic well. Fig. 2a shows the superficial-gas velocity (v_{sg}) and the critical-transition-velocity-profile in the well (v_{gc}). The v_{sg} increases in the well from bottomhole to wellhead. Since the flowing pressure decreases as we rise to the wellhead inside the wellbore, gas expands and accelerates. This is countered to some extent by the decreasing temperature as the fluid rises up the wellbore; requiring temperature computation. In this example, the lower part of the well is experiencing slug flow i.e. $v_{sg} < v_{gc}$, and the upper part contains annular flow, i.e. $v_{sg} > v_{gc}$. In Fig. 2b the effect of the flow regime on the different pressure gradients is shown. Accelerational pressure gradient is ignored since it is insignificant compared to the other two components. The hydrostatic pressure gradient is the largest contributor to the total pressure gradient throughout the wellbore. However the disparity between the two pressure gradient components is significantly higher in the slug flow regime. The sudden drop in the pressure heads going from slug to annular flow is caused by the increase in gas-volume fraction, f_g, which causes the mixture density to decrease significantly.

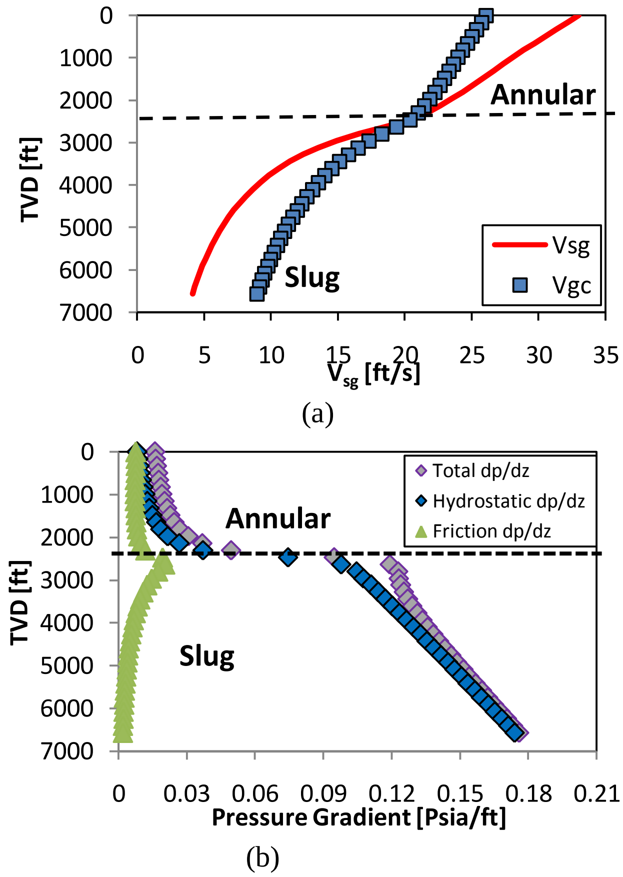

Fig. 2 – Effect of Flow Regime on (a) Gas Velocity and critical transition velocity (b) pressure gradient.

Fig. 2 also suggests that the onset of liquid loading takes place towards the bottom of the well from where the liquid loading front moves up the wellbore and eventually reaches the wellhead. Relying on the wellhead information to predict the onset of liquid loading therefore does not bode well since by the time the wellhead superficial gas velocity has become less than the critical transition velocity, the wellbore is already loaded up. Fig. 3 shows the comparison of a few critical loading velocity models where it can be seen that the actual gas velocity, v_{sg}, at the wellhead is greater than the critical liquid loading velocity as predicted by all the different models. Therefore none of the models diagnose the well to be loaded since they are all based on wellhead conditions. However as can be seen, the bottomhole conditions tell another story entirely.

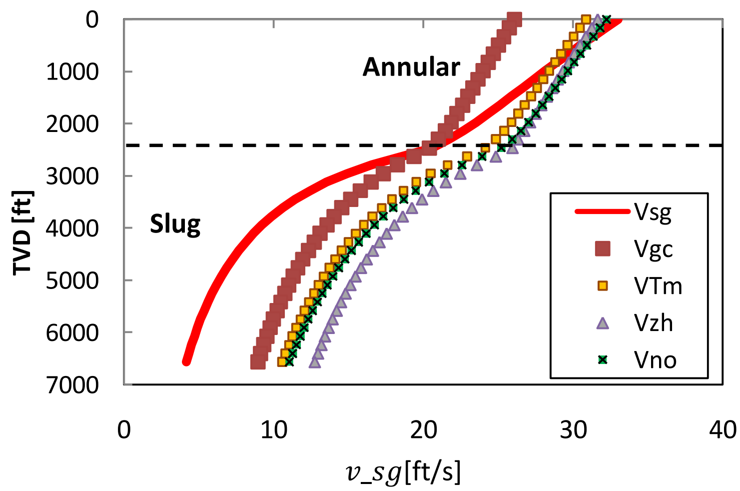

Fig. 3 – Gas superficial velocity, critical loading velocitiy models on the entire wellbore indicate missleading use of wellhead condition to predict liquid loading

It seems counterintuitive that the well may ever behave otherwise, so the conclusion thus drawn from the example that the transition from annular flow to slug or churn flow will always be triggered at the bottomhole may seem logical in an obvious way. However this may not be valid since the gas velocity is also affected by fluid temperature in a reverse manner. It can be shown that in wells with high temperature and low pressure gradients, the gas velocity at bottomhole may be very similar to that at the wellhead. Therefore, for those wells, applying the critical loading criterion at the wellhead may work. This concept becomes more important with rising complexities in the completion of the well. Varying tubulars and properties may result in different conditions of flow regimes in the entire well and therefore the entire wellbore should be acknowledged when checking for the ciritical loading velocity criterion.

METHODOLOGY

In the reservoir-wellbore coupled system proposed in this work, we need to contend with pressure drops in the reservoir and the well; i.e., both the reservoir and the wellhead pressure are known quantities. As for the bottomhole pressure, it is the common parameter in both systems. It is the end point of the gas inflow coming from the reservoir and the starting point for the gas in the wellbore flowing upward to wellhead pressure. Physically, there is only one value satisfying pressure drop in both systems. It is an iterative process in which bottomhole pressure, p_{wf}, is guessed. Then, gas flow rate is calculated from Eq 3. With the calculated flow rate, we back calculate bottomhole pressure from the wellhead pressure from Eq. 14. If the calculated p_{wf} is different from the assumed one, a new p_{wf} is calculated from the equation below,

$$p_{wf\,,new\ assumed} = 0.5\, p_{wf\,,old\ assumed} + 0.5\, p_{wf\,,calculated} \qquad (18)$$

The process is continued until p_{wf} calculated in succesive steps are “close enough” (within 1 psia). After p_{wf} has been calculated with appropriate convergence tolerance at any time-step, material balance is used to calculate depletion and a new reservoir pressure so that Eq. 18 may be used to calculate a new p_{wf} for the next time-step and the wellbore model is used to calculate a new bottomhole pressure as well as the two-phase flow regime in the wellbore. The iterative procedure is repeated and a production histry of gas and liquid rates are computed as a funtion of time, along with two-phase flow regime in the wellbore. This allows us to estimate when liquid loading will be initiated in the well and how long the well can continue producing after that before it is killed.

RESULTS

In the following, we present results computed from our coupled model. For the computations, Table 1 lists the data for the reservoir and the wellbore that were used as inputs.

Table 1 – Generic gas reservoir parameters used to study liquid loading phenomenon

Reservoir			Wellbore			Stream		
$_i$	5000	psia	p_{wh}	300	psia	T_{pc}	348	°R
	200	°F	T_{wh}	129.2	°F	p_{pc}	663	psia
	200	acres	d	3	in	MW	20.28	lbm/lb-mol
	2	md	ε	6.00E-03	ft	γ_g	0.7	
	30	ft	θ	90	°			
	0.12		r_w	0.328	ft			
$_{wi}$	0.25		Depth	9,000	ft			

Bottomhole pressure is a vital parameter in evaluating liquid loading phenomena. As we discussed, when gas velocity is not high enough to carry the liquid to the surface, liquid (or water in our case) starts accumulating in the well, which naturally increases bottomhole pressure. In one way, we can detect liquid loading onset from the sudden increase in bottomhole pressure which can be seen clearly in Fig. 4. The sudden decrease in bottomhole pressure is associated with a transition in flow pattern from annular to slug. Even though liquid loading onset is on day 978, the well is still producing. It dies after 23 days. An intervention must take place in the form of plunger lift or other means to sustain gas production. Near the death of the well, even water production declines because reservoir drawdown has decreased significantly to a point that there is no sufficient energy to move the fluid.

To provide a glimpse of flow pattern determined in the entire wellbore, Table 2 shows a flow pattern chart that provides flow pattern determined at different depths in the wellbore at different point in time. As can be seen, flow pattern starts changing towards the bottom first. This is because of high pressure and low gas velocity whereas at the top pressure is less on gas molecules allowing velocity to be higher. While most researchers agree on flow pattern transition from annular flow is the point of liquid loading onset, some use wellhead conditions to determine this point. If we rely on wellhead conditions, liquid loading starts on day 987 which is not correct. The onset of liquid loading happens when anywhere in the wellbore flow pattern transition from annular takes place which is on day 978. That is 9 days earlier than what is predicted by the wellhead condition. This example just reiterates the assertion above. Identifying liquid loading onset as early as possible can prevent the significant loss of gas production.

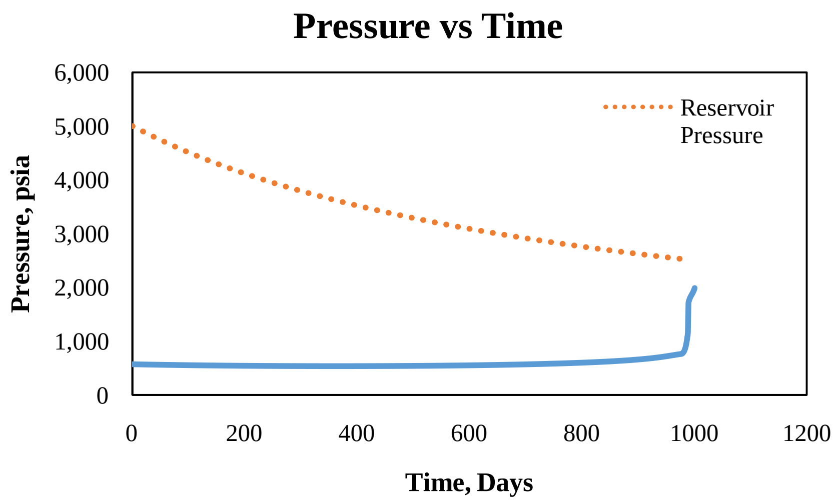

Fig. 4 – Bottomhole pressure increases steeply after transition from annular takes place

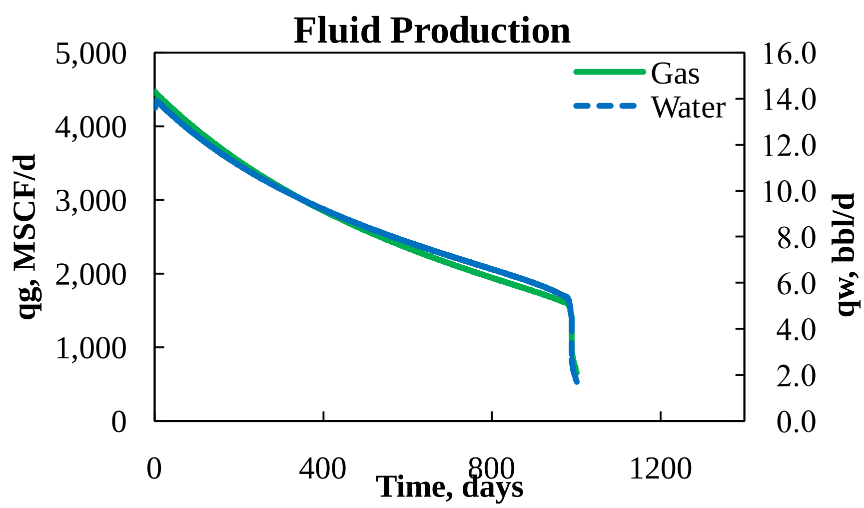

Fig. 5 – Gas production declines rapidly due to high gas compressibility

A closer look at the bottom of the well where transitition from annular takes place first in the wellbore can be seen in Fig. 6. Liquid holdup at the bottom of the well is plotted against time. A sharp increase happens exactly when flow pattern changes from annular to slug flow. At this time, gas cannot leave liquid dropet and liquid film reversal is triggered. This agrees with a simulation excuted with OLGA and Shell reservoir simulation software on a study conducted in the Netherlands. Gas mass flow rate and bottomhole pressure for the simulation are plotted against time in Fig. 7.

Table 2 – Flow pattern map inside the wellbore for different days

<table>
<tr><td>Depth</td><td colspan="10">Days</td></tr>
<tr><td>ft</td><td>978</td><td>979</td><td>980</td><td>981</td><td>982</td><td>983</td><td>984</td><td>985</td><td>986</td><td>987</td></tr>
<tr><td>0</td><td rowspan="29">Annular</td><td rowspan="26">Annular</td><td rowspan="23">Annular</td><td rowspan="19">Annular</td><td rowspan="14">Annular</td><td rowspan="8">Annular</td><td rowspan="6">Annular</td><td rowspan="4">Annular</td><td rowspan="2">Annular</td><td>Churn</td></tr>
<tr><td>4,410</td><td>Slug</td></tr>
<tr><td>4,500</td><td>Churn</td><td>Slug</td></tr>
<tr><td>5,400</td><td>Slug</td><td>Slug</td></tr>
<tr><td>5,490</td><td>Churn</td><td>Slug</td><td>Slug</td></tr>
<tr><td>6,210</td><td>Slug</td><td>Slug</td><td>Slug</td></tr>
<tr><td>6,300</td><td>Churn</td><td>Slug</td><td>Slug</td><td>Slug</td></tr>
<tr><td>6,930</td><td>Slug</td><td>Slug</td><td>Slug</td><td>Slug</td></tr>
<tr><td>7,020</td><td>Churn</td><td>Slug</td><td>Slug</td><td>Slug</td><td>Slug</td></tr>
<tr><td>7,110</td><td>Churn</td><td>Slug</td><td>Slug</td><td>Slug</td><td>Slug</td></tr>
<tr><td>7,200</td><td>Churn</td><td>Slug</td><td>Slug</td><td>Slug</td><td>Slug</td></tr>
<tr><td>7,290</td><td>Churn</td><td>Slug</td><td>Slug</td><td>Slug</td><td>Slug</td></tr>
<tr><td>7,380</td><td>Churn</td><td>Slug</td><td>Slug</td><td>Slug</td><td>Slug</td></tr>
<tr><td>7,470</td><td>Slug</td><td>Slug</td><td>Slug</td><td>Slug</td><td>Slug</td></tr>
<tr><td>7,560</td><td>Churn</td><td>Slug</td><td>Slug</td><td>Slug</td><td>Slug</td><td>Slug</td></tr>
<tr><td>7,650</td><td>Churn</td><td>Slug</td><td>Slug</td><td>Slug</td><td>Slug</td><td>Slug</td></tr>
<tr><td>7,740</td><td>Churn</td><td>Slug</td><td>Slug</td><td>Slug</td><td>Slug</td><td>Slug</td></tr>
<tr><td>7,830</td><td>Churn</td><td>Slug</td><td>Slug</td><td>Slug</td><td>Slug</td><td>Slug</td></tr>
<tr><td>7,920</td><td>Slug</td><td>Slug</td><td>Slug</td><td>Slug</td><td>Slug</td><td>Slug</td></tr>
<tr><td>8,010</td><td>Churn</td><td>Slug</td><td>Slug</td><td>Slug</td><td>Slug</td><td>Slug</td><td>Slug</td></tr>
<tr><td>8,100</td><td>Churn</td><td>Slug</td><td>Slug</td><td>Slug</td><td>Slug</td><td>Slug</td><td>Slug</td></tr>
<tr><td>8,190</td><td>Churn</td><td>Slug</td><td>Slug</td><td>Slug</td><td>Slug</td><td>Slug</td><td>Slug</td></tr>
<tr><td>8,280</td><td>Slug</td><td>Slug</td><td>Slug</td><td>Slug</td><td>Slug</td><td>Slug</td><td>Slug</td></tr>
<tr><td>8,370</td><td>Churn</td><td>Slug</td><td>Slug</td><td>Slug</td><td>Slug</td><td>Slug</td><td>Slug</td><td>Slug</td></tr>
<tr><td>8,460</td><td>Churn</td><td>Slug</td><td>Slug</td><td>Slug</td><td>Slug</td><td>Slug</td><td>Slug</td><td>Slug</td></tr>
<tr><td>8,550</td><td>Slug</td><td>Slug</td><td>Slug</td><td>Slug</td><td>Slug</td><td>Slug</td><td>Slug</td><td>Slug</td></tr>
<tr><td>8,640</td><td>Churn</td><td>Slug</td><td>Slug</td><td>Slug</td><td>Slug</td><td>Slug</td><td>Slug</td><td>Slug</td><td>Slug</td></tr>
<tr><td>8,730</td><td>Churn</td><td>Slug</td><td>Slug</td><td>Slug</td><td>Slug</td><td>Slug</td><td>Slug</td><td>Slug</td><td>Slug</td></tr>
<tr><td>8,820</td><td>Slug</td><td>Slug</td><td>Slug</td><td>Slug</td><td>Slug</td><td>Slug</td><td>Slug</td><td>Slug</td><td>Slug</td></tr>
<tr><td>8,910</td><td>Churn</td><td>Slug</td><td>Slug</td><td>Slug</td><td>Slug</td><td>Slug</td><td>Slug</td><td>Slug</td><td>Slug</td><td>Slug</td></tr>
</table>

9,000	Slug	Slug	Slug	Slug	Slug	Slug	Slug	Slug	Slug	Slug

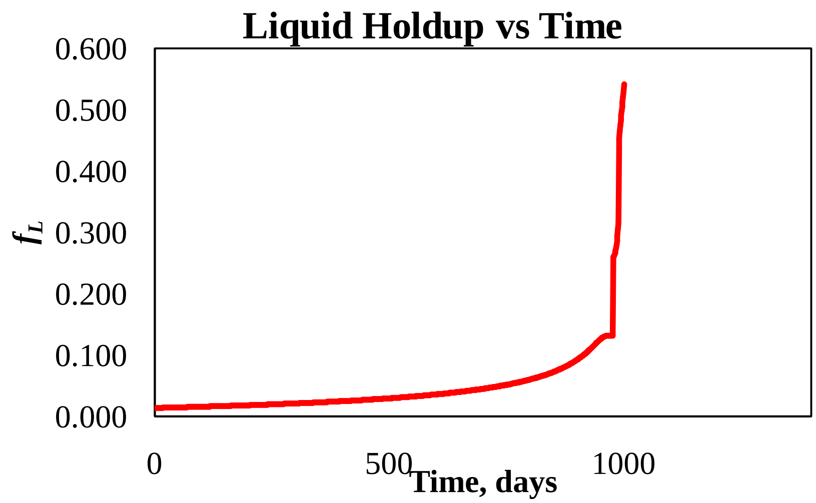

Fig. 6 – Liquid holdup at the bottom of the well

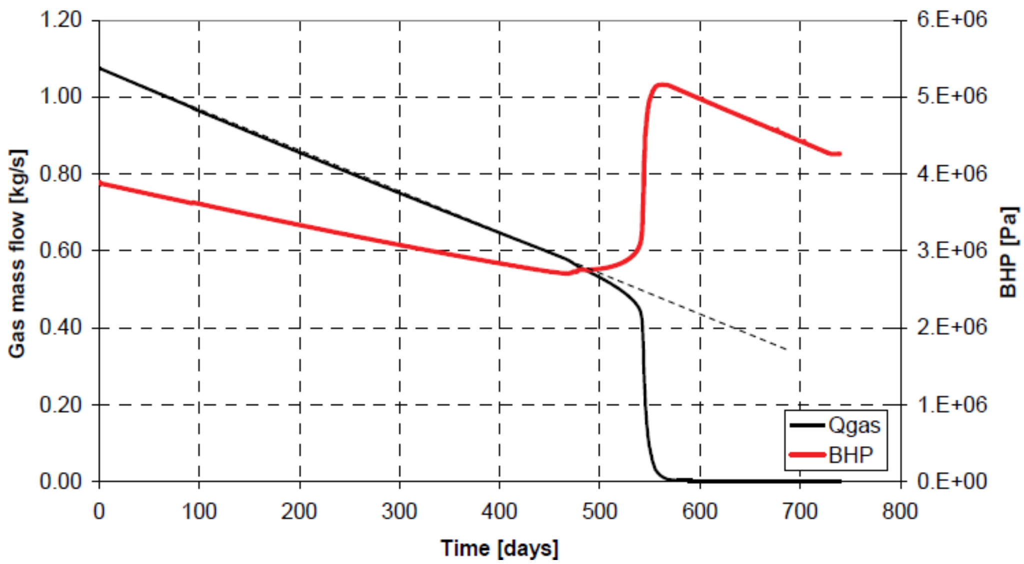

Fig. 7 – Simulation for the Netherlands study.

REMEDIATION

Once it has been established that liquid loading is taking place, remediation should be considered. We propose that more often than not, plunger lift would be cost-effective for many operations where liquid loading is timely diagnosed. Plunger lift uses the built up energy of a temporarily shut-in well to move much of the accumulated liquid up from the well bottom to the surface.

Plunger lift operate on the basis that when gas production rate starts to decline because of lowering pressure, the plunger would be allowed to drop and shut-off flow up the tubing; allowing pressure to buildup at the well bottom. Once the bottomhole pressure has increased enough, the plunger is lifted along with the incoming reservoir fluid. Obviously, with producing time, pressure will start to decline again, and the plunger will be lowered again to repressurize the well. To efficiently run this cyclic process of shutting in and restarting production, the well should not be shut-in for too long; yet, it must be shut-in for long enough for the pressure to build up to a certain level that allows continuous production for quite some time. The objective here is to develop a model that allows estimation of pressure buildup in the well after shut-in that allows subsequent sustained production.

The plunger should be released from the bottom seat only after the annular pressure has increased high enough so that the tubinghead pressure reaches above the line pressure upon expansion of fluids, and arrival of the plunger and liquid to the wellhead. We analyze the process by examining the energy available just before the plunger starts ascending and compare that to the final state of the process when the plunger has moved all the way up. We use the pressures at the tubinghead (p_t) and casinghead (p_c) to represent the pressure in the entire tubing and casing, respectively.

Energy available in the annular gas just before the plunger is released is the pressure-volume (pV) work that equals p_cV_c (ft-lbf), where V_c is the total volume of the gas in the tubing/casing annulus. This energy must be at least equal to the final pV work that is given by $(pV)_{\text{total}} = (p_tV_c + p_tV_t)$. In addition, energy must be spent to move the plunger, and water and gas on top of it to the wellhead (potential energy), and overcoming friction in doing so. The gain in potential energy of the plunger-fluid system is proportional to the total mass of plunger (m_p) plus fluid on top of the plunger (m_L+m_g). Therefore, energy balance is written as

$$p_cV_c = p_t(V_c + V_t) + (m_p + m_L + m_g)\left(\frac{g}{g_c}\right)D + F \tag{19}$$

The frictional loss of energy depends on the mass of the fluid plunger system, in addition to the well depth. For simplicity we assume that the frictional loss F is small compared to the other terms and is included in the gas static-head term as a small fraction C. Therefore, Eq. 18 is rewritten as

$$p_cV_c = p_t(V_c + V_t) + (m_p + m_L + (1 + C)m_g)\left(\frac{g}{g_c}\right)D \tag{20}$$

Eq. 20 allows us to estimate the optimum casing pressure, p_c. Thus, before the tubinghead valve is opened to allow the plunger to move up, the casing pressure must rise to a value given by the following expression:

$$p_c = \frac{p_t(V_c + V_t) + (m_p + m_L + (1 + C)m_g)\left(\frac{g}{g_c}\right)D}{V_c} \tag{21}$$

We used the data offered by Luo and Kelkar (2014) to validate the proposed plunger lift modeling approach. Their work provided data from four wells. To avoid repetition, only one of the examples has been reproduced below.

Fig. 8 presents daily production data along with tubinghead pressures for Well 1 in the Luo-Kelkar study. The decline in gas flow rate, with consequent rise in tubing pressure, signifies liquid loading. The schedule followed in the field data for the first plunger cycle is given below; subscript 1 represents conditions just prior to shut-in and subscript 2 represents conditions when the well is opened up again and the plunger begins its ascent:

p_{c1} = 240 psi $\qquad$ p_{t1} = 178 psi
p_{c2} = 255 psi $\qquad$ p_{t2} = 185 psi

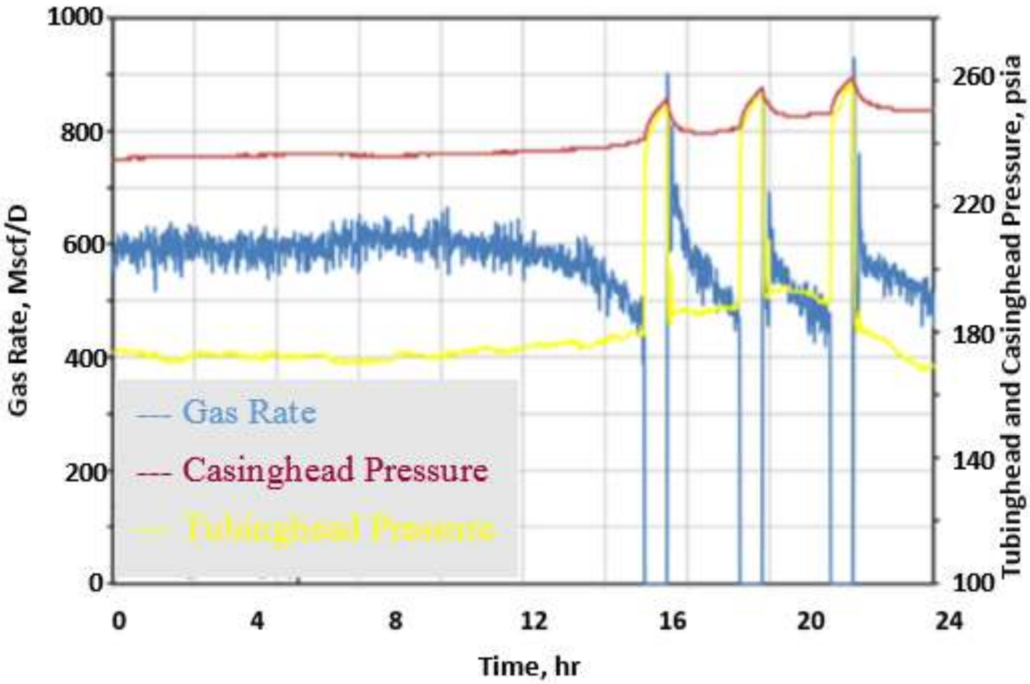

Fig. 8─Production data for Well 1 (Luo and Kelkar, 2014).

This vertical well has a depth of 3,440 ft; other pertinent data and sample calculations are presented in Appendix A. Our model (Eq. 21) calculated the required casing pressure for sustained production to be 269 psig, which is higher than the field schedule. Fig. 8 clearly shows that the field practice of releasing the plunger at 255 psig casinghead pressure did not allow production for more than a couple of hours.

Our contention is that if the plunger is allowed to stay long enough for the casinghead pressure to reach 269 psia, sustainable production can be achieved. To validate that contention, we need the reservoir response to reflect the desired casinghead pressure. However, Luo and Kelkar did not provide any reservoir information. We, therefore, built a reservoir model honoring the available production and pressure data. Estimation of reservoir influx provides a synergy that allows for a holistic approach to modeling the plunger lift system. **Fig. 9** presents daily production data along with tubinghead pressures for Well 1 in the Luo-Kelkar study in addition to showing the match that we were able to obtain using the numerical reservoir modeling. The match allowed reasonable prediction of the future production which could then be compared to the simulations made using the proposed model as shown later.

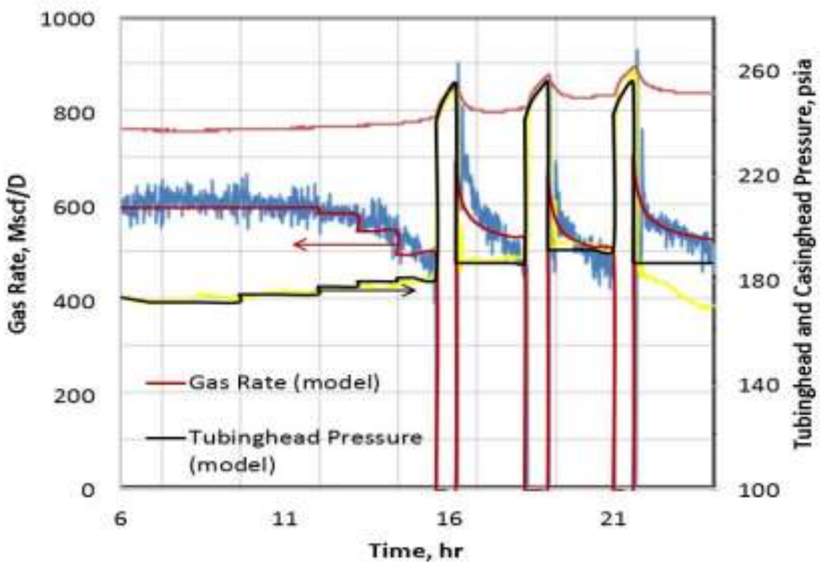

Fig. 9─History matching production performance in Well 1.

We think that the required casinghead pressure given by Eq. 21 is also the optimum value. In other words, our contention is that cumulative production over a period of time should be greater using the casinghead pressure given by Eq. 21, than using either a higher or a lower casinghead pressure. We used Well 1 of the Luo-Kelkar study to make this point. We tested the model with a 5% higher and a 5% lower casinghead pressure than was estimated with Eq. 21. As expected, both simulations yielded a lower cumulative production than that estimated by following the schedule suggested by Eq. 21. These results are shown in **Fig. 10** and **Fig. 11**, where we compare the effects of aiming for higher (Fig. 10) or lower (Fig. 11) target casinghead pressures.

Fig. 10 clearly shows that a higher target casinghead pressure requires the plunger to sit at the bottom longer than in the optimum case above. However, this longer shut in does not create much of a change in the eventual gas flow rate; the cumulative production for a higher casing pressure case ends up being lower than the optimum suggested by Eq. 21.

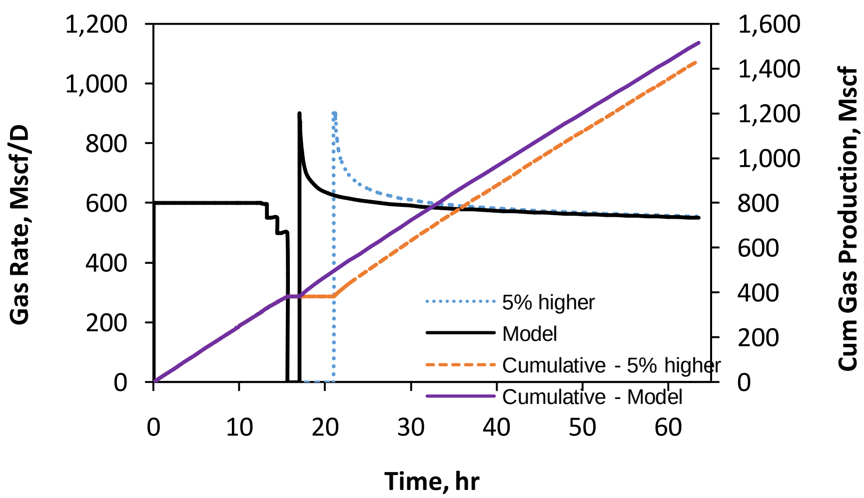

Fig. 10─Comparison of production between optimum and above optimum casing pressure, Well 1.

Fig. 11 represents similar data for a lower than optimum casing pressure. In contrast to the higher casing pressure case shown in Fig. 10, this one requires shorter shut-in time than is optimum. However, in this case, the pressure does not build up enough to sustain a high enough rate to maximize production; the cumulative production offered by the casing pressure calculated with Eq. 21 ends up being slightly higher. Overall, the results of Figs. 10 and 11 validate that the target casing pressure calculated by the proposed model is in fact optimum in a given situation.

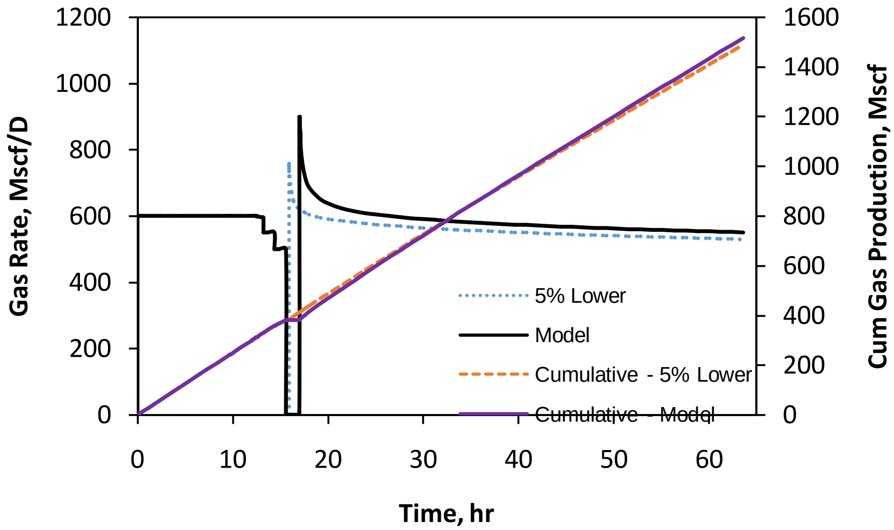

Fig. 11─Comparison of production between optimum and suboptimal casing pressure, Well 1.

CONCLUSION AND DISCUSSION

This paper presents a coupled wellbore/reservoir model to help estimate the onset of liquid loading in a gas well and forecast the productive period of the well after liquid loading has began. Such estimates of productive life of a gas well is useful to determine if some type of remediation would be economically effective.

The paper also suggests that plunger lift could be an attractive remediation of the liquid loading issue for many operators. We present a model for plunger lift operation to assess the desired casinghead pressure for release of the plunger for optimal performance.

We believe that the fluid flow in the entire wellbore must be in annular-flow regime for a well to be free from liquid loading. Since pressure is greatest near the bottom of the wellbore, the gas velocity is expected to be the lowest there, meaning transition from annular flow is most likely to occur at bottom first, as Sutton et al. (2010) deduced. Most authors use wellhead condition to calculate the critical loading velocity. In this study, the critical velocity is calculated throughout the entire wellbore based on local conditions.

This work also makes use of Vogel's empirical relationship for inflow performance in reservoirs with multiphase flow. The method requires some tuning to adapt it to the gas-water flow case as presented in this paper, since it was originally developed for oil-water flow. Though in our examples, the correlation works really well, reservoir simulation should be used for more thorough vetting in order to cover all bases. The physics of the flow being the same at least in conventional systems, we expect the tuned model to have very similar results as the oil-water flow.

In the example shown in the paper, liquid loading onset could be predicted 9 days before it was observed at the wellhead using the model described. We expect this time period to vary considerably in other cases, especially where high pressure and high temperature wells are concerned. This time period could very well turn into months or even a year, which significantly enhances the utility of such a model for forewarning timely remediation.

Another observation of the finer details of modeling reveals that the transition criterion from annular to slug or churn flow may in some cases predict abrupt switchovers to these flow regimes. This is a relic of discrete formulations that can be addressed by introducing smoothing parameters in the transition criteria. However the aspect merits some more investigation into making the transition more accurate and smooth, which is an item deferred for future study.

Proposed modeling also helps determine wells' candidacy for plunger lift. Wells producing gas-condensate fluids are also good candidates for plunger lift, particularly those below 100 STB/MMscf. In light of paucity in drilling in current business climate, some operators have experienced the need for artificial lift for about 50% of their wells. Given the low-cost operation, plunger lift is an attractive option and our approach to optimize the plunger lift cycle for cumulative production makes this lift option to operate more effectively.

NOMENCLATURE

A = drainage area of the reservoir, acres, L^2
B = formation volume factor, RB/STB
C = friction pressure loss as a fraction of gas potential energy change, dimensionless
C_o = flow parameter, dimensionless
c_p = specific-heat capacity of fluid, Btu/lbm-°F
D = depth of well, ft, L
d = pipe or well diameter, in, L
F = frictional loss, ft-lbf, mL^2/t^2
f_m = two-phase mixture friction factor, dimensionless
g = acceleration owing to gravity, ft/s^2, L/t^2
g_c = conversion factor, 32.17(lbm-ft)/(lbf-s^2)
g_g = geothermal gradient, °F/ft, T/L
G_i = Initial gas-in-place, Scft, L^3
h = reservoir thickness, ft, L
k = permeability, md, L^2
k_r = relative permeability, md, L^2
k_{rg} = relative permeability of gas, md, L^2
k_{rw} = relative permeability of water, md, L^2
L_R = relaxation parameter as defined by Hasan et al. 2009
m_g = mass of gas on top of plunger, m, lb_m
m_L = mass of fluid on top of plunger, m, lb_m
m_p = mass of plunger, m, lb_m
p = pressure, psia, m/Lt^2
p_c = pressure at casinghead, psia, m/Lt^2
p_i = initial pressure in the reservoir, psia, m/Lt^2
p_t = pressure at tubinghead, psia, m/Lt^2
p_{wh} = pressure at top of gas column, psia, m/Lt^2
$\bar{p}$ = average reservoir pressure, psia, m/Lt^2
p_{wf} = bottomhole pressure, psia, m/Lt^2

q_g = volumetric gas production rate, Scft/D, L^3/t
$q_{g,max}$= maximum volumetric gas production rate, Scft/D, L^3/t
q_w = volumetric water production rate, STB/D, L^3/t
r_e = reservoir radius, ft, L
r_w = wellbore radius, ft, L
S = Saturation, dimensionless
T *or* T_f = fluid temperature, °F, T
T_{ei} = undisturbed earth, or formation, temperature, °F, T
T_{eij} = undisturbed earth, or formation, temperature at z_j, °F, T
T_{fj} = fluid temperature at z_j, °F, T
V_c = Volume of tubing/casing annulus, ft^3, L^3
V_t = Volume of tubing, ft^3, L^3
v_{gc} = critical gas velocity needed for annular two-phase flow, ft/s, L/t
v_m = two-phase mixture velocity, ft/hr, L/t
v_{sg} = superficial gas velocity, ft/hr, L/t
$v\infty$ = terminal rise velocity of single bubble, ft/hr, L/t
z = variable well depth from surface, ft, L
Z = gas compressibilty factor, dimensionless
γ = specific gravity, dimensionless
θ = well deviation from horizontal, degree
μ = fluid viscosity, cp, m/Lt
ρ = density, lb_m/ft^3, m/L^3
σ = surface tension, lb_m/sec^2
φ = porosity, dimensionless
φ_T = lumped parameter as defined by Hasan et al. 2009

Subscripts
c = critical
g = gas
gc = critical gas
gi = initial gas
gr = residual gas
i = initial
j = space coordinate
l = liquid
n = timsestep
pc = pseudocritical
pn = cumulative produced
w = water
wh = wellhead
wi = initial water
1 = condition prior to plunger release
2 = final condition after plunger release

REFERENCES

Agarwal, R.G. 1967. Unsteady-State Performance of Water-Drive Gas Reservoirs, Ph.D. Thesis, Texas A&M University, College Station, Texas, USA.

Agrawal, S. and Sharma, M. M. 2013. Impact of Liquid Loading in Hydraulic Fractures on Well Productivity. Presented at the SPE Hydraulic Fracturing Conference, The Woodlands, TX, USA, 4-6 February. SPE-163837-MS. http://dx.doi.org/10.2118/163837-MS.

Alamu, M. B. 2012. Gas-Well Liquid Loading Probed With Advanced Instrumentation. *SPE J.* **17** (1): 251-270. SPE-153724-PA. http://dx.doi.org/10.2118/153724-PA.

Barnea, D. 1986. Transition from annular flow and from dispersed bubble flow-unified models for the whole range of pipe inclinations. *Int. J. Multiphase Flow* **12** (5): 733-744. http://dx.doi.org/10.1016/0301-9322(86)90048-0.

Barnea, D. 1987. A unified model for predicting flow-pattern transitions for the whole range of pipe inclinations. *Int. J. Multiphase Flow* **13** (1): 1-12. http://dx.doi.org/10.1016/0301-9322(87)90002-4.

Chava, G.K., Falcone, G., and Teodoriu, C. 2008. Development of a New Plunger-Lift Model Using Smart Plunger Data. Paper SPE-115934-MS presented at the SPE Annual Technical Conference and Exhibition, 21-24 September, Denver, Colorado, USA. SPE-115934-MS. http://dx.doi.org/10.2118/115934-MS.

Chava, G., Falcone, G., and Teodoriu, C. 2010. Plunger-Lift Modeling Toward Efficient Liquid Unloading in Gas Wells. *SPE Projects, Fac & Const* **5** (1): 38–45. SPE-124515-PA. http://dx.doi.org/10.2118/124515-PA.

Coleman, S. B., Clay, H. B., McCurdy, D. G. et al. 1991. Understanding Gas-Well Load-Up Behavior. *J Pet Technol* **43** (3): 334-338. SPE-20281-PA. http://dx.doi.org/10.2118/20281-PA.

Dousi, N., Veeken, C. A. M., and Currie, P. K. 2006. Numerical and Analytical Modeling of the Gas-Well Liquid-Loading Process. *SPE Prod & Oper* **21** (4): 475-482. SPE-95282-PA. http://dx.doi.org/10.2118/95282-PA.

Foss, D. L. and Gaul, R. B. 1965. Plunger-life Performance Criteria with Operating Experience-Ventura Avenue Field. *Drill and Prod Practice*, New York, New York. API.

Hasan, A. R. and Kabir, C. S. 2002. *Fluid Flow and Heat Transfer in Wellbores*. Richardson, Texas, USA: SPE Textbook Series.

Hasan, A. R., Kabir, C. S., and Wang, X. 2009. A Robust Steady-State Model for Flowing-Fluid Temperature in Complex Wells. *SPE Prod & Oper*. **24** (2): 269-276. SPE-109765-PA. http://dx.doi.org/10.2118/109765-PA.

Hashmi, G. M., Hasan, A. R., and Kabir, C. S. 2016. Design of Plunger Lift for Gas Wells. Presented at the SPE North American Artificial Lift Conference and Exhibition, The Woodlands, TX, USA, 25-27 October. SPE-181220-MS. http://dx.doi.org/10.2118/181220-MS.

Hu, B., Veeken, K., Yusuf, R. et al. 2010. Use of Wellbore-Reservoir Coupled Dynamic Simulation to Evaluate the Cycling Capability of Liquid-Loaded Gas Wells. Presented at the SPE Annual Technical Conference and Exhibition, Florence, Italy, 19-22 September. SPE-134948-MS> htpp://dx.doi.org/10.2118/134948-MS.

Jackson, D. F. B., Virues, C. J. J., and Sask, D. 2011. Investigation of Liquid Loading in Tight Gas Horizontal Wells With a Transient Multiphase Flow Simulator. Presented at the Canadian Unconventional Resources Conference, Calgary, 15-17 November. SPE-149477-MS. http://dx.doi.org/149477-MS.

Lea, J.F. 1982. Dynamic Analysis of Plunger Lift Operations. *J Pet Technol* **34** (11): 2,617–2,629. SPE-10253-PA. http://dx.doi.org/10.2118/10253-PA.

Luo, S. and Kelkar, M., 2014. Effective Method to Predict Installation of Plunger in a Gas Well. *J Energy Resour Technol*, **136** (2): 024501. http://dx.doi.org/10.1115/1.4025799.

Mulyadi, H., Amin, R., Kennaird, T. et al. 2000. Measurement of Residual Gas Saturation in Water-Driven Gas Reservoirs: Comparison of the Various Core Analysis Techniques. Presented at the International Oil and Gas Conference and Exhibition, Beijing, China, 7-10 November. SPE-64710-MS. http://dx.doi.org/10.2118/64710-MS.

Nosseir, M. A., Darwich, T. A., Sayyouh, M. H. et al. 2000. A New Approach for Accurate Prediction of Loading in Gas Wells Under Different Flowing Conditions. *SPE Prod & Fac* **15** (4): 241-246. SPE-66540-PA. http://dx/doi.org/10.2118/66540-PA

Riza, M.F., A.R. Hasan, and C.S. Kabir. 2015. A Pragmatic Approach to Understanding Liquid Loading in Gas Wells. *SPE Prod Oper*. SPE-170583-PA. http://dx.doi.org/10.2118/170583-PA.

Sutton, R. P., Cox, S. A., Lea, J. F. et al. 2010. Guidelines for the Proper Application of Critical Velocity Calculations. *SPE Prod & Oper* **25** (2): 182-194. SPE-120625-PA. http://dx.doi.org/10.2118/120625-PA.

Taitel, Y., Bornea, D. and Dukler, A. E. 1980. Modeling Flow Pattern Transitions for Steady Upward Gas-Liquid Flow in Vertical Tubes. *AIChE J*. **26** (3): 345-354. http://dx.doi.org/10.1002/aic.690260304.

Tang, Y. and Liang, Z., 2008, January. A New Method of Plunger Lift Dynamic Analysis and Optimal Design for Gas Well Deliquification. Presented at the SPE Annual Technical Conference and Exhibition, 21-24 September, Denver, Colorado, USA. SPE-116764-MS. http://dx.doi.org/10.2118/116764-MS.

Turner, R. G., Hubbard, M. G., and Dukler, A. E. 1969. Analysis and Prediction of Minimum Flow Rate for the Continuous Removal of Liquids from Gas Wells. *J Pet Technol* **21** (11): 1475-1482. SPE-2198-PA. http://dx.doi.org/10.2118/2198-PA

Rubis – Multipurpose Numerical Model. Kappa Engineering, (https://www.kappaeng.com/software/rubis/overview).

van't Westende, J. M. C., Kemp, H. K., Belt, R. J. et al. 2007. On the role of droplets in concurrent annular and churn-annular pipe flow. *Int J Multiphase Flow* **33** (6): 595-615. http://dx.doi.org/10.1016/j.ijmultiphaseflow.2006.12.006.

Veeken, K., Hu, B., and Schiferli, W. 2010. Gas-Well Liquid-Loading-Field-Data Analysis and Multiphase-Flow Modeling. *SPE Prod & Oper* **25** (3): 275-284. SPE-123657-PA. http://dx.doi.org/10.2118/123657-PA.

Wallis, G. B. 1969. *One-Dimensional Two-Phase Flow*. New York: McGraw-Hill.

Yuan, G., Pereyra, E., Sarica, C. et al. 2013. An Experimental Study on Liquid Loading of Vertical and Deviated Gas Wells. Presented at the SPE Production and Operations Symposium, Oklahoma City, Oklahoma, USA, 23-26 March. SPE-164516-MS. http://dx.doi.org/10.2118/164516-MS.

Zhang, H., Falcone, G., and Teodoriu, C. 2010. Relative Permeability Hysteresis Effects in the Near-Wellbore Region During Liquid Loading in Gas Wells. Presented at the SPE Latin American and Carribean Petroleum Engineering Conference, Lima, Peru, 1-3 December. SPE-139062-MS. http://dx.doi.org/10.2118/139062-MS.

Zhang, H., Falcone, G., Valko, P. et al. 2009. Numerical Modeling of Fully-Transient Flow in the Near-Wellbore Region During Liquid Loading in Gas Wells. Presented at the SPE Latin American and Carribean Petroleum Engineering Conference, Cartagena de Indias, Colombia, 31 May-3 June. SPE-122785-MS. http://dx.doi.org/10.2118/122785-MS.

Zhou, D. and Yuan, H. 2010. A New Model for Predicting Gas-Well-Loquid Loading. *SPE Prod & Oper* **25** (2): 172-181. SPE-120580-PA. http://dx.doi.org/10.2118/120580-PA.

APPENDIX A ─ EXAMPLE CALCULATIONS

Well 1. Estimating desired casinghead pressure. The following sample calculation shows how the proposed approach works using Luo and Kelkar (2014) data. The following data were available:

Tubing pressure after plunger travel, p_{t2} = 185 psia
Casing volume V_c = 436 ft^3. Tubing volume V_t = 169 ft^3.
Vertical well depth = 3,443 ft. Liquid column on plunger top = 40 ft.
Gas gravity = 0.62

The following quantities were derived from these field data:

Gas pressure at tubing bottom, p_{tb} = 185 $p_{bh} = 185e^{(gMh)/(RZTg_c)}$ = 198 psia
Gas density for average tubing pressure (~pM/RT) = 0.573 lbm/ ft^3
Mass of gas in the tubing (= tubing volume × gas density) = 106.6 lbm
Mass of liquid on top of plunger (= liquid volume × liquid density) = 612.6 lbm

We can use Eq. 21 to calculate the required casing pressure before the plunger release for sustained production:

$$p_c = \frac{p_t(V_c+V_t)+\left(m_p+m_L+(1+C)m_g\right)\left(\frac{g}{g_c}\right)h}{V_c} = 269 \text{ psia.} \qquad \textbf{(A-1)}$$

The actual casinghead pressure at the time of plunger release was 255 psia, which is 14 psig lower than that recommended by Eq. 21. As a result, the well did not sustain continued production.

International Conference on Petroleum Engineering 2016 (ICPE-2016)
Bangladesh University of Engineering & Technology (BUET)
Dhaka-1000, Bangladesh

ICPE (2016-033)

Re-completion of KTL-5 well: An investigation of excessive water production

Hasan Mahmud*[1],Mohammad Mojammel Huque[2], Mohammed Mahbubur Rahman[3], Howleder Ohidul Islam[4]

Sylhet Gas Fields Limited, Sylhet, Bangladesh[1],
Process Engineering Department, Memorial University of Newfoundland, Canada[2],
Petroleum and Mineral Resources Engineering Department, Bangladesh University of Engineering and Technology, Dhaka,Bangladesh[3],
Bangladesh Petroleum Exploration and Production Company Limited, Dhaka, Bangladesh[4]

ABSTRACT

This paper presents an analysis of the excessive water production problem in the well KTL-5, and explores the remedial measures that may be taken to revive the well. KTL-5 is a gas well in the Kailashtilla gas field. It began production in 2006, but had to be shut down two times between 2009 to 2013 due to excessive water production. The Kailashtilla field has three gas bearing formations. These are called the Upper (UGS), the Middle (MGS), and the Lower (LGS) gas sands. It is also recognized that the UGS is the most potential formation. There are three more wells, namely KTL-2, 3, and 6, producing from the same sand. However, these three wells have low and steady water production. Thus, it is suspected that the water source for KTL-5 may be elsewhere. Production data, wireline log, and cement bond log data for KTL-5 were analyzed to investigate this problem. It is found that the cementing is weak just above the permeable sand (UGS). It may cause channeling behind the casing and water from adjacent formation may have invaded the UGS. To confirm this, further investigation is recommended. Neutron log based cased hole reservoir evaluation tool should be run to check cross flow and to confirm the current water level. Gas saturation also should be estimated from this log to confirm gas amount. If the results are encouraging, a cement squeeze job above the UGS section should be performed. Then the well can be revived by perforating in 2,387-2,435.3m (MD) section.

Keywords: Well re-completion, Water production, Wire line log, Cement squeeze.

* Corresponding Author address
Email: hmplus02@gmail.com

INTRODUCTION

The Kailashtilla field is located at about 15 km east of the town of Sylhet in northeastern Bangladesh. The field was discovered in 1960 by Pakistan Shell Oil Company (PSOC), developed by the Bangladesh National Company and is now operated by Sylhet Gas Fields Limited.

The Kailashtilla structure is located in the northeast Surma basin of Bangladesh. The Surmabasin contains almost exclusively clastic sequences of deltaic, fluvial, and to a lesser degree marine sandstones, siltstones, shale and claystones. The Kailashtilla structure is a north-South elongated, slightly asymmetric anticline. It is approximately 12 km long and 5 km wide.[1]

The hydrocarbon of Kailashtilla field is primarily contained within three distinct horizons: Upper Gas Sand (UGS), Middle Gas Sand (MGS), and Lower Gas Sand (LGS). The gas initially in place (GIIP) estimated by two different organizations at two different times is shown in Table1.

Table 1: Potential Sands in Kailashtilla Reservoir [1, 2].

Potential Sands	Depth, Meter	GIIP, TCF	
		RPS, 2009	BAPEX, 2012
UGS	7483-7662	1.79	0.972
MGS	9665-9734	0.72	0.312
LGS	9808-9990	1.10	0.245

The first well in Kailashtillafield, KTL-1, was drilled in 1961-62 up to a total depth of 13,577 ft.Subsequently six more wells, KTL-2 to KTL-7, were drilled at different times.Out of these 7 wells, KTL-1, 2, 3, 5 and 6 were completed in the UGS. Production from this field started in 1983. The cumulative gas and condensate production from thisfield are about 316.158 BCF (from 1983 to December 2015). Currently the field produces about 57 MMSCF of gas per day[3]. Summary of the KTL wells are shown in Table 2.

Table 2 Summary of KTL wells in UGS [3, 4]

Wells	Formation	Perforation (ft)	Tubing size (inches)	Production period
KTL-1	LGS and UGS (dual completion)	7,487-7,547(UGS) 9,810-9,870(LGS)	2-7/8	Jun 83 to Jan 98
KTL-2	UGS	7,390-7,430	3-1/2	Feb 95 to present
KTL-3	UGS	7,391-7,526	3-1/2	Jul 06 to present
KTL-5	UGS	7,580-7,612	4-1/2	Sep 10 to Mar 14
KTL-6	UGS	7,480-7,628	4-1/2	Aug 07 to present

Table-2 shows that production from UGS through KTL-1 and KTL-5 were stopped from January 1998 and March 2014 respectively. KTL-1 was producing through dual completion and it was shut-in due to excessive water production from the LGS. KTL-5 was also shut-in for severe water production, but its production history is quite different from the rest of the wells producing from the same sand (UGS). The study is focused on this anomalous production history of KTL-5, and the motivation of the work is to see whether it is possible to revive this well [3, 4].

PROBLEM STATEMENT

KTL-5 was shut in twice during its life time. Initially it started production from the high resistivity zone (HRZ) from September 2006, but had to be shut in due to excessive water productionfrom October 2009. The water gas ratio (WGR) reached as high as 540 bbl/MMSCF,and the well head pressure (FWHP)fell down to 1495 psig.To resume production, KTL-5 was recompleted by setting a bridge plug and cementing above the HRZ, and then it was perforated at 2,413-2,425 m MD of the UGS.It came back to production in in September 2010, with gas rate of 14 MMSCFD, and WGR of 0.21 bbl/MMSCF. After January 2011, WGR was increasing and wellhead pressure was decreasing gradually. By February 2013, gas rate fell to 6.00 MMSCFDand WGR increased to 25 bbl/MMSCF. Finally, in March 2013, WGR abruptlyclimbed to 600 bbl/MMSCF and lowered the FWHP to 1,260 psig, resulting in the second shut in of the well.

It is most interesting to note that, three other wells, namely KTL-2, KTL-3, KTL-6 are also producing from the UGS, without any dramatic increase of WGR (Figure 1). Thus it is reasonable to assume that this excessive water from KTL-5 is not the formation water, but the water source is elsewhere, and there is a good chance to revive the well by identifying the water source [4]

In this paper we attempt to identify the water source by analyzing the available data- namely, production history, wireline log, and cement bond log.

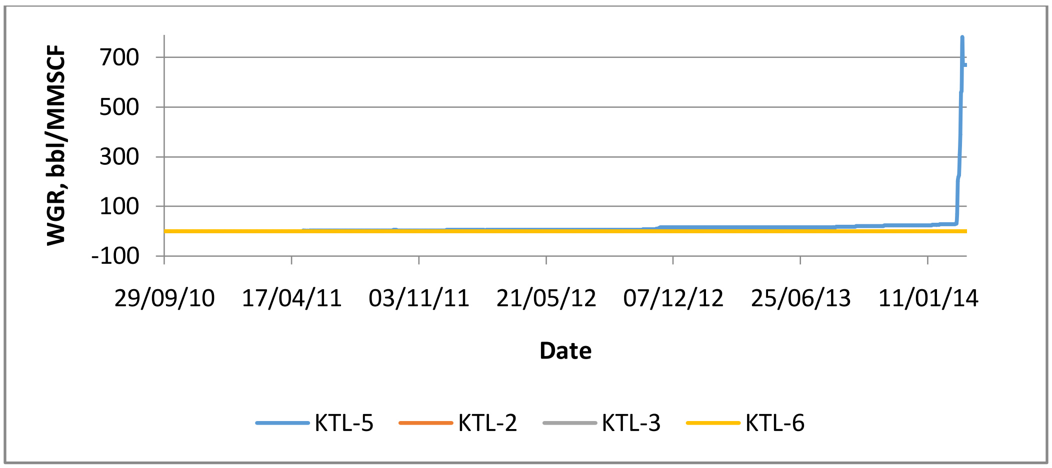

Fig: 1 WGR vs time plot of KTL-2, 3, 5 and 6 wells.

Production History Analysis

The gas rate, flowing well head pressure and WGR of KTL-5 is shown in Figure 2 and 3. The gas rate varied from 14-12 MMSCFD from October 2010 to March 2012. After that, an increasing trend of WGR(3-4bbl/MMSCF) is noticed, with a reduced gas rate of 8 MMSCFD. The increasing trend of WGR continued upto25 bbl/MMSCF, which further reduced the gas rate to 5 MMSCFD. Meanwhile the well head pressure fell from 2,680 to 2,450 psig. Finally a huge and sudden increase in water production(WGR about 780 bbl/MMSCF) was encountered in March 2014, and the gas rate became nearly zero, with well head pressure of 1,250 psig[4].

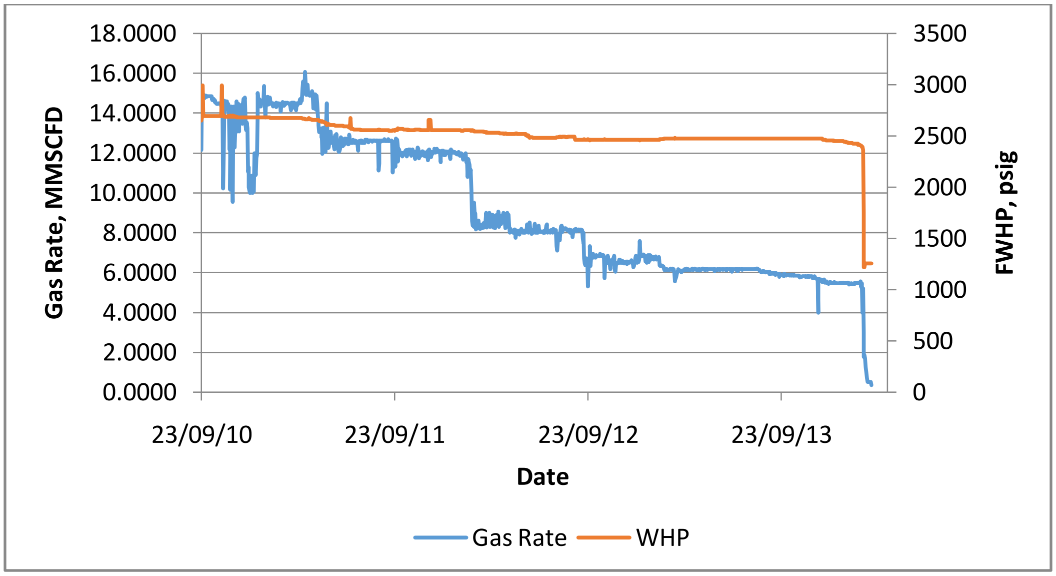

.

Fig: 2 Gas Rate andFWHP versus time plot of KTL-5

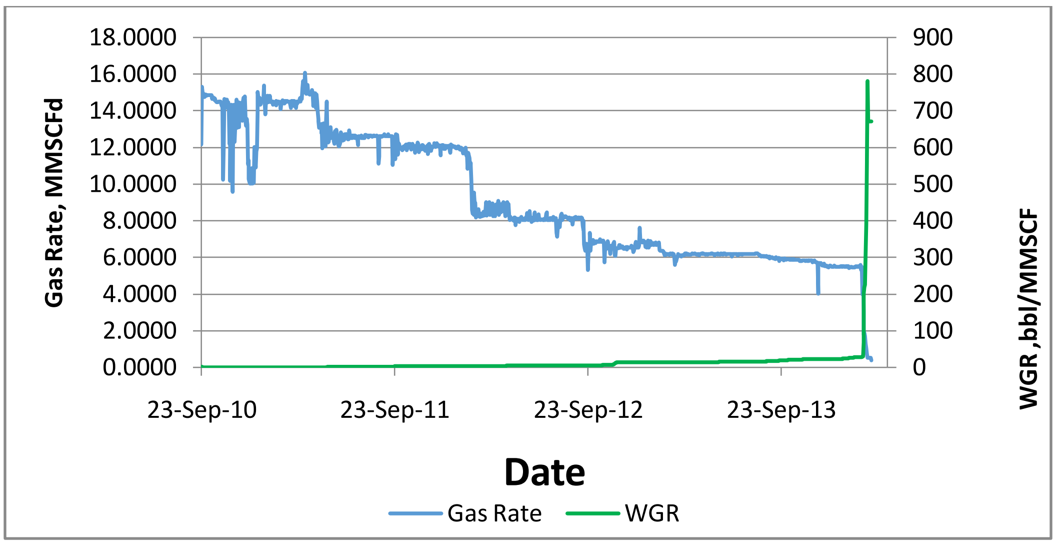

Fig: 3 Gas Rate and WGR versus time plot of KTL-5

Master log and wireline log interpretation

Figure 4 shows the composite logs in the UGS interval of KTL-5. It indicates gas bearing zonefrom 2,387.7 to 2,406.7m and from 2,413.0 to 2,435.3m. The gas zone is separated by a shale zone. The Master log shows the total gas saturation from 0.4% to 29.1 % in this sand. A clear "excavation effect" is seen in the Neutron-Density log, which indicates a gas bearing zone. From the wireline log data, porosity, permeability, and water saturation are obtained as 22.7%, 477 md and 42% respectively. Gas water contact is estimated at a depth of 2,435.3m MD.[5]

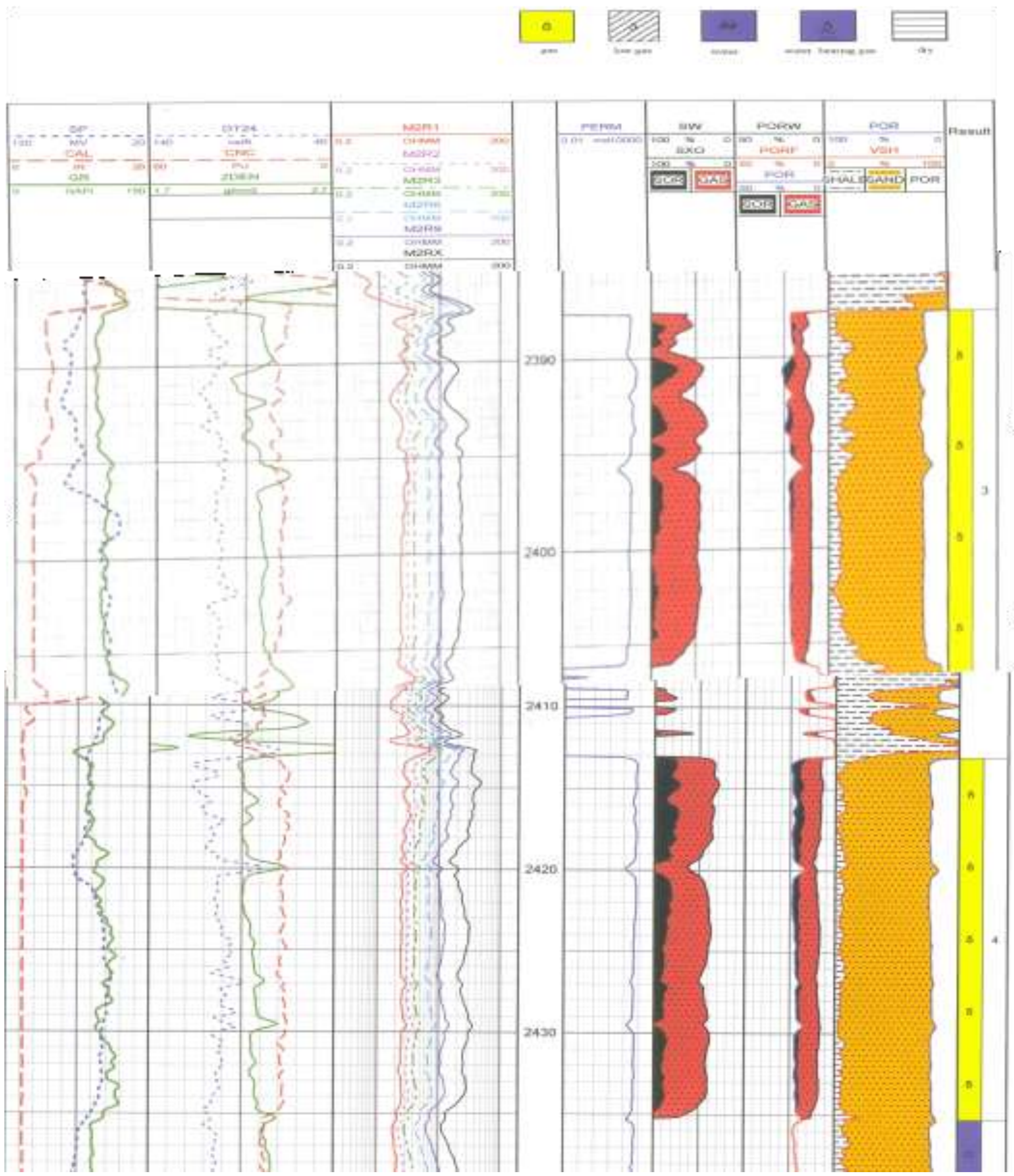

Figure 4 Composite logof KTL-5 well in UGS section.

Cement bond log analysis

Cement bond log of KTL-5 in the UGS section is shown in Figure 5.It shows that bellow theUGS (2,387-2,435.3m), the cement bond is good enough but above the zone cementing is not good except 2,405-,2410 m as pipe amplitude is more than 50 mV. Thus, there is a chance of channeling of water from nearby aquifer through this weak bonded cemented area [5].

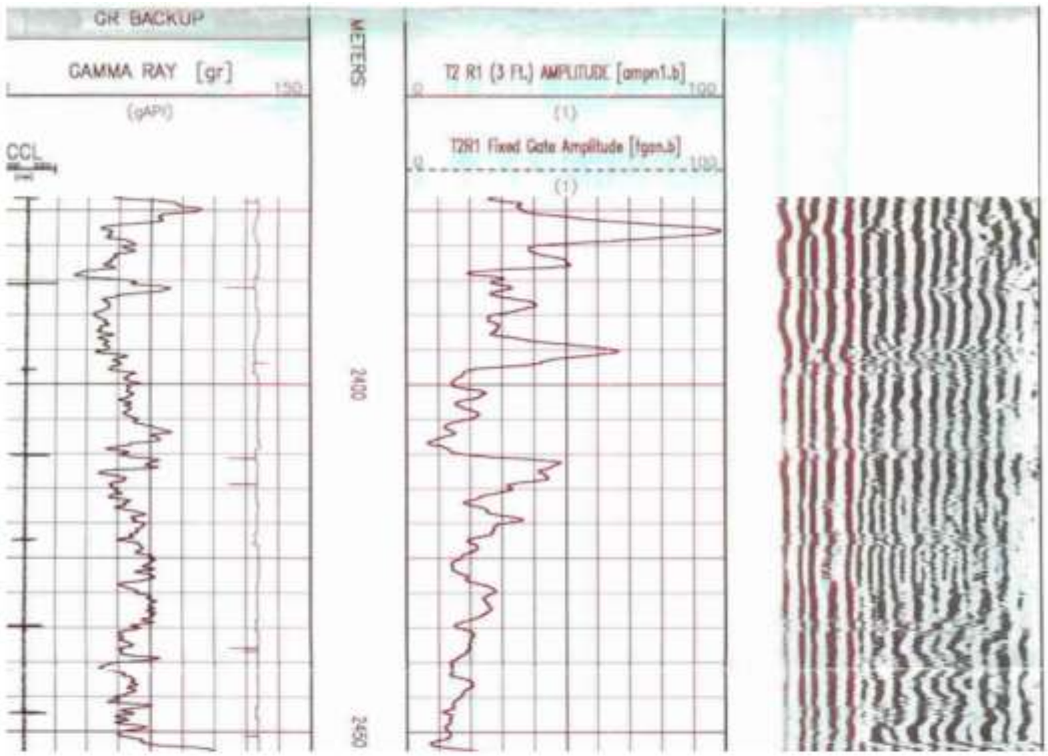

Fig 5 CBL-VDL of KTL-5.

DISCUSSION

The most potential sand of KTL field is UGS. There is no indication of excessive water production from this sand by KTL -2, 3, and 4. Unlike other wells in the same sand, increasing trend of water production was remarkablein KTL-5 which was noticed within six month of production, and ultimately the well was shut in due to excessive water production. This excessive water could not be formation water.Again, Cement Bond Log(CBL) - Variable Density Log(VDL) indicates weak cement bond above the permeable zone. Thus it is quite possible that a channel was created, which brought water from a nearby aquifer or water bearing formation. Further investigation should be conducted to confirmthe water source. A neutron log based cased-hole reservoir evaluation tool may be run to identify the cross-flow effect of aquifer water to the upper portion of UGS and to measure current water level. If the channeling is confirmed, this well can be brought back to production by squeezing cement above UGS, and re-perforating in the 2,387-2,435.3m interval.[6]

CONCLUSION

The UGS is not the source of excessive water which killed KTL-5. The cementing is weak just above the UGS. Therefore, channeling of water from nearby formation is suspected.

RECOMMANDATION

To make KTL-5 producible again, the following activities are recommended:

a) Run CBL-VDL log to check current cement bond.

b) Run neutron log based Cased hole reservoir evaluation tool to check cross flow and to confirm the current water level. Gas saturation also should be estimated from this log to confirm gas amount. In this case, how much water has already been dumped in the reservoir have to be considered. The decision for further perforation in the upper portion of UGS depends on this log result.

c) In case of positive result from step (b), squeeze cement above the UGS section.

d) Again run CBL-VDL to check the cementation.

e) Make the well producible by perforating in 2,387-2,435.3 m (MD) section.

REFERENCES

1. RPS Energy, . 2009. Resource Estimation for Rashidpur Field, Prepared for petrobangla.
2. BAPEX, .2012. Rashidpur 3D Interpretation Report. Prepared for Sylhet Gas Fields Limited.
3. RPS Energy, .2009. Rashidpur petroleum Engineering Report, Prepared for petrobangla.
4. Petrobangla MIS Reports of 2010-2014. Available at www. petrobangla.org.bd
5. CNPC Logging Corporation, .2006. KTL-5 Completion Interpretation Report.
6. Elkington, Peter A. S., Pereira, Alex & Smworth, Roger, .2006. A novel cased hole Density Neutron log characteristics and Interpretation. SPE Asia Pacific Oil & Gas Conference and Exibition, Australia.

International Conference on Petroleum Engineering 2016 (ICPE-2016)
Bangladesh University of Engineering & Technology (BUET)
Dhaka-1000, Bangladesh

ICPE (2016-049)

Analyzing Physico-Chemical Properties of Bioethanol and Bioethanol Blended Fuels

Samavi Farnush Bint-E-Naser[1,†], Laila Hossain[1,†], Mrittika Debnath[2], Proma Prodipti Barua[1], Mohidus Samad Khan[1,*]

[1]Department of Chemical Engineering, Bangladesh University of Engineering & Technology, Dhaka - 1000, Bangladesh

[2]Applied Chemistry and Chemical Engineering, Dhaka University, Dhaka – 1000, Bangladesh

[†]Equally first author: both authors contributed equally

ABSTRACT

In Bangladesh, development of industrial and agricultural sectors has led to an ever increasing demand of petroleum products. The annual demand of petroleum products is met primarily by refining imported crude oils from overseas, which is processed with a small quantity of oil from the Haripur Gas Field at Sylhet, Bangladesh . Bioethanol, produced from biomass, could be a potential alternative fuel for Bangladesh to meet the future energy demand and to save foreign exchange. As a quasi-renewable energy source, bioethanol is considered the cleanest alternative to fossil fuel . Although Bangladesh does not commercially produce bioethanol to date, there are few initiatives at the private sector level in this regard; therefore, it is important to understand the physico-chemical properties of bioethanol and bioethanol blended petrol and octane . This chapter aims to measure and analyze different fuel properties, namely, specific gravity & API gravity, gross calorific value, Reid vapor pressure, viscosity, copper strip corrosion, ASTM distillation, sulfur content, water content, ASTM color of bioethanol and bioethanol blend petrol and octane at various blending rates (0, 5, 10%) . This chapter will be highly useful in providing the baseline properties of bioethanol and bioethanol blend petrol and octane as engine fuel.

Keywords: bioethanol, physico-chemical properties, ASTM method, bioethanol blend.

* Corresponding Author address
Email: mohid@che.buet.ac.bd

Samavi Farnush Bint-E-Naser1,†, Laila Hossain1,†, Mrittika Debnath2, Proma Prodipti Barua1, Mohidus Samad Khan1,*

INTRODUCTION

Ethanol is the most used liquid biofuel either as a fuel or as a gasoline enhancer [1]. It is generally obtained from the conversion of carbon-based feedstocks, which are often locally available and can be converted into secondary energy carriers [2]. Bioethanol is easily biodegradable. Bioethanol as a vehicle fuel produces less greenhouse gas (GHG) emissions compared to petrol or octane. Carbon dioxide (CO_2) released when ethanol is used in vehicles is offset by the CO_2 captured when crops used to make the ethanol are grown [3]. Bioethanol is completely miscible with water in all proportions, while gasoline and water are immiscible [4]. This may cause the blended gasoline to contain water, and further result in corrosion related problems on the mechanical components, especially for components made of copper, brass or aluminum [5].

Bioethanol is a safer alternative to methyl tertiary butyl ether (MTBE), the most common additive to gasoline, used to provide cleaner combustion. However, MTBE is a toxic chemical compound, and has been found to contaminate groundwater. In contrast, ethanol has greater octane booster properties, and introduces less contamination to water sources [2]. Ethanol contains 35% oxygen by mass which implies a smaller amount of the additive will be required; moreover, ethanol facilitates better fuel combustion and reduces the amount of particulate emission resulting from combustion [6]. In order to use ethanol as engine fuel, it is important to understand its physico-chemical properties, as well as its effects on engine performance. In this chapter, selected physico-chemical properties of the bioethanol sample, and bioethanol blends of petrol and octane prepared in the laboratory, were measured as per ASTM guidelines.

MATERIALS & METHODOLOGY

Sample Collection & Preparation

Bioethanol sample was collected from Mojj Engineering Systems Limited, India through Sunypun Organics Limited, Bangladesh. The collected bioethanol sample was produced from a multi feedstock which was converted to monomeric sugars via enzymatic hydrolysis, followed by fermentation using yeast for conversion of sugars into ethanol. The produced bioethanol was purified in a multi-pressure distillation column with integrated evaporator operating under vacuum at low temperature, and then, dehydrated to obtain the final product. Octane and petrol were collected from local market.

High quality petrol and octane (almost 100%) were purchased from local fuel station. The 5% and 10% bioethanol blends of petrol and octane were prepared in the laboratory using the collected bioethanol sample, petrol and octane. While conducting the experiments, the blended sample s w ere remixed at regular interval (at least once a month) to prevent phase seperation.

Methodology

The fuel properties of the seven samples (pure bioethanol, petrol, octane, 5 and 10% bioethanol blends of petrol and octane) were tested according to ASTM specification. The test methods are listed in Table 1. Each test was performed thrice (n=3) and the average results obtained were used for further analysis.

Table 1. ASTM test methods.

Parameter tested	ASTM test method
Specific gravity & API gravity	ASTM D 1298-99
Calorific value	ASTM D 2014-96
Reid vapor pressure	ASTM D 323-99a
Viscosity	ASTM D 88-94
Copper strip corrosion	ASTM D 130-04
ASTM distillation	ASTM D 86-04b
Sulfur contnent	ASTM D 3177-89
Water content	ASTM D 95-70
ASTM color	ASTM D 1500-03

RESULTS

Table 2: Results for specific gravity, API gravity, gross calorific value, Reid vapor pressure, viscosity and Cu strip corrosion test.

Sample	Sample no	Specific gravity at 25°C	API gravity (°)	GCV (MJ/kg)	Reid vapor pressure (kPa)	Viscosity (cSt)	Cu strip corrosion at 50°C
Bioethanol	1	0.785	49.0	27.33	14.25	1.03	1a
Petrol	2	0.757	56.5	40.72	45.75	0.55	1a
5% bioethanol blend petrol	3	0.761	56.0	40.44	43.00	0.56	1a
10% bioethanol blend petrol	4	0.762	55.5	39.38	43.00	0.57	1a
Octane	5	0.777	51.8	40.59	50.00	0.55	1a

5% bioethanol blend octane	6	0.781	51.5	40.07	48.00	0.57	1a
10% bioethanol blend octane	7	0.784	50.8	40.08	47.60	0.58	1a

Table 3: Results for ASTM distillation, sulfur content, water content and ASTM color.

Sample no	ASTM distillation				Sulfur content (wt %)	Water content (%)	ASTM color
	IBP (ºC)	FBP (ºC)	Total recovery (vol %)	Percent loss (vol %)			
1	81.0	83.0	99.50	0.50	0.036	Nill	-
2	54.2	266.4	99.05	0.95	0.048	Nill	L ASTM Color 1
3	60.3	286.5	99.05	0.95	0.054	Nill	L ASTM Color 1
4	49.9	239.8	97.93	2.07	0.048	Nill	L ASTM Color 1
5	46.2	224.4	97.23	2.77	0.035	Nill	L ASTM Color 1.5
6	48.9	223.9	97.10	2.90	0.041	Nill	L ASTM Color 1.5
7	48.2	248.4	97.24	2.76	0.065	Nill	L ASTM Color 1

DISCUSSIONS

Specific Gravity, API Gravity and Water Content

Lighter fuel oils can be transported through pipelines. Greater the specific gravity (SG), greater the mass of fuel that can be stored in a given tank. Fuel density generally increases with increasing molecular weight of the fuel molecules. Generally, an increase in density increases the overall performance of engines [7]. Figure 1 shows graphical representation of experimental and theoretical values [8, 9] of SG of the samples. As shown in the figure, specific gravity increases slightly with increasing amounts of bioethanol in the blended fuels, as the SG of bioethanol is higher than petrol and octane. The American Petroleum Institute gravity (API gravity), is another means to determine petroleum lightness with respect to water: if the API gravity is greater than 10, the petroleum fuel is lighter and floats on water; if less than 10, it is heavier and sinks. API gravity is an inverse measure of a petroleum liquid's density relative to water (also known as specific gravity), as is shown in Figure 2. API gravity is gradated in degrees on a hydrometer. API gravity values of most petroleum liquids fall between 10 and 70 degrees.

Determining the water content of fuels and biofuels is important for quality control, meeting trade specifications, protecting financial value, enhancing process optimization and for taking necessary steps to reduce risks from corrosion, safety problems, and infrastructure damage. Petrol, octane and bioethanol samples were tested according to ASTM D 95-70 which yielded no water content in the samples (table 3) since the moisture content of the samples was very low.

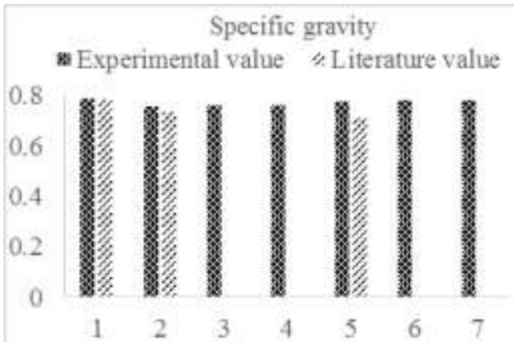

Figure 1: Specific gravity of fuel samples

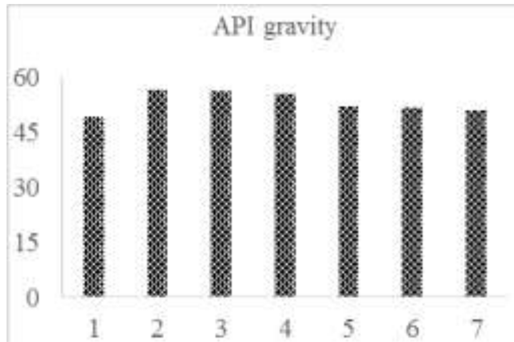

Figure 2: API gravity of fuel samples

Gross Calorific Value

The combustion rate of a fuel is proportional to its calorific value. A low calorific value indicates more water vapor absorption. Gross caloric values (GCV) of the samples are shown in Figure 3. For samples 1, 2, and 5, the experimentally obtained values are lower than literature values [10, 11]. Possible explanation of this discrepancy may include the presence of small amount of water, which lowers the calorific value of fuel. For samples 3, 4, 6, and 7, blending of ethanol lowers the GCV of petrol and octane. The higher the percentage of ethanol, the lower the GCV.

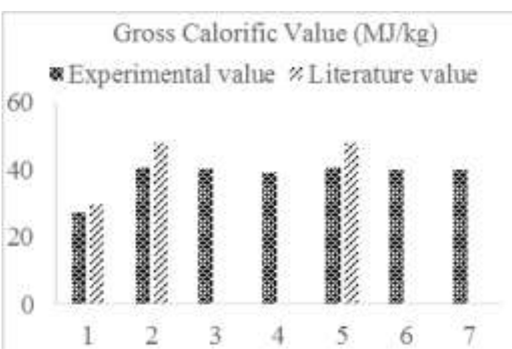

Figure 3: GCV of fuel samples

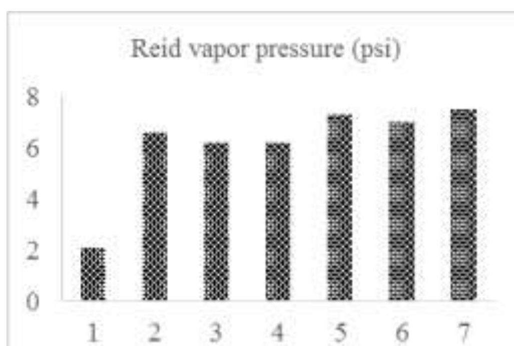

Figure 4: RVP of fuel samples

Reid Vapor Pressure

Reid vapor pressure (RVP) is defined as the absolute pressure (i.e., psia, kPa or bar) exerted by a mixture, determined at 100 ºF (37.8 ºC). This is different than the true vapor pressure which is defined as the pressure of a vapor in equilibrium with its condensed phase at a specific temperature. According to

Renewable Fuel Association (RFA) guidelines, unless other more volatile blending components are used, the addition of ethanol should not result in a vapor pressure increase above 1.0 psi in conventional gasoline [12]. The experimental measurements as demonstrated in Figure 4 shows that blending of bioethanol caused increase in RVP lower than 1.0 psi for all petrol-bioethanol and octane-bioethanol blends. The 10% bioethanol blend octane showed the highest RVP, which is similar to the findings of Andersen et.al. [13].

Viscosity

Viscosity is a measure of oil's resistance to flow. It decreases (thins) with increasing temperature and vice-versa. Oil's viscosity is determined most commonly by measuring kinematic viscosity, which is measured in the time it takes for a specific volume of oil to flow through a special device called a capillary tube and reported in a unit called the centistoke (cSt). Figure 5 shows the effect of blending bioethanol on the viscosity of petrol and octane. As shown in Figure 5, blending ethanol up to 10% volume content causes only a small increase in viscosity, although, viscosity of ethanol is almost double the viscosity of petrol and octane.

Sulfur Content

Sulfur and its compounds are present in almost all petroleum products and lubricants, from crude oils to the ultra-low sulfur fuels of the future. Figure 6 shows the effect of blending bioethanol on the sulfur content of petrol and octane. For 5% bioethanol blended fuel, sulfur content is higher than pure petrol and bioethanol and for 10% bioethanol blend petrol, sulfur content is same as pure petrol, which is higher than bioethanol. For octane, blending of bioethanol resulted in increased amounts of sulfur in samples containing 5 and 10% bioethanol blended octane. However , the sulfur contents of all samples were found to be sufficiently low, implying that the samples do not demand further purification.

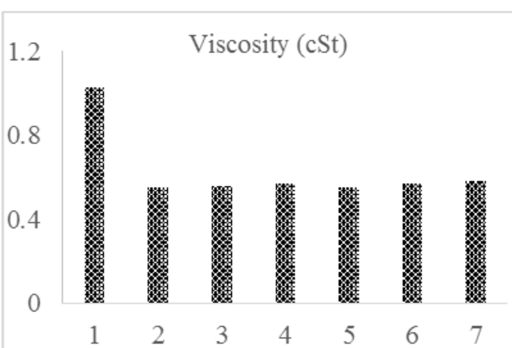

Figure 5: Viscosity of the fuel samples

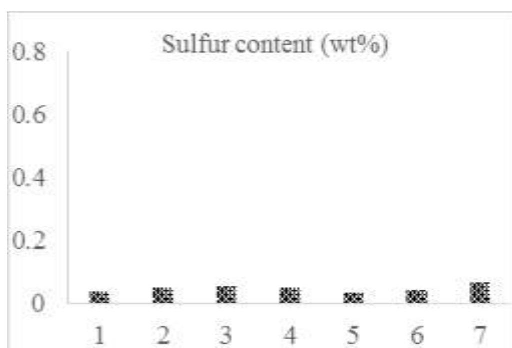

Figure 6: Sulfur content of the fuel samples

ASTM Distillation

The distillation curves are shown in Figure 7 and Figure 8. The temperatures obtained during distillation are plotted against the percentages distilled.

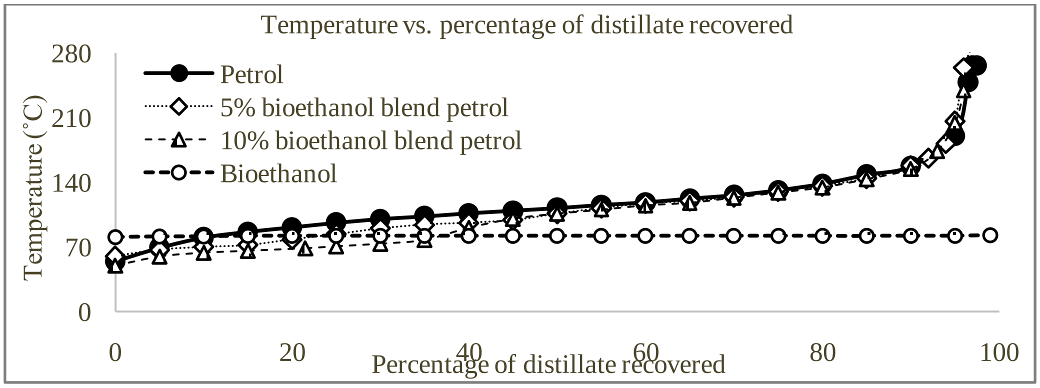

Figure 7: Effect of blending bioethanol on boiling point of petrol

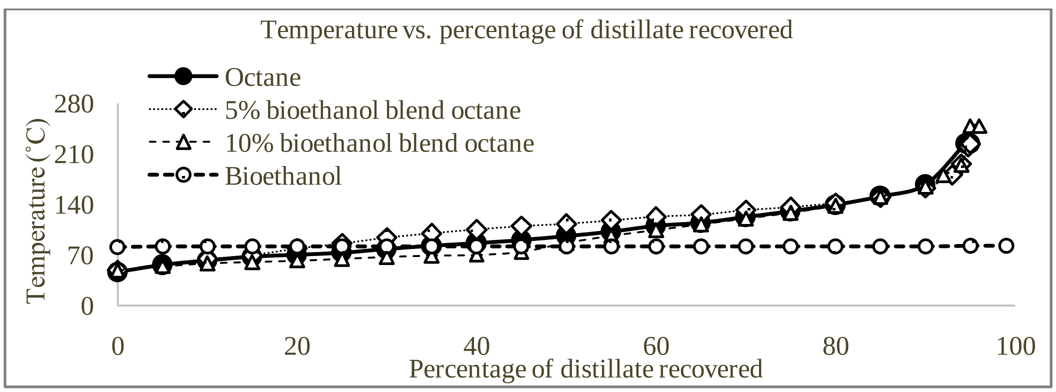

Figure 8: Effect of blending bioethanol on boiling point of octane

For efficient combustion, the distillation curve need to be smooth and straight [14]. The distillation range is important in judging the ignition properties of oil. Figure 7 and Figure 8 show the degree of spread between the initial boiling point and the end point. Mixing bioethanol up to 10% with petrol and octane slightly change the boiling point range of the blended petrol and octane.

Cu Strip Corrosion and ASTM Color

Crude petroleum contains sulfur compounds, most of which are removed during refining. However, of the sulfur compounds remaining in the petroleum product, some can have corroding effects on various metals, and this corrosivity may not be directly related to the total sulfur content. The effect can vary according to the types of the sulfur compounds present. The copper strip corrosion test is designed to assess the relative degree of corrosivity of a petroleum product. All samples under analysis generated a slight tarnish (1a) color of the copper strip.

Determination of the color of petroleum products serves as an indication of the degree of refinement of the material; given the color range of a particular product is known, a variation outside the established range may indicate possible contamination with another product. Table 3 shows that blending bioethanol does not contribute to the ASTM color.

CONCLUSION

The inevitable depletion of world's energy supply has resulted in a worldwide interest in alternative sources of energy to ensure fuel security. In Bangladesh, the present annual demand of petroleum products is about 3.7 MMT. Bangladesh imports about 1.3 MMT of crude oil and another 2.7 MMT (approximately) of refined petroleum products per annum. Considering the limited amount of global fossil fuel reserves, the amount of foreign currency required to import the petroleum products, and concern regarding environmental challenges, particularly greenhouse gas (CO_2) emission, it is vital for Bangladesh to look for alternate renewable fuels for its sustainable development. While renewable energy sources such as solar, wind and hydro energies may be used to generate electricity or heat either directly or indirectly, biomass is the only renewable energy source capable of producing liquid fuels (biofuels) for storage and also as a transport fuel [15]. Bioethanol blended with petrol and octane are in early stage of development compared to other alternatives such as CNG or LPG. These blends also have the potential to reduce greenhouse gas emissions. This experimental study provides baseline properties of bioethanol and bioethanol blend (5% and 10%) petrol and octane as fuel.

ACKNOWLEDGEMENTS

This research was supported by BCEF Academic Research Fund and CASR Research Fund. The authors would like to acknowledge Sunypun Organics Limited, Bangladesh and Mojj Engineering Systems Limited, India for bio-ethanol samples, and Mr J. Bishwash of Fuel Lab, ChE, BUET, for providing technical support.

REFERENCES

1. Sanchez, O.J. and C.A. Cardona, *Trends in biotechnological production of fuel ethanol from different feedstocks.* Bioresource technology, 2008. **99**(13): p. 5270-5295.

2. Von Blottnitz, H. and M.A. Curran, *A review of assessments conducted on bio-ethanol as a transportation fuel from a net energy, greenhouse gas, and environmental life cycle perspective.* Journal of cleaner production, 2007. **15**(7): p. 607-619.

3. *Fuels & Vehicles: Ethanol Vehicle Emissions*. [cited 2016 November 20]; Available from: http://www.afdc.energy.gov/vehicles/flexible_fuel_emissions.html.

4. Furey, R.L. and K.L. Perry, *Composition and reactivity of fuel vapor emissions from gasoline-oxygenate blends*. 1991, SAE Technical Paper.

5. Coelho, E.P., et al., *Fuel injection components developed for Brazilian fuels*. 1996, SAE Technical Paper.

6. Lin, Y. and S. Tanaka, *Ethanol fermentation from biomass resources: current state and prospects.* Applied microbiology and biotechnology, 2006. **69**(6): p. 627-642.

7. *Fuel Density*. [cited 2016 August 10]; Available from: http://members.axion.net/~enrique/space_fueldensity.html.

8. *Specific Gravity of Liquid Table*. [cited 2016 August 10]; Available from: http://www.csgnetwork.com/specificgravliqtable.html.

9. *Liquids-Specific Gravities*. [cited 2016 August 10]; Available from: http://www.engineeringtoolbox.com/specific-gravity-liquids-d_336.html.

10. *Calorific values od solid, liquid and gaseous fuels*. [cited 2016 August 29]; Available from: http://www.kayelaby.npl.co.uk/chemistry/3_11/3_11_4.html.

11. *Fuels-Higher Calorific Values*. [cited 2016 August 30]; Available from: http://www.engineeringtoolbox.com/fuels-higher-calorific-values-d_169.html.

12. Association, R.F., *Fuel Ethanol: Industry Guidelines, Specifications, and Procedures*. 2005: The Association.

13. Andersen, V.F., et al., *Vapor pressures of alcohol− gasoline blends.* Energy & Fuels, 2010. **24**(6): p. 3647-3654.

14. Schmidt, P.F., *Fuel oil manual*. Vol. 10. 1985: Industrial Press Inc.

15. Adams, J.M., J.A. Gallagher, and I.S. Donnison, *Fermentation study on Saccharina latissima for bioethanol production considering variable pre-treatments.* Journal of applied Phycology, 2009. **21**(5): p. 569-574.

International Conference on Petroleum Engineering 2016 (ICPE-2016)
Bangladesh University of Engineering & Technology (BUET)
Dhaka-1000, Bangladesh

ICPE (2016-051)

Studying Growth Kinetics of Chlorella vulgaris, a Microalgae with High Lipid Content, to Produce Biodiesel in Local Condition

Anika Ferdous[1], Farid Ahmad[1,2], Md. Shajid Khan[1], John Liton Munshi[3], Chapol Kumar Roy[3], Husna Parvin Nur[3], Mohidus Samad Khan[1*]

1 Department of Chemical Engineering, Bangladesh University of Engineering and Technology (BUET). Dhaka-1000, Bangladesh.

2 Institute of Appropriate Technology, Bangladesh University of Engineering and Technology (BUET). Dhaka-1000, Bangladesh.

3Biological Research Division, BCSIR Laboratories, Dhaka.Dhaka-1205, Bangladesh

ABSTRACT

Biofuel derived from edible and non-edible sources is considered to be a promising alternative to conventional fossil fuel. Biofuels are renewable, carbon neutral and cause less environmental damages than fossil fuel. However, edible biofuel sources, such as: soybean, corn, jatropha, and sunflower have raised concerns due to their demand as food crops. On the other hand, non-edible sources like microalgae have received considerable interest since it does not compete with food supply. The lipid content of microalgae may vary depending on the microalgae strain. To make biofuel production from microalgae economically viable and sustainable, it is important to identify microalgae strains with high lipid content and to find an optimized mass culture technique for local condition. Different research groups have reported that locally available microalgae strain, such as *Spirulina*, contains low lipid content (less than 10 per cent), which is unfavorable for the commercial production of biofuel from microalgae. Therefore, it is important to identify and culture a microalgae strain with high lipid content, which can be cultured in high volume in local condition. In this study, microalgae strain *Chlorella vulgaris*, collected from CSIRO Australia, was used to grow in local condition. *Chlorella vulgaris* contains up to 50 per cent lipid (dry weight). Growing a foreign microalgae strain in local condition is highly challenging and time consuming, and requires right kind of nutrient and environment to grow. The first part of this systematic study aims to identify a suitable growth media and growth condition to grow *Chlorella vulgaris* in local environment, which will be used for the future production of *Chlorella vulgaris* in industrial scale. Different growth media, such as: MLA, BB, and CH, were used to grow *Chlorella vulgaris* in laboratory scale. The growth patterns of *Chlorella vulgaris* was analyzed for the proposed growth media in the local conditions.

Keywords: Biodiesel, microalgae, nutrient media, growth patterns, lipid

* Corresponding Author address
Email: mohid@che.buet.ac.bd

INTRODUCTION

Along with the economic development, the demand of energy is growing throughout the world. To meet the growing demand, researchers and technologists all over the world are looking for sustainable alternative fuel sources [1]. Biofuel produced from different edible and non-edible sources could be a potential alternative of traditional fossil fuel. The first generation biofuel feedstock, such as: sunflower, palm, rapeseed, soybean, maze, sugarcane, and coconut have been used to produce biofuel. However, the above items also have demand as food crops. Different non-edible crops have also been used to produce biodiesel, but the yield is often not satisfactory. Alternatively, researches have shown that average biofuel production from microalgae can be 10 to 20 time higher than the yield of oleaginous seeds and/or vegetable oil [2, 3]. Because of the high photosynthetic ability, high biomass production, and fast growth rate, microalgae can be a favorable source of biofuel production. The critical factors to culture microalgae and to produce biofuel from extracted lipid contents are: environmental condition, growth media, lipid extraction methods, esterification techniques, and cost effectiveness of the overall process [4]. The lipid content of microalgae may vary from 5 per cent to 65 per cent (or higher) depending on the microalgae strain; Table 1 presents the lipid contents of different microalgae strains [5]:

Table 1: Lipid content of different microalgae strains (% dry matter)

Species	Lipid
Scenedesmus obliquus	11–22/35–55
Scenedesmus dimorphus	6–7/16–40
Chlorella emersonii	63
Chlorella protothecoides	23/55
Chlorella sorokiana 22	22
Chlorella minutissima	57
Dunaliella bioculata	8
Dunaliella salina	14–20
Neochloris oleoabundans	35–65
Spirulina maxima	4–9

In Bangladesh, only *Spirulina* is produced in a high volume (pilot plant set by BCSIR). However, the lipid content of *Spirulina* is very low (Table 1), which indicates low yield of biofuel from *Spirulina*. Therefore, it is important to select and grow a microalgae with high lipid content at the local condition. The growth of microalgae heavily depends on growth media and growth environment. Finding the best growth media for a certain microalgae strain can mitigate the algal production cost and improve the product quality significantly. The elements required for the growth of green algae are: N, P, K, Mg, Ca, S, Fe, Cu, Mn and Zn. Often the growth media is designed by analyzing the chemical environment in which

the natural algae can thrive [6, 7]. However, the combination and concentration of the required chemical elements may vary according to the algae strain and culture environment.
This article presents the first part of a systematic study to identify and grow a microalgae strain with high lipid contents in local condition. In this study, *Chlorella vulgaris,* collected from Commonwealth Scientific and Industrial Research Organization (CSIRO) Australia, was selected as the potential microalgae strain. *Chlorella vulgaris* is reported as the fast growing high yield green microalgae with high lipid content; researchers reported that on an industrial scale, in a glasshouse area of 10,000 m^2, 130-150 tons of dry algal biomass can be obtained annually [8]. Some researchers also reported that during the nutrient starvation phase, the lipid content in *Chlorella vulgaris* could be increased between 50 and 70 per cent [9, 10]. However, growing a microalgae strain in a new condition is highly challenging, time consuming, and could be unsuccessful if right nutrient and environment is not ensured. It is to be noted that it took more than two years for the local and international experts to successfully culture *Spirulina* in a pilot scale in Bangladesh condition. Therefore, identifying the growth medium and culture conditionfor *Chlorella vulgaris* would be the most critical factor for the industrial production of biofuel from microalgae. Studying the growth kinetics is important to evaluate and to improve the performance of microalgae culture systems [11]. In this study, three different growth media: Bold's Basal (BB), MLA and CH media, were used to study the growth patterns of *Chlorella vulgaris*. The growth patterns of *Chlorella vulgaris* in the above nutrients have been observed and analyzed.

MATERIAL AND METHOD

Materials

The analytical grade of the following chemicals were used to prepare growth media for *Chlorella vulgaris*: $MgSO_4.7H_2O$, $NaNO_3$, K_2HPO_4, KH_2PO_4, H_3BO_3, H_2SeO_3, $NaHCO_3$, $CaCl_2.2H_2O$, KNO_3, $FeSO_4.7H_2O$, $CaSO_4.2H_2O$, NaCl, EDTA, KOH, H_2SO_4, Biotin, Vitamin B12, Thiamin HCl, Na_2EDTA, $FeCl_3$, $MnCl_2.4H_2O$, $CuSO_4.5H_2O$, $ZnSO_4.7H_2O$, $CoCl_2.6H_2O$, $Na_2MoO_4.2H_2O$, $MnCl_2.4H_2O$, MoO_3, $Co(NO_3)_2.6H_2O$. Laboratory grade ultra-pure water was used for solution preparation and dilution.
The microalgae *Chlorella vulgaris* was collected from Commonwealth Scientific and Industrial Research Organization (CSIRO), Australia.

Microalgae Culture

The microalgae was cultured in 250 ml Erlenmeyer flasks. Experiments for each medium were repeated six times. Different batches of the experiments for each medium were conducted in series. The flasks were first filled with 200 ml nutrient medium and then autoclaved for 20 minutes. After cooling down to the room temperature, each flask was inoculated with 5 ml of algae stock solution. The flasks were kept in a plant-growth room having a controlled temperature of 25±2°C, and lit with 1200 lux/m^2 fluorescent light with a photoperiod of 8 hours a day (Figure 1). The change in color of the culture medium has been observed with the passing of time.

Figure 1: Growing *Chlorella vulgaris* in controlled environment using different growth media

RESULTS AND DISCUSSION

Three growth media were used to culture *Chlorella vulgaris*: BB, MLA, and CH media. Among the proposed growth media, CH was formulated using trial and error method. Composition of the above growth media used in this study are presented in Table 2.

After collecting the microalgae *Chlorella vulgaris*, the major concern was to ensure the survival of the stock solution. There were several factors that could be crucial for the algae culture, such as: composition and quality of the nutrient media, temperature of the culture room, aseptic condition of the culture room, and light intensity. If the above factors are not maintained accurately, the whole batch of mother culture could be contaminated or die. Moreover, the time required for the microalgae to response to the new environment was also a matter of concern, because it took longer to response than usual (2-3 days) [12]. For the first batch of culture it took round 6 weeks to show the first response, however for the third batch, it took around 4 weeks to respond.

The time dynamic behavior of *Chlorella vulgaris* growth in the above growth media are presented in Table 3. *Chlorella vulgaris* found to grow in all the media. However, the respond was found satisfactory in CH medium, followed by MLA medium, and BB medium. The first and second batch of *Chlorella vulgaris* culture did not respond well to the new environment, although, the third batch adapted to the local environment and the response was very well. The microscopic images presented in Figure 2 show the healthy cells of *Chlorella vulgaris* growing in MLA media.

Table 2: Composition of the three media (MLA, BB, and CH)

Name of the chemicals	Concentration (g/L)		
	MLA	BB	CH
$MgSO_4.7H_2O$	49.4	7.5	10.42×10^{-3}
$NaNO_3$	85.0	25	-
K_2HPO_4	6.96	7.5	40.42×10^{-3}
KH_2PO_4	-	17.5	-
H_3BO_3	2.47	11.42	-
H_2SeO_3	1.29×10^{-3}	-	-
$NaHCO_3$	16.9	-	-
$CaCl_2.2H_2O$	29.4	2.5	-
KNO_3	-	-	1.0833
$FeSO_4.7H_2O$	-	4.98	5×10^{-3}
$CaSO_4.2H_2O$	-	-	2×10^{-3}
NaCl	-	-	-
EDTA	-	50	-
KOH	-	31	-
H_2SO_4	-	1 ml/L	-
Biotin	50×10^{-9}	-	-
Vitamin B_{12}	50×10^{-9}	-	-
Thiamin HCl	0.1×10^{-3}	-	-
Na_2EDTA	4.36	-	-
$FeCl_3$	1.58	-	-
$MnCl_2.4H_2O$	0.36	1.44	-
$CuSO_4.5H_2O$	0.01	1.57	-
$ZnSO_4.7H_2O$	0.022	8.82	-
$CoCl_2.6H_2O$	0.01	-	-
$Na_2MoO_4.2H_2O$	6×10^{-3}	-	-
MoO_3	-	0.71	-
$Co(NO_3)_2.6H_2O$	-	0.49	-

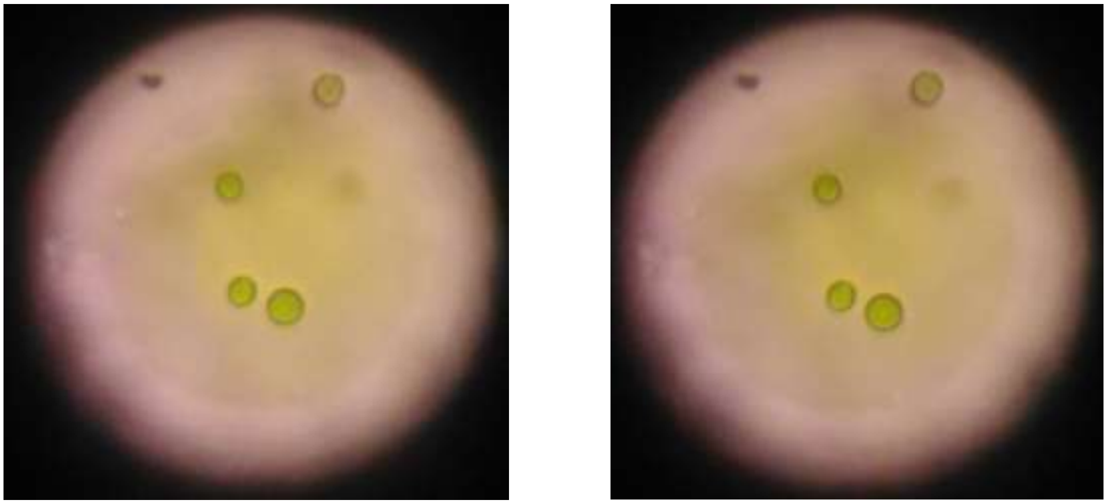

Figure 2: Microscopic images of *Chlorella vulgaris* cells (4 weeks inoculation) growing in MLA growth media at 25°C

Table 3: Growth of *Chlorella vulgaris* in growth media: MLA, CH, and BB

Time	Algae Growth in MLA Medium	Algae Growth in CH Medium	Algae Growth in BB Medium
4 weeks after inoculation			
6 weeks after inoculation			
8 weeks after inoculation			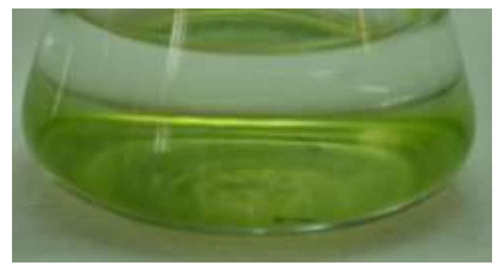

CONCLUSION

In Bangladesh, *Spirulina* is produced in high volume as a food supplement. However, the lipid content of *Spirulina* is less than 10 per cent, which is not favorable for biofuel production from algae. Therefore, it is important to identify a microalgae strain with high lipid content, and to grow it in local condition. *Chlorella vulgaris,* a microalgae strain with high lipid content, was collected from CSIRO, Australia to grow in Bangladesh. Often the microalgae strain, collected from foreign environment, do not survive in a foreign environment, or get contaminated because of adverse culture environment. The initial success of this study was to keep the mother stock surviving in Bangladesh condition, and to propagate in locally prepared growth media. In this study, the growth pattern of *Chlorella vulgaris* is reported based on a visual color change and microscopic images in different growth media: BB, MLA and CA. The preliminary study has shown the difference in response in the media over a period of time. This study will be highly useful to produce *Chlorella vulgaris* in high volume in Bangladesh, and hence, to produce biodiesel as the alternative fuel source.

ACKNOWLEDGEMENTS

This research was supported by BCEF Academic Research Fund and CASR Research Fund.

REFERENCES

1. Saifullah, A.Z.A., Karim,A.Md., Yazid,A.A., Microalgae: An Alternative Source of Renewable Energy. American Journal of Engineering Research (AJER), 2014. 3(3): p. 9.
2. BLINOVA, L., BARTOSOVA,A.,GERULOVA,K., CULTIVATION OF MICROALGAE (*Chlorella vulgaris*) FOR BIODIESEL PRODUCTION. RESEARCH PAPERS, FACULTY OF MATERIALS SCIENCE AND TECHNOLOGY IN TRNAVA SLOVAK UNIVERSITY OF TECHNOLOGY IN BRATISLAVA, 2015. 23(36): p. 10.
3. Darzins, A., Pienkos,P.,Edye,L., Current Status and Potential for Algal Biofuels Production. August, 2010.
4. Hannon, M., Gimpel, J., Tran, M., Rasala, B., and Mayfield, S., Biofuels from algae: Challanges and Potentials. PMC. PMC, August 2011. 1(5): p. 11.
5. Gouveia L, O.A., Microalgae as a raw material for biofuels production. journal of Industrial & Microbial Biotechnology, Februaru 2009. 36(2).
6. Vonshak, A., Laboratory techniques for the cultivation of microalgae, in Handbook of microalgal mass culture, A. Richmond, Editor. 1986, CRC Press: Boca Raton, FL. p. 117-145.
7. Blair, M.F., Kokabian,B., Gude,V.G., Light and growth medium effect on Chlorell vulgaris biomass production. Journal of Environmental Chemical Engineering, 2013: p. 10.

8. Pulz, O., Photobioreactors: Production system for phototrophic microorganisms. Applied Microbiology and Biotechnology, 2001. 57: p. 5.
9. Scragg, A.H., Illman,A.M., Carden,A., Shales,S.W., Growth of microalgae with increased calorific values in a tubular bioreactor. Biomass and Bioenergy, 2002. 23: p. 6.
10. Yeh, K.L., Chang,J.S., Effects of cultivation conditons and media composition on cell grwoth and lipid productivity of indigenous microalga *Chlorella vulgaris* ESP-31. Bioresource Technology, 2012. 105: p. 7.
11. Sandnes, J.M., Ringstad,T., Wenner,D., Heyerdahl,P.H., Kallqvist,T., Gislerod,H.R., Real-time monitoring and automatic density control of large-scale microalgal cultures using near infrared (NIR) density sensors. Journal of Biotechnology, 2006. 122: p. 6.
12. Kim, J., Lee,J-Y., Keener, T.C., Growth Kinetic Study of *Chlorella vulgaris*, in AIChE Annual Meeting. 2009, ResearchGate.